Synthesis and Characterization of Zinc(II) Complexes with Diamines and Thiolates

A Dissertation Submitted to the Department of Chemistry,
Quaid-i-Azam University, Islamabad, Pakistan
in Partial Fulfillment of the Requirements for the Degree of

Doctor of Philosophy

in

Inorganic/Analytical Chemistry

By

Muhammad Akhtar
Department of Chemistry
Quaid-i-Azam University
Islamabad, Pakistan

2016

Declaration

This is to certify that this dissertation submitted by Mr. Muhammad Akhtar is accepted in its present form by the Department of Chemistry, Quaid-i-Azam University, Islamabad Pakistan, as satisfying the partial requirement for the degree of Doctor of Philosophy in the field of Inorganic/Analytical Chemistry.

External Examiner (1) _____

External Examiner (2) _____

Supervisor: _____
Prof. Dr. Muhammad Mazhar
Department of Chemistry
Quaid-i-Azam University
Islamabad

Co-Supervisor: _____
Prof. Dr. Saeed Ahmad
Department of Chemistry
UET. Lahore

Head of Section: _____
Prof. Dr. Amin Badshah
Department of Chemistry
Quaid-i-Azam University
Islamabad

Chairman _____
Prof. Dr. Muhammad Siddiq
Department of Chemistry
Quaid-i-Azam University
Islamabad

Dedicated

to

My Family and Friends

CONTENTS

		Page
Acknowledgements		**i-ii**
Preface		**iii**
Abstract		**iv-vi**
Objectives of the Work		**vii**
List of Abbreviations		**viii-x**
List of Tables		**xi-xii**
List of Schemes		**xiii**
List of Figures		**xiv-xvii**
Chapter-1	**Introduction**	**1-30**
1.1	Coordination chemistry of zinc(II)	**2**
1.2	Zinc(II) complexes with nitrogen donor ligands	**4**
	1.2.1 Zinc(II) diamine complexes	**5**
1.3	Zinc(II) thiocyanate complexes	**9**
1.4	Zinc(II) cyanide complexes	**11**
1.5	Zinc(II) Schiff base complexes	**12**
1.6	Complexes with oxygen donor ligands	**15**
	1.6.1 Zinc(II)-acetylacetonate complexes	**15**
1.7	Complexes with sulfur donor Ligands	**17**
	1.7.1 Zinc(II) thiolate complexes	**20**
1.8	Biological importance of zinc	**27**
Chapter-2	**Binary Zinc(II) Complexes of Thiolates**	**31-82**
2.1	Introduction	**31**
2.2	Experimental	**33**
	2.2.1 Chemicals	**33**

	2.2.2	Synthesis of complexes	**33**
	2.2.3	IR, NMR and thermal measurements	**36**
	2.2.4	X-ray structure determination	**36**
	2.2.5	Computational details	**36**
	2.2.6	Antimicrobial activities	**37**
2.3		Results and discussion	**42**
	2.3.1	Spectroscopic characterization	**42**
	2.3.2	Description of X-ray Structures	**53**
	2.3.3	Comparative geometrical analysis of the ligands (CymH and Cym-Cym) and the corresponding Zn(II) Complexes	**60**
	2.3.4	Vibrational analysis of $[Zn_4Cym_4Cl_4]$ (1) and $[Zn(Cym\text{-}Cym)Cl_2]_n$ (2)	**64**
	2.3.5	Antimicrobial activities	**79**
		Conclusions	**81**
Chapter-3		**Zinc(II) Complexes of Diamines**	**83-134**
3.1		Introduction	**83**
3.2		Experimental	**84**
	3.2.1	Chemicals	**84**
	3.2.2	Synthesis of complexes (6-13)	**84**
	3.2.3	IR and NMR measurements	**86**
	3.2.4	Theoretical (DFT) calculations	**87**
	3.2.5	X-ray structure determination	**88**
3.3		Results and discussion	**94**
	3.3.1	IR studies	**94**
	3.3.2	NMR studies	**96**
	3.3.3	DFT calculations	**98**
	3.3.4	Description of X-ray structures	**117**

	Conclusions	**134**
Chapter-4	**Zinc(II) Complexes of Phenanthroline**	**135-147**
4.1	Introduction	**135**
4.2	Experimental	**136**
	4.2.1 Materials	**136**
	4.2.2 Synthesis of complexes	**136**
	4.2.3 X-Ray structure determination	**137**
4.3	Results and discussion	**139**
	4.3.1 Crystal structure description of (15)	**142**
	Conclusions	**147**
	References	**148-162**
	List of Publications	**163**

ACKNOWLEDGEMENTS

All praises to the Almighty Allah, the most gracious and the most benevolent, Who enabled me to accomplish my Ph.D research work. Peace and Blessings of Allah be upon His Last Holy Prophet (PBUH) who exhorted his followers to seek knowledge from cradle to grave and is the source of knowledge as well as guidance for the entire world forever.

I am extremely grateful to my learned and experienced worthy supervisor Prof. Dr. Muhammad Mazhar, Department of Chemistry, Quaid-i-Azam University, Islamabad and Co-supervisor Prof. Dr. Saeed Ahmad, Department of Chemistry, UET Lahore, for their inspiring guidance, pleasant attitude, valuable suggestions, invigorating encouragement, excellent cooperation and for providing all the necessary research facilities throughout the period of my research work. Without their generous help, the completion of this work would have not been possible for me.

I am highly indebted to Prof. Dr. Muhammad Siddique, Chairman, Department of Chemistry, Quaid-i-Azam University, Islamabad for providing an opportunity to complete my Ph.D degree. A special word of thanks is due to Prof. Dr. Amin Badshah, Department of Chemistry, Quaid-i-Azam University, Islamabad for his essential advice, sympathetic behavior and research support during my study period. I am highly obliged to Dr. S. A. Trimazi, Dr. Saqib Ali, Dr. Shahid Hamid, Dr. Ilyas Sarwar and Dr. Imtiaz-ud-Din for their valuable discussions and support during my stay at department. I am also thankful to all faculty members of Chemistry Department for their kind cooperation.

I am extremely thankful for the technical help provided by Dr. Tobias Rüffer, Inorganic Chemistry Division, Institute of Chemistry, Faculty of Natural Sciences, Technische Universitaet, Chemnitz, Germany and Dr. Muhammad Nawaz Tahir, Department of Physics, University of Sargodha for X-ray structure determination; and Dr. Ivelina Georgieva, Institute of General and Inorganic Chemistry, Bulgarian Academy of Sciences, Sofia, Bulgaria and Dr. Wiktor Zierkiewicz, Faculty of Chemistry, Wroclaw University of Technology, Wroclaw, Poland, for theoretical calculations.

I am also obliged to Prof. Anvarhusein A. Isab, Department of Chemistry, King Fahd University of Petroleum and Minerals, Dhahran, Saudi Arabia and Dr. Muhammad Saleem, Department of Civil Engineering, Jubail University College, Saudi Arabia for their guidance in analytical work and for antimicrobial studies respectively.

Last but not least, I would like to acknowledge Dr. Muhammad Monim-ul-Mehboob and Dr. Muhammad Rafiq for their cooperation and necessary guidance. My sincere thanks to my friends and class fellows, particularly Dr. Muhammad Khawar Rauf, Dr. Irshad Ali, Dr. Muhammad Sultan, Dr. Muhammad Rizwan (Late), Dr. Shahid Saeed, Dr. Liaqat Ali, Dr. Sajjad Shoukat, Dr. Azadar Hussain and Dr. Mahmood-ul-Hassan Khan for extending their cooperation. I would like to acknowledge Mr. Tayyab Razzaq for technical support in NMR measurements.

I wish to thank to administrative staff and other supporting staff of Chemistry Department, especially Mr. Shamas Pervaiz, Mr. Sharif Chohan, Mr. Mehmood Hussain, Mr. Muhammad Hanif Tahir and Mr. Amir Hussain for their support and cooperation. I am appreciative of the moral support, prayers and patience of my family.

MUHAMMAD AKHTAR

PREFACE

The thesis entitled, “Synthesis and Characterization of Zinc(II) complexes with Diamines and Thiolates” describes the synthesis and characterization of some new zinc(II) complexes of thiolates or diamines and their use as antimicrobial agents. The thesis is divided into four chapters.

Chapter 1 highlights the general coordination chemistry of zinc. The complexes of zinc discussed here include those with nitrogen donor ligands including diamines and cyanide, oxygen donor ligands including diacetylacetonate and alkoxide, sulfur donor ligands including thiocyanates and thiolates, and mixed ligands including thiolate-diamine and thiocyanate-diamine and Schiff base ligands. The biological importance of such complexes is also briefly highlighted.

The second chapter deals with the preparation and characterization of binary zinc(II)-thiolates. These complexes are characterized by spectroscopic techniques, thermal studies and single crystal X-ray analysis. The crystal structures of two new complexes are discoursed. The structural features of zinc(II) thiolates are discussed and compared with results of other studies. Moreover, the biological activity of zinc(II) thiolate complexes is evaluated against six microorganisms.

The third chapter deals with the coordination of diamine ligands towards zinc(II) in the presence of other ancillary ligands, including thiolates and thiocyanate. In this regard, the crystal structures of five new complexes are described.

The fourth chapter describes the synthesis of two zinc(II) complexes of 1,10-phenanthroline, [Zn(phen)(Mnt)Cl] and a cyanido-bridged Zn(II)-Ag(I) bimetallic coordination polymer, $\{[Zn(phen)_2(H_2O)\{Ag(CN)_2\}][Ag(CN)_2]\cdot MeOH\}_n$. Attempts to prepare the mixed ligand zinc(II) complexes of phenanthroline and thiolates led to the formation of $[Zn(Phen)Cl_2]$ except in case of 2-mercaptonicotinic acid. The biological activities of some zinc thiolates were also evaluated.

ABSTRACT

Recent studies on the biochemical role of zinc(II) complexes of thiolates and amino acids encouraged our attention in the spectral and structural chemistry of zinc. Thus, the better insight of the role of zinc demands further systematic structural studies on the model compounds. The present dissertation describes the synthesis, spectral and structural characterization of zinc(II) complexes containing thiolate, diamine and 1,10-phenanthroline ligands. The first series consists of five new zinc(II) thiolate complexes; $[Zn_4(Cym)_4Cl_4]$ (**1**) with space group *P*-21/n, $[Zn(Cym\text{-}Cym)Cl_2]_n$ (**2**) with space group *P21/c*, $[Zn(Cys)Cl]\cdot H_2O$ (**3**), $[Zn(Msa)_2]$ (**4**) and $[Zn(Mnt)_2(H_2O)]$ (**5**), where Cym-H = cysteamine, Cym-Cym = cystamine, Cys-H = cysteine, Msa-H = 2-mercaptosuccinic acid and Mnt-H = 2-mercaptonicotinic acid. The second series comprises eight zinc(II) diamine complexes; $[Zn(Dach)_2][ZnCl_4]$ (**6**) with space group Pna21, $[Zn(Dach)(NCS)_2]$ (**7**) with space group Pbca, $[Zn(Dap)(NCS)_2][Zn(Dap)(NCS)_2]_n$ (**8**) with space group Pbca, $[Zn(TMEDA)(NCS)_2]$ (**9**), $(TMEDA\text{-}H_2)^{2+}[ZnCl_4]^{2-}$ (**10**) with space group *P*-1, $[Zn(Mnt\text{-}Mnt)(en)].H_2O$ (**11**) with space group *P*-1, [Zn(Dap)(Mnt)Cl] (**12**) and $[Zn(en)(NCS)_2]$. (**13**), where Dach = *cis*-1,2-diaminocyclohexane, TMEDA = *N,N,N´,N´* -tetramethylethylenediamine, en = 1,2-diaminoethane, Dap = 1,3-diaminopropane, Mnt-H = 2-mercaptonicotinic acid. In the third series two new zinc(II) complexes of 1,10-phenanthroline (phen); [Zn(Phen)(Mnt)Cl] (**14**) and $\{[Zn(phen)_2(H_2O)\{Ag(CN)_2\}][Ag(CN)_2]\cdot MeOH\}n$ (**15**) with space group *P* -1 are presented. The complexes were characterized by CHNS analysis, FTIR and NMR (^1H, ^{13}C) spectroscopy. The FTIR and NMR spectroscopic data indicated the coordination of the ligands to the metal centre and were discussed in terms of the nature of bonding. The crystal structures of eight complexes; (**1**)**,** (**2**), (**6**), (**7**), (**8**), (**10**), (**11**) and (**15**) were determined by X-ray crystallography. The structure of $[Zn_4(Cym)_4Cl_4]$ (**1**) shows that the complex exists in the form of a tetranuclear molecule in which zinc atoms are bridged by S atoms of Cym forming an eight-membered ring. The complex consists of two crystallographically independent Zn(II) ions. Zn1 and symmetry related ion are coordinated by two sulfur atoms and two nitrogen atoms of Cym, while Zn2 and symmetry related ion exhibit a ZnS_2Cl_2 setup. In both coordination environments, zinc atom adopts a distorted tetrahedral geometry. The complex (**2**), $[Zn(Cym\text{-}Cym)Cl_2]_n$ exists in the form of a polymer consisting of $Zn(Cym\text{-}Cym)Cl_2$

monomeric units in which each zinc atom acquires a tetrahedral environment and it is coordinated by two chloride ions and two nitrogen atoms of bridging Cym-Cym ligands. The sulfur atoms of cystamine retained the disulfide linkage instead of coordinating to metal center. The structure of complex (**6**) is composed of $[Zn(Dach)_2]^{2+}$ cations and $[ZnCl_4]^{2-}$ anions. The Zn atoms in both ionic species adopt a distorted tetrahedral geometry. In $[Zn(Dach)(NCS)_2]$ (**7**), the Zn(II) atom is bonded to one 1,2-diaminocyclohexane molecule and to two terminal thiocyanate ions via the nitrogen atoms adopting a slightly distorted tetrahedral geometry. The crystal structure of complex $[Zn(Dap)(NCS)_2][Zn(Dap)(NCS)_2]_n$ (**8**) consists of two types of molecules, a discrete monomer and a polymeric one. The asymmetric unit of $(TMEDA\text{-}H_2)^{2+}[ZnCl_4]^{2-}$ (**10**) consists of one tetrachloridozincate(II) anion and two halves of tetramethylethylenediaminium cations. Each of the two diaminium ions is located on an inversion center and one of them is disordered over two sites in a 0.780 (17):0.220 (17) ratio. The cations and anions are connected *via* N---H...Cl hydrogen bonds into chains extending along the [011] direction. In the crystal structure of complex $[Zn(Mnt\text{-}Mnt)(en)]\cdot H_2O$ (**11**), the asymmetric unit consists of a zinc(II) ion bound to two Mnt ligands (in the form of a disulfide) and an ethylenediamine molecule, and a water of crystallization. The asymmetric units are joined together to form a one-dimensional polymeric chain. Each zinc atom is five coordinated with three carboxylic oxygen atoms of Mnt and two N atoms of bidentate en ligand. The crystal structure of a heterobimetallic coordination polymer $\{[Zn(phen)_2(H_2O)\{Ag(CN)_2\}]\ [Ag(CN)_2]\bullet MeOH\}n$ (**15**) consists of dinuclear $[Zn(Phen)_2(H_2O)\{Ag(CN)_2\}]^+$ cations, $[Ag(CN)_2]^-$ anions and a methanol molecule. The non-coordinated $[Ag(CN)_2]^-$ anions are linked to $[Zn(Phen)_2(H_2O)\{Ag(CN)_2\}]^+$ cations through Ag---Ag (argentophilic) interactions resulting into the formation of chains. H-bonds and π-π interactions further connect these chains to constitute a 3D network. The complexes (**1**), (**2**), (**6**), (**7**), (**8**), (**9**) and (**13**) were also investigated by DFT modeling and frequency calculations. The complexes (**1)** and (**2**) were investigated in the solid state by infrared spectroscopic measurements, DFT modeling and frequency calculations using periodic DFT methodology. The vibrational modes sensitive to the N and S ligand coordination to Zn(II) and to the coordination polyhedron were determined. The C-S stretching vibrations appeared in the most characteristic modes are able to distinguish different binding behaviour of the CS donor group in the two Zn(II) ions. The structures of $[Zn(Dach)_2][ZnCl_4]$ (**6**),

$[Zn(Dach)(NCS)_2]$ (**7**), $[Zn(Dap)(NCS)_2][Zn(Dap)(NCS)_2]_n$ (**8**) and $[Zn(TMEDA)(NCS)_2]$ (**9**) as well as of $[Zn(en)(NCS)_2]$ (**13**) were predicted using theoretical DFT method. The structure of $[Zn(Dach)(NCS)_2]$ (**7**) is also compared with its octamer, $[Zn(Dach)(NCS)_2]_8$. The interaction energy (ΔE) values for NCS^- anions obtained by B3LYP-D3 method are about –140 kcal mol^{-1}, while the calculated ΔE for neutral organic ligands are about twice smaller. The atomic charges and second-order interaction energies between orbitals were calculated with natural bond orbital (NBO) analysis. In compound (**8**), the weak chalcogen bonds play an additional role in its stabilization. Antimicrobial activities of zinc(II) thiolate complexes were assessed by minimum inhibitory concentration (MIC) in μg/mL against six microorganisms. The complexes exhibited significant activities against gram-negative bacteria such as, *Escherichia coli* and *Pseudomonas aeruginosa*, while moderate activities were detected against molds such as, *Aspergillus niger and Penicillium citrinum* and yeasts such as, *Candida albicans* and *Saccharomyces cerevisiae*.

OBJECTIVES OF THE WORK

Recent studies on the biochemical role of zinc(II) complexes of thiolates and amino acids stimulated our interest in the spectral and structural chemistry of zinc. Thus, understanding the interactions between zinc and its protein ligands (amino acid residues) is imperative for elucidating the structural role of Zn in proteins. The better understanding of the role of zinc requires further systematic structural studies on the model compounds. Therefore, in this study we planned to carry out some work on the synthesis, characterization and biological activities of zinc(II) complexes with thiolates and diamines as ligands.

The prime objective of the present research project is to utilize simple methodology to: prepare Zn(II) complexes with diamines, thiolates and thiocyanate ligands; characterize them by various physico-chemical techniques, such as melting point, elemental analysis, FTIR, NMR, TG/DTG and single crystal X-ray analysis for their stoichiometry and structure; and assess them for efficacy against various types of microorganisms for their application as drugs.

The main components of the present study are summarized as follows:

1) Synthesis of binary zinc(II) complexes of thiolates
2) Synthesis of zinc(II) complexes with diamines
3) Synthesis of mixed ligand zinc(II) complexes of thiolates and diamines
4) Characterization of the complexes by elemental analysis, IR and NMR methods
5) Determination of crystal structure of crystalline complexes by X-ray crystallography
6) Theoretical investigation of some of the complexes by DFT method
7) Evaluation of the antimicrobial activities of some of the complexes

LIST OF ABBRIVEATIONS

Abbreviation/Acronym/Symbol	Name of Compound/Term
Ada	Azodicarbonamide
ATCC	American Type Culture Collection
BIQ	bis(2-(benzimidazol-2-yl)quinolinato
BSSE	Basis Set Superposition Error
Cym	Cysteamine
Cym-Cym·2HCl	Cystamine dihydrochloride
Cys	Cysteine
Dach	1,2-Diaminocyclohexane
Dap	1,3-Diaminopropane
Dea	Diethanolamine
DFT	Density Functional Theory
DMF	N,N'-Dimethyl formamide
DMSO	Dimethyl sulphoxide
DNA	Deoxyribonuleic acid
DTA	Differental thermal analysis
en	Ethylenediamine
FTIR	Fourier transform infrared spectroscopy
GGA	Generalized Gradient Approximation
GP	Glucose and polypeptone
His	Histidine
LFSE	Ligand Field Stablization Energy
LP(N)	Lone pair (non-bonding)
Mnt-H	2-Mercaptonicotinic acid
Msa	2-Mercaptosuccinic acid

MT	Metallothioniene
MTCC	Microbial Type Culture Collection
NBO	Natural Bond Orbital
NMR	Nuclear magnetic resonance spectroscopy
OLED	Organic light emitting device
ORTEP	Oak Ridge Thermal Ellipsoid Plot
PAW	Projector-augmented-wave
PBE	Perdew, Burke and Ernzerhof
PDA	Pyridine-2,6-dicarbaldehyde
pH	Reciprocal of logarithm of H^+ ion concentration
phen	1,10-Phenanthroline
pia	Picolinamde
pm	Picometers
pn	1,2-Propylenediamine
PW	Plane-wave
Py	Pyridine
RNA	Ribonucleic acid
SCD	Soybean, Casein and Digest
SDTA	Structural Dynamic Test Article
SN_2	Bimolecular Nucleophilic Substitution
Tea	Triethanolamine
Ten	Triethylenediamine
terpy	Terpyridine
TG	Thermogram
TGA	Thermogravimetric analysis
THF	Tetrahydrofuran
TMEDA	*N*,*N*,*N´*,*N´*-tetramethylethylenediamine

TMS	Tetramethylsilane
UV	Ultraviolet
VASP	Vienna ab initio simulation package

LIST OF TABLES

Table	Title	Page
1.1	Coordination geometries of Zn (II)	**3**
2.1	Elemental analysis and melting points of zinc(II)-thiolate complexes	**35**
2.2	Crystal data and refinement details for compound (**1**)	**40**
2.3	Crystal data and refinement details for compound (**2**)	**41**
2.4	Selected IR absorptions (cm^{-1}) of thiolates and their zinc(II) complexes	**43**
2.5	Experimental ^{1}H NMR and ^{13}C NMR data of ligands; CymH, Cym-Cym and Zn(II) complexes; (**1)** and (**2**) recorded in DMSO-d_6 and calculated (at PBE1PBE/**B1** level) ^{13}C chemical shifts (δ_i) of the model compounds in DMSO	**47**
2.6	^{13}C chemical shifts (δ, ppm) of RSH ligands and their zinc(II) complexes	**48**
2.7	Selected bond distances (Å) and bond angles (˚) for (**1**)	**55**
2.8	Hydrogen bonds in complex (**1**) (Å, º)	**55**
2.9	Selected bond distances (Å) and bond angles (˚) for (**2**)	**59**
2.10	Hydrogen bonds in complex (**2**) (Å, º)	**59**
2.11	Selected experimental and calculated bond lengths (in Å) of polymeric $[Zn(Cym\text{-}Cym)Cl_2]_n$, cyclic $[Zn_4Cym_4Cl_4]$ and $[ZnCymCl]_4$ complexes, compared to the cystamine (Cym-Cym·2HCl) and cysteamine (Cym, zwitterionic tautomer) ligands parameters	**63**
2.12	Experimental IR and calculated harmonic frequencies (in cm^{-1}) of cyclic $[Zn_4Cym_4Cl_4]$ complex (Z = 4). Comparison with the experimental (Raman) frequencies of deprotonated cysteamine and CymH·HCl ligand in the solid state	**68-71**
2.13	Experimental IR and calculated harmonic frequencies (in cm^{-1}) of polymeric $[Zn(Cym\text{-}Cym)Cl_2]_n$ complex (Z = 4) compared to the experimental IR data of [Cym-Cym·2HCl] ligand	**72-75**
2.14	Antimicrobial Activities of zinc(II) complexes evaluated by minimum inhibitory concentration (MIC: $\mu g\ mL^{-1}$)	**80**
3.1	Elemental analysis and melting points of zinc(II) complexes of diamines	**89**
3.2	Crystal data and refinement details for compound (**6**)	**90**
3.3	Crystal data and refinement details for compounds (**7**) and (**8**)	**91**

3.4	Crystal data and refinement details for compound (**10**)	**92**
3.5	Crystal data and refinement details for compound (**11**)	**95**
3.6	Selected structural parameters of $\{[Zn(Dach)_2][ZnCl_4]\}_3$ $(\mathbf{6})_3$ complex	**102**
3.7	NBO charges [e] on selected atoms of the central $[Zn(Dach)_2][ZnCl_4]$ complex in $(\mathbf{6})_3$	**103**
3.8	Selected structural parameters (bond distances in Å, angles in degrees) of $[Zn(Dach)(NCS)_2]_8$ $(\mathbf{7_8})$, $[Zn(Dach)(NCS)_2]$ (**7**), $[Zn(TMEDA)(NCS)_2]$ (**9**) and $[Zn(en)(NCS)_2]$ (**13**) complexes	**107**
3.9	DFT calculated interaction energies (ΔE in kcal mol^{-1}) corrected for the BSSE between selected ligand and the rest of the complex in $[Zn(Dach)(NCS)_2]$ (**7**), $[Zn(TMEDA)(NCS)_2]$ (**9**) and $[Zn(en)(NCS)_2]$ (**13**) complexes	**108**
3.10	NBO charges [e] on selected atoms of the $[Zn(Dach)(NCS)_2]$ (**7**), $[Zn(TMEDA)(NCS)_2]$ (**9**) and $[Zn(en)(NCS)_2]$ (**13**) complexes	**109**
3.11	Selected bond distances (Å) and bond angles (°) for $[Zn(Dach)_2][ZnCl_4]$ (**6**)	**119**
3.12	Hydrogen bonds in complex $[Zn(Dach)_2][ZnCl_4]$ (**6**) (Å, º)	**120**
3.13	Selected bond distances (Å) and bond angles (˚) for (**7**)	**123**
3.14	Hydrogen bonds in the complex (**7**) (Å, º)	**123**
3.15	Selected bond distances (Å) and bond angles (˚) for (**8**)	**126**
3.16	Hydrogen bonds in complex (**8**) (Å, º)	**127**
3.17	Selected bond distances (Å) and bond angles (˚) for (**10**)	**129**
3.18	Hydrogen bonds in complex (**10**) (Å, º)	**129**
3.19	Selected bond distances (Å) and bond angles (˚) for (**11**)	**133**
3.20	Hydrogen bonds in complex (**11**) (Å, º)	**133**
4.1	Crystal data and refinement details for complex (**15**)	**138**
4.2	Selected bond lengths (Å) and bond angles (º) for compound (**15**)	**146**
4.3	Selected bond lengths (Å) and bond angles (º) in hydrogen bonds of (**15**)	**146**

LIST OF SCHEMES

Scheme	Title	Page
1.1	Structures of diamines and phenanthroline used in this study	**6**
1.2	Structures of some thiolate ligands used in this study	**22**

LIST OF FIGURES

Figure	Title	Page
1.1	Octahedral structure of $[Zn\{C_6H_9(NH_2)_3\}_2]^{2+}$	**4**
1.2	Structure of $[ZnCl_2(terpy)]$ complex	**5**
1.3	Structure of $[ZnCl_2\{CH_3–NH–CH_2–CH_2–N–(CH_3)_2\}]$	**7**
1.4	Structure of $[ZnBr_2(CH_3)_2N–CH_2–CH_2–N(CH_3)_2]$	**8**
1.5	Structure of Zn(II) complex with picolinamide (*pia*) representing two polymorphs of monomeric $[Zn(SCN)_2(pia)_2]$ units	**10**
1.6	Structure of *bis*(salicylaldiminato)zinc(II) complexes (R = H, Cl, NO_2, OCH_3)	**13**
1.7	Structure of trinuclear $[Zn_3(saldmen)_3(OH)](ClO_4)_2·0.25H_2O$	**14**
1.8	Structure of Zn-acetylacetonate dihydrate complex	**16**
1.9	Structural arrangement of Zn-acetylacetonate monohydrate complex	**16**
1.10	Structure of anhydrous $[Zn(acac)_2]$ complex	**17**
1.11	Structure of a typical $[Zn(dithiolene)_2]^{2-}$ complex	**17**
1.12	Structure of $[(Me_2NCS_2)_4Zn_2]$ complex	**18**
1.13	Centrosymmetric dimer of $[Zn_2(PDTC)_4]$	**19**
1.14	Molecular structure of $[Zn(Diaz)_2Cl_2]$	**20**
1.15	ORTEP diagram of a zinc(II) thiolate complex	**24**
1.16	Structure of *N*-(2-mercaptoisobutyl)(2-pyridin-2-yl-ethyl)methylamine-Zn-Cl	**25**
1.17	Molecular structure of *N*-(2-mercaptoisobutyl)(2-pyridin-2-yl-ethyl)methylamine-Zn–SC_6H_5	**26**
1.18	Structure of *E. Coli* Ada protein showing ZnS_4 environment	**28**
1.19	Active site of human carbonic anhydrase featuring a first coordination shell of three histidine residues and an activated water molecule	**29**
2.1	IR spectrum of Zn-Cysteine complex (**3**)	**44**
2.2	^1H NMR data of cystamine dihydrochloride and its $[Zn(Cym-Cym)Cl_2]_n$ (**2**) complex in DMSO	**49**
2.3	$^{13}C\{^1H\}$ NMR spectrum of complex (**1**) in DMSO	**50**

2.4	^{13}C NMR data of cystamine dihydrochloride and its $[Zn(Cym\text{-}Cym)Cl_2]_n$ complex (**2**) in DMSO	**51**
2.5	Thermogravimetric curve of complex $[Zn(Cys\text{-}H)Cl].0.5H_2O$ (**3**)	**52**
2.6	Molecular structure of compound (**1**), including the atomic numbering scheme(i = -x,-y,-z)	**54**
2.7	Crystal packing diagram of (**1**) showing hydrogen bonding interactions	**54**
2.8	The asymmetric unit of (**2**) with thermal ellipsoids drawn at 50 % probability level	**57**
2.9	A projection perpendicular to ***b*** axis showing the formation of one dimensional polymeric chains along the *a* axis in (**2**)	**57**
2.10	Crystal packing diagram of (**2**) showing H-bonding interactions	**58**
2.11	Optimized geometry structure of $[ZnCymCl]_4$ (**1A**) in gas phase at DFT/PBE1PBE/**B1** level	**62**
2.12	Experimental IR spectra of [Cym·HCl] ligand and cyclic $[Zn_4Cym_4Cl_4]$ (**1**) complex	**65**
2.13	Experimental IR spectra (2000-400 cm^{-1}) of [Cym-Cym·2HCl], cyclic $[Zn_4Cym_4Cl_4]$ (**1**) and polymeric $[Zn(Cym\text{-}Cym)Cl_2]_n$ (**2**) complexes	**66**
2.14	Experimental IR spectra (4000-2000 cm^{-1}) of [Cym-Cym·2HCl] ligand, cyclic $[Zn_4Cym_4Cl_4]$ (**1**) and polymeric $[Zn(Cym\text{-}Cym)Cl_2]_n$ (**2**) complexes	**67**
3.1	IR Spectrum of $[Zn(Dap)(NCS)_2][Zn(Dap)(NCS)_2]_n$ (**8**)	**95**
3.2	IR Spectrum of $[Zn(TMEDA)(NCS)_2]$ (**9**)	**95**
3.3	^1H NMR Spectrum of $[Zn(Dap)(NCS)_2][Zn(Dap)(NCS)_2]_n$ (**8**) in DMSO	**96**
3.4	$^{13}C\{^1H\}$ NMR Spectrum of $[Zn(Dap)(NCS)_2][Zn(Dap)(NCS)_2]_n$ (**8**) in DMSO	**97**
3.5	$^{13}C\{^1H\}$ NMR Spectrum of $[Zn(TMEDA)(NCS)_2]$ (**9**) in DMSO	**97**
3.6	Fully DFT optimized structure of the $[Zn(Dach)_2][ZnCl_4]$ (**6**) complex in the gas phase	**99**
3.7	Optimized structure of the central $[Zn(Dach)_2][ZnCl_4]$ (**6**) complex surrounded by two frozen units in the $\{[Zn(Dach)_2][ZnCl_4]\}_3$complex $(\mathbf{6})_3$	**99**
3.8	Optimized structures of the most (a) and the less (b) stable $[Zn(Dach)Cl_2]_2$ complexes	**101**

3.9	Fully optimized structure of the model [Zn(Dach)$(NCS)_2$] (**7**) complex surrounded by seven frozen complexes. Calculations performed at the B3LYP-D3 level	**104**
3.10	Fully optimized structure of the [Zn(Dach)$(NCS)_2$] (**7**) complex without additional frozen molecules	**105**
3.11	Optimized structure of the model [Zn(Dach)$(NCS)_2$] (**7**), [Zn(TMEDA)$(NCS)_2$] (**9**) and [Zn(en)$(NCS)_2$] (**13**) complexes with frozen positions of sulfur atoms	**105**
3.12	Optimized structures of the models of (**8**), [Zn(Dap)$(NCS)_2$][Zn(Dap)$(NCS)_2]_3$ and simple polymeric structure (**8b**), [Zn(Dap)$(NCS)_2]_4$	**110**
3.13	Molecular surface of electrostatic potential (ESP, kcal mol^{-1}) of neutral isolated HNCS molecule computed on the 0.001 a.u. contour of the electrostatic density at the B3LYP-D3/Def2TZVP level. Color ranges, in kcal mol^{-1}, are: red greater than 20, yellow between 20 and 10, green between 0 and 10, blue less than 0. Selected surface critical point, $V_{s,max}$ on the sulfur atom is indicated (its value is 2.78 kcal mol^{-1}). The σ-hole on the sulfur atom is demonstrated as a green circle	**112**
3.14	Fragment of the crystal structure of complex (**8**) with DFT optimized positions of hydrogen atoms. Selected distances are in Å. The dashed lines represent the S···π chalcogen and S···H hydrogen bonds	**114**
3.15	Plots of the non-covalent interactions (NCI) for [Zn(Dap)$(NCS)_2$]···[Zn(Dap)$(NCS)_2$] complex. The green parts of surfaces mean attractive interactions, while the red mean repulsive interactions	**116**
3.16	ORTEP diagram (50 % ellipsoid probability) of the molecular structure of (**6**) according to the orientation of the $[Zn(Dach)_2]^{2+}$ cation towards the $[ZnCl_4]^{2-}$ anion in the asymmetric unit. All carbon bonded hydrogen atoms are omitted for clarity. Dotted lines refer to interionic hydrogen bonds	**118**
3.17	Molecular Structure of (**7**) along with crystallographic numbering scheme of the molecular unit	**122**
3.18	The packing diagram of (**7**) showing H-bonds	**122**
3.19	Molecular structure of (**8**) along with crystallographic numbering scheme	**125**
3.20	The packing diagram of compound (**8**) showing H-bonds	**125**

3.21	Molecular structure of compound (**10**) showing the atomic numbering scheme	**128**
3.22	Packing diagram of compound (**10**) showing the hydrogen-bonding interactions	**128**
3.23	The asymmetric unit of (**11**) with thermal ellipsoids drawn at 50 % probability level	**131**
3.24	Formation of one-dimensional polymeric chains along the ***b*** axis in (**11**)	**131**
3.25	Crystal packing diagram of (**11**) showing hydrogen bonding interactions	**132**
4.1	A comparison of ^{13}C NMR of [Zn(Phen)Cl_2] (lower) and expected [Zn(Phen)(Cys)Cl] product (upper)	**140**
4.2	$^{13}C\{^{1}H\}$ NMR of [Zn(Phen)(Mnt)Cl] (**14**) showing the resonances of both ligands	**141**
4.3	Graphical representation of a selected part of the chains formed by (**15**) in the solid state due to argentophilic interactions and interactions with the MeOH molecules in chains. All *C*-bonded hydrogen atoms of the phen ligands are omitted for clarity	**143**
4.4a	Selected part of the 3D network of (**15**) in the solid state. Hydrogen bonds are indicated by dotted lines. π-π interactions in aromatic rings are filled with black and grey colours. MeOH molecules and *C*-bonded hydrogen atoms are omitted. Labels 'A' to 'I' refer to a first to the ninth symmetry-generated asymmetric unit of (**15**)	**144**
4.4b	Graphical illustration of the parallel-displaced sandwich type π-π interactions of phen ligands in (**15**) in the solid state, where *d* gives the distances of interacting phen ligands and ∢ the interplanar angles, respectively. The labelling refers to the code given in Figure 4.3a	**145**

Chapter – 1
INTRODUCTION

Zinc is the second most abundant element of the transition series found in human body after iron [1]. It is a constituent of more than 300 enzymes and plays essential roles in biological systems. The zinc ions in Zn-containing proteins are frequently coordinated by a combination of histidine and cysteine residues.This coordination mode is for example, found in the zinc-finger proteins.The common donor atoms of zinc in proteins are the nitrogen of histidine, oxygen(s) of glutamate/aspartate and sulfur of cysteine [1-12]. In addition to atoms that coordinate directly to the zinc ions, the side chains of amino acids have groups that can donate or accept hydrogen bonds from other groups. These secondary interactions can help to stabilize the zinc-binding sites, can contribute to protein folding and stability, and can participate in interactions with other macromolecules [12].Zinc(II) thiolate complexes are reported comprehensively in the scientific literature [13-24]. These studies establish that thiolates coordinate tozinc(II) through sulfur donor atom, leading to a tetrahedral geometry.

Zinc being an inexpensive and non-toxic metal also makes its use attractivein catalysis [25]. Several zinc(II)-diamine complexes are known to possess catalytic properties [25-28]. In view of this importance, zinc(II) complexes containing diamine (or ammine) ligands have been studied extensively [28-50].

Owing to the presence of thiolates and nitrogen donor groups in the coordination sphere of zinc(II) ions in metalloproteins, the zinc(II) complexes with N,S-donor ligands are of great importance from a bioinorganic point of view. The study of these complexes would thus help to understand the mechanism of biochemical reactions of the zinc-containing enzymes as well as in designing new metal-based therapeutic agents. The better understanding of the role of zinc requires further systematic structural investigation on the model compounds.Therefore, in the present study, we have prepared a number of zinc(II) complexes using various thiolate and diamine ligands. The complexes were characterized by elemental analysis, IR and NMR (^{1}H, ^{13}C)spectroscopy and X-ray crystallography. DFT (density functional theory) calculations were also performed to validate the

experimentally determined structures, to predict the geometrical structures and to carry out the solid state vibrational analysis for some of the prepared complexes.

1.1 Coordination chemistry of zinc(II)

Zinc(II)is a Lewis acid of borderline strength and generally forms stable complexes with nitrogen, oxygen, sulfur and carbon donor ligands. The coordination number of zinc in these complexes varies from two to six. Due to having d^{10} configuration, Zn^{2+} ions show no preference for a particular geometry. Two and three coordinate complexes are rare for zinc. Five coordination bipyramid shape is not common but there are complexes, which have trigonal bipyramid shape such as $[Zn(terpy)Cl_2]$ where terpy = 2,6-*bis*(2-pyridyl)pyridine. Zinc(II) occurs usually infourcoordinationas tetrahedral complexes. Zinc also forms several six coordinate octahedral complexes but they are less stable due to its smaller size. There are a few examples with coordination number of 7 and 8. An example of coordination number 8 is $[Zn(NO_3)_4]^{2-}$ [51,52].

As zinc(II) is a d^{10} system, there is no ligand field stabilization energy (LFSE) associated with it. Therefore, the compounds of zinc are usually colorless and diamagnetic. In view of the stability of the filled d^{10} shell, the elements of group 12 show few properties of the transition metals. Thus, zinc shows resemblance to the main group metal magnesium. It resembles the transition elements to form complexes with N,O and S donor ligands. The Zn^{2+} as well as Cd^{2+} and Hg^{2+} ions do not form π-complexes with CO, NO or olefins (alkenes) due to the stability of their d^{10} configuration and their inability to provide electrons for π-back bonding. The filled d^{10} shell also hinders π-acceptance and thus the complexes with cyclopentadienide ($C_5H_5^-$, abbreviated as Cp^-) ions are σ rather than π bonded [51-54]. The geometries of Zn(II) complexes are described in Table 1.1.

Table 1.1 Coordination geometries of Zn(II)complexes

S. No	Coordination Number	Geometry	Examples
1	2	Linear	$[Zn(CH_3)_2]$
2	3	Triangular Planar	$[ZnMe(NPh_3)]_2$
3	4	Tetrahedral	$[Zn(CN)_4]^{2-}$, $ZnCl_2$ (solid)
4	5	Trigonal bipyramid	$[Zn(SCN)\ tern]^+$, $[Zn(terpy)Cl_2]$
5		Square pyramid	$[Zn(acac)_2H_2O]$, $[Zn(S_2CN)_2]_2$
6	6	Octahedral	$[Zn(NH_3)_6]^{2+}$, $[Zn(en)_3]^{2+}$
7	7	Pentagonal bipyramid	$[Zn(H_2dapp)(H_2O)_2]$
8	8	Dodecahedral	$[(Ph_4As)_2Zn(NO_3)_4]$

1.2 Zinc(II) complexes with nitrogen donor ligands

The synthesis of nitrogen containing complexes is of great interest because a large number of natural products and pharmaceuticals contain amine or amide moieties [55,56]. Zinc(II) shows strong affinity towards nitrogen donor ligands. It forms numerous complexes with the am(m)ine ligands ranging from NH_3[29] through diamines such as ethylenediamine (en)[41-50] to a variety of macrocycles [57, 58]. Pyridines, imidazoles and pyrazoles are also good ligands in this context [59-62]. With 1-methylimidazole, a tetrahedral complex, $[Zn(C_4H_6N_2)_4]^{2+}$ is formed [62].The structure of the zinc(II) complex of *cis*-cyclohexanetriamineconsists of octahedral molecular units [63] as shown in Figure 1.1.

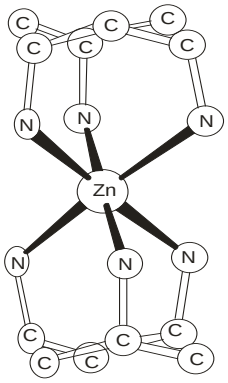

Figure 1.1 Octahedral structure of $[Zn\{C_6H_9(NH_2)_3\}_2]^{2+}$

A typical zinc(II) complex having a distorted trigonal bipyramidal shape is $[ZnCl_2(terpyridyl)]$ [52]. $[ZnCl_2(terpyridyl)]$contains the tridentate terpyridyl ligand havinganequatorial and two axial positions resulting intotrigonal bipyramidal shape as depicted in Figure 1.2.

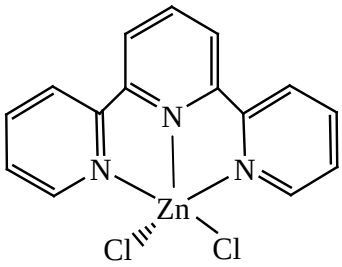

Figure 1.2 Structure of $[ZnCl_2(terpy)]$ complex

Polycyclic heterocyclic ligands like, 2,2-bipyridine and 1,10-phenthroline yield chelate complexes. The geometry of zinc varies between tetrahedral to octahedral [64-69]. With redox active metals, they are able to form complexes with wide range of oxidation states, as in the redox series given below [70].

$$[Cr(bipy)_3]^{3+}, [Cr(bipy)_3]^{2+}, [Cr(bipy)_3]^{+}, [Cr(bipy)_3]^{0}, [Cr(bipy)_3]^{-}$$

1.2.1 Zinc(II) diamine complexes

Organic compounds containing two amino (NH_2) groups in their skeleton are called diamines. The chemistry of amines is dominated by the lone pair of electrons on nitrogen atom.Amines are more basic than alcohols, ethers or water. These have higher boiling points than the corresponding alkanes. Another characteristic of amines is their odour. Low molecular weight amines like trimethylamine have a distinctive fish like aroma while diamines such as cadaverine (1,5-pentanediamine) have names that are self-explanatory [71].Zinc(II) complexes with certain diamines act as catalyst in the ring opening polymerization (ROP) [28]. Diamines usually bind as bidentate chelating ligands but the complexes with bridging diamines are also known [42]. The structures of diamine ligands used in this study are given in Scheme 1.1.

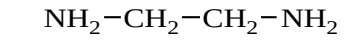

Ethylenediamine (en)

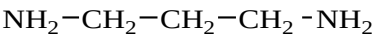

1,3-Diaminopropane (Dap)

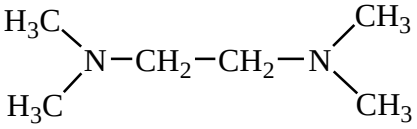

N,N,N′,N′ -
Tetramethylethylenediamine (TMEDA)

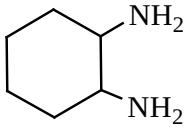

1,2-Diaminocyclohexane (Dach)

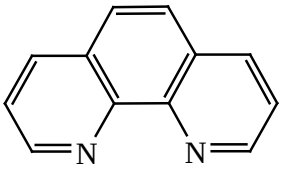

1,10-Phenanthroline(phen)

Scheme 1.1 Structures of diamines and phenanthroline used in this study

Some of the representative complexes of zinc(II)containing diamine ligandsare being discussed briefly in the following lines.

The complexes of the type, $[Zn(diamine)_2]^{2+}$and $[Zn(diamine)X_2]$ have mainly tetrahedral configuration [31-41] whereas the complexes like $[Zn(en)_3]^{2+}$ exhibit octahedral geometry [44-49]. For example, $[Zn(Dach)_2](ClO_4)_2$ (Dach = 1,2-diaminocyclohexane) involves a *bis* chelated tetrahedral environment [37], while in $[Zn(Dach)_2(H_2O)_2]Cl_2$ and some other complexes of Dach or its derivatives, zinc atom is also octahedrally coordinated [48-50]. There are relatively few five coordinate complexessuch as $[Zn(pn)_3Cl_2]\cdot 2H_2O$ (pn =1,2-diaminopropane)[42,43].The crystal structure of *cis-bis*(ethylenediamine)(nitrito-O,O´) zinc(II) nitrite comprises one chelating nitrite, another nitrite ion acts as a counter ion. The coordination polyhedron about the metal ion may be described as a distorted octahedron [47].

The compound $[ZnCl_2\{CH_3–NH–CH_2–CH_2–N–(CH_3)_2\}]$ crystallizes as tetrahedral monomer, as shown in Figure 1.3. The complex is chiral but forms racemic crystals. Intermolecular N—H---Cl hydrogen bonds; H---Cl = 2.56 Å forms infinite chains. Since $[ZnCl_2$(trimeda)] (trimeda = trimethylethylenediamine) is stereochemically labile and racemizes in solutions. Apart from the stereogenic center N atom, the complex also shows another element of chirality. The five membered trimeda–zinc chelating ring is conformationally chiral. Molecules having R-configuration at nitrogen have a delta (δ) conformation of five membered chelate ring and those having S-configuration have lambda (λ) confirmation [34].

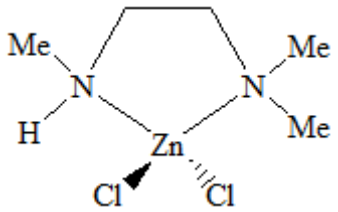

Figure 1.3 Structure of $[ZnCl_2\{CH_3–NH–CH_2–CH_2–N–(CH_3)_2\}]$

Johansson et al. (2004) crystallized the tetramethylethylenediamine (TMEDA) complex, $[ZnCl_2\}(CH_3)_2N\text{-}CH_2CH_2\text{-}N(CH_3)_2\}]$ as a tetrahedral monomer. The complex is chiral

but forms racemic crystals. Intermolecular N-H---Cl hydrogen bonds; H---Cl = 2.56 (4) Å form infinite chains [35]. The structure of the analogous bromide complex, $[ZnBr_2(CH_3)_2N–CH_2–CH_2–N–(CH_3)_2]$ is shown in Figure 1.4. The asymmetric unit contains two molecules on general positions. It is a worth-mentioning that weak interactions exist between Br atoms and their neighboring H atoms as evidenced by short Br---H bond distances [36].

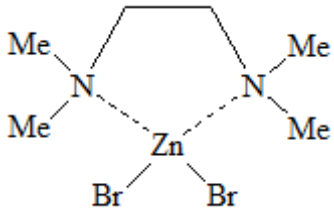

Figure 1.4 Structure of $[ZnBr_2(CH_3)_2N–CH_2–CH_2–N(CH_3)_2]$

Cusack and co-workers (2004) synthesized the zinc ethylxanthate (S_2COEt) complex of *N,N,N′,N′*-tetramethylethylenediamine (TMEDA), $[Zn(TMEDA)(S_2COEt)_2]$ and characterized it with FTIR and ^1H as well as ^{13}C NMR spectroscopy, and X-ray crystallography. The zinc complex contains four coordinate $\{ZnS_2N_2\}$ zinc with two monodentate xanthate groups [72]. In an analogous complex of 4-methylpiperidinecarbodithioate (4-mpipdtc), $[Zn(TMEDA)(4\text{-mpipdtc})_2]$ zinc possesses a distorted octahedral environment with a ZnS_4N_2 chromophore. The Zn–S distances are longer than those in parent $[Zn(4\text{-mpipdtc})_2]$. The acceptance of an additional neutral ligand by the $[Zn(4\text{-mpipdtc})_2]$ to form an octahedral adduct causes an increase in the Zn–S bond lengths and a lowering of the S–Zn–S bite angle. The piperidine ring in the dithiocarbamate fragment is in the normal chair conformation [73].

Luo et al. (2006) described the preparation of four zinc(II)complexes; $[ClZnN(CH_2CH_2NMe_2)_2]_2$, $[EtZnN(CH_2CH_2NMe_2)_2]_2$, $\{Zn[N(CH_2CH_2NMe_2)_2]_2\}_2$ and $[iBu_2NZnN(CH_2CH_2NMe_2)_2]_2$ using a tridentate amido-diamine ligand bearing a formula, $N(CH_2CH_2NMe_2)_2$. The NMR data proposed dimeric structures for all the four compounds. The crystal structures of $[EtZnN(CH_2CH_2NMe_2)_2]_2$ and $\{Zn[N(CH_2CH_2NMe_2)_2]_2\}_2$ were determined by X-ray crystallography[74]. In both structures, one NMe_2 group in each bridging ligand is bonded to a Zn center forming a

five-membered ring. Both compounds were centrosymmetric containing a four-membered Zn_2N_2 ring with bridging amido ligands.

1.3 Zinc(II) thiocyanate complexes

Thiocyanate (NCS^{-1}) ion is an ambidentate ligand, binding through N or S or as a bridging M–NCS–M. The canonical structures of the thiocyanato ligand are shown below:

$$S{=}C{=}N^{-1} \rightleftharpoons S^{-1}{-}C{\equiv}N$$

When acting as terminal ligand it can use its hard (N) or soft (S) donor atom depending on the hardness of the metal centre [53,75]. In thiocyanate ion negative charge is almost equally shared between sulfur and nitrogen atoms. As a result, thiocyanate can act as a nucleophile at either S or N atom. Experimental evidences concluded that hard acids (metals) can form N-bonded thiocyanate complexes, whereas, soft line metal ions can form S-bonded thiocyanate complexes [42]. In mercury(II) complexes, thiocyanate is normally bound from the *S* side [76,77], while in zinc(II)complexes [39-41], thiocyanate appears to coordinate exclusively through the *N* atom.

Petrusenko et al. (1997) reported the method of synthesizing zinc thiocyanate complexes with triethylenediamine (Ten). The main peculiarities of interaction of zinc oxide with non-aqueous (methanol, acetonitrile, N,N-dimethylformamide = DMF, dimethylsulfoxide = DMSO) solutions of ammonium thiocyanate in the presence of Ten were investigated. The crystal structures of the compounds $[Zn_2(NCS)_4(NH_3)_2(Ten)]$, $(HTen)_2[Zn(NCS)_4]$ and $[Zn(NCS)_2(Ten)(DMSO)]$ were determined by X-ray diffraction. The complexes contain four (in $[Zn_2(NCS)_4(NH_3)_2(Ten)]$) and five (in $[Zn(NCS)_2(Ten)DMSO]$) coordinate zinc atoms linked by μ_2-bridging nitrogen atoms of Ten forming the dimeric and polymeric molecules respectively.The complex $(HTen)_2[Zn(NCS)_4]$ has an ionic-type crystal lattice composed of $(HTen)^+$ cations and $[Zn(NCS)_4]^{2-}$ anions [78].

Cameron et al.(1998) described the crystal structures of neutral tetrahedral dithiocyanato zinc(II) complexes with methylated derivatives of ethylenediamine. It was found that the H(N) hydrogen atoms were exhaustively engaged in N–H(N)---S bonds. The majority of

these bonds are branched (bifurcated or trifurcated). The H bonding is discussed comprehensively, in terms of correlations between the N-H(N)-S angles and the H(N)---S lengths as well as between the analogous N-H(N)-S/H(N)---S pairs in the bifurcated N-H(N)---2S bonds [41].

Daković́a and his co-workers (2001) prepared three new heteroleptic thiocyanato complexes of zinc(II), cadmium(II) and mercury(II) containingchelating picolinamide (*pia*) ligand. The crystal structures of complexeswere determined by X-ray crystallography. The structure of Cd(II) compound presents a polymer $[Cd(SCN)_2(pia)]_n$ and compound of Hg(II) shows dimerof $[Hg(SCN)_2(pia)]_2$ units. The compound of Zn(II) produces two polymorphs of monomeric $[Zn(SCN)_2(pia)_2]$ units as shown below in Figure 1.5[79].

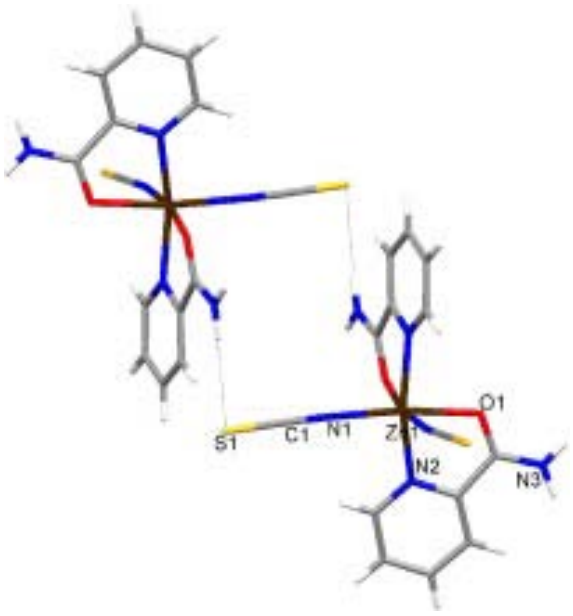

Figure 1.5 Structure of the of Zn(II)complex of picolinamide (*pia*) representing two polymorphs of monomeric $[Zn(SCN)_2(pia)_2]$ units

Sadhu and his colleagues (2015) synthesized a new tetradentate ligand,*N*,*N´-bis*(3,5-dimethyl-1H-pyrazol-1-yl)methyl-N_2-phenylethane-1,2-diamine (*bdpab*) and prepared itsCu(II) and Zn(II) mononuclear mixed ligand complexes, [M(*bdpab*)(NCS)]Y [M = Cu(II), Zn(II) and Y=PF_6^-, ClO_4^-] by treating metal nitrate/perchlorate, tetradentate N_4-coordinated ligand (*bdpab*), NCS^- and PF_6^- ions using appropriate mole ratio. Crystal structures of the compounds [Cu(*bdpab*)(NCS)]ClO_4 and [Zn(*bdpab*)(NCS)]PF_6were

measured by X-ray crystallography. Structural analysis revealedthat copper(II) and Zinc(II) complexes have five coordination with distorted square pyramidal for copper(II) or trigonal bipyramidal for zinc(II) geometry [80].

In the present study we have extended the investigations on zinc thiocyante complexes by carrying out the X-ray and DFT studies of a number of zinc(II) complexes of diamines and thiocyanate [81,82].

1.4 Zinc(II) cyanide complexes

An important field of Inorganic Chemistry is the study of compounds containing C≡N bonds. The complexation of cyanide ion with group 12 transition elements(Zn^{2+}, Cd^{2+} and Hg^{2+}) can occur in aqueous solution. The CN^- ion is unidentate and a strong nucleophile. It occupies higher position in the spectrochemical series. It usually exhibits sharp, intense bands between2200-2000 cm^{-1} in IR region and always binds through carbon but since the N atom of cyanide ion has a lone pair of electrons, so it can act as a bridge giving M–C–N–M links. Such bridges are found in many crystalline cyanides such as AuCN, $Zn(CN)_2$ and $Cd(CN)_2$. These are polymeric with chain structures [53]. Cyanide ion is the conjugate base of the weak acid hydrocyanic acid. Thus the solution of sodium cyanide is not only toxic but also very basic due to the presence of the OH^- base [83].

$$CN^- + H_2O \quad \rightarrow \quad HCN + OH^-$$

The cyanide ion may coordinate either through C atom as a monodentate ligand or through the C and N atoms as a bridging ligand producing 1, 2 or 3 D polymers. Zn^{2+} ions in the cyanide complexes generally contain a four coordination number [46]. The cyanide ion has a marked tendency to form linear bridges such as, Zn–C≡N–Zn. In general bridging CN^{-1} ions tend to be distorted so that C and N are not distinguishable. This makes possible, the formation of a great variety of unusual frame work structures. In fact, isomorphous $Zn(CN)_2$ itself has a very unusual structure consisting of two inter-penetrating diamond like networks. Due to the length of the Zn–C≡N–Zn units (5.11 Åfor

Zn) each network has distinct cavities, each of which is occupied by an atom of metal and its connected cyano groups of the other one [53].

Zinc cyanide can be prepared by adding HCN to zinc acetate dissolved in glacial acetic acid. Industrially zinc cyanide is used in the electrorefining and electroplating of zinc [84]. The reaction is shown as follows.

$$2HCN + Zn(CH_3COO)_2 \rightarrow Zn(CN)_2 + 2CH_3COOH$$

Zinc(II) is used to complex cyanide for the isolation of precious metals in the cyanadation [85]. Therefore, the complexation of zinc(II) with cyanide is very important from metallurgical point of view. In spite of this importance, there are only very few reports on the crystal structures of zinc cyanide-dia(i)mine systems [46,86-88].

1.5 Zinc(II) Schiff base complexes

Schiff bases provide a very important class of ligands which form a variety of coordination complexes with transition metals. They are the compounds, which contain the azomethine group (–CH=N–) and are represented by the general formula, $RR_1C=NR_2$ in which RR_1C is an aklylidene group representing an aldehyde or ketone and = N–R_2 is an imine residue of a primary amine. Schiff bases obtained from aromatic amines for example aniline are more stable than those obtained from aliphatic amines because CH=N– bond is conjugated with the aryl group. They can be prepared by mixing aldehyde with either aliphatic or aromatic and primary amine in equimolar quantities under reflux [53,89-91]. The reaction proceeds according to the following scheme.

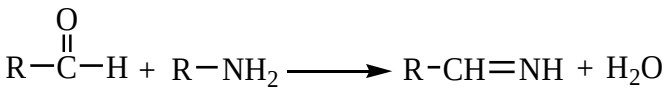

Schiff bases have been employed as chelating ligands in coordination chemistry to get thermotropic liquid crystalline polymers [92]. Many Schiff base complexes of metal ions show high catalytic activity [91,93]. These ligands usually contain both N and O donor

atoms, although purely N as well as N,S donors also exist. Schiff bases are generally mono, bi, tri or tetradentate ligands capable of forming very stable chelates with most of the transition metals. [94]. One of the best known Schiff base ligand is *bis*(salicylaldehyde)ethylenediamine which acts as an acidic tetradentate ligand [53,95]. Its preparation is represented by the following reaction scheme.

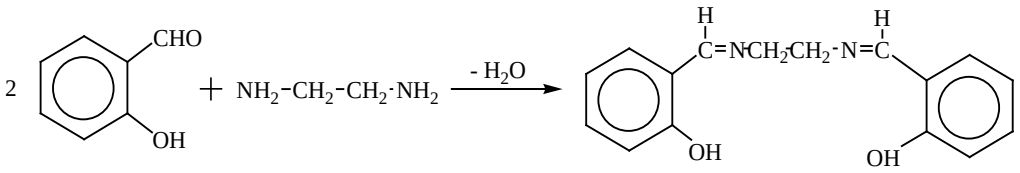

Zinc(II) assumes the coordination number 4,5 or 6 [53,96-100]. Seven is an unusual coordination number for most elements and is rare for zinc [100]. In *bis*(salicylaldiminato)zinc(II) complexes (R = H, Cl, NO_2 OCH_3),zinc(II) exhibits thecoordination number of 4 [96] as shown in Figure 1.6.

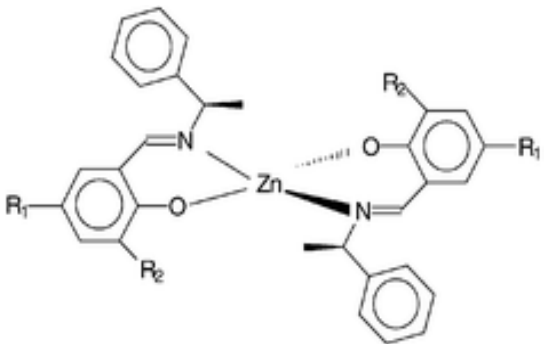

Figure 1.6 Structure of *bis*(salicylaldiminato)zinc(II) complexes (R = H, Cl, NO_2, OCH_3)

The Schiff base ligands, (*R* or *S*)-N-1-(Ar)ethyl-2-oxo-1-naphthaldiminate (*R*- or *S*-N,O), diastereo-selectively provide zinc(II)complexes having two chelate ligands coordinated to zinc(II) in a tetrahedral mode [97].The Schiff base complex of *N*-[2-(*N*,*N*-dimethyl-amino)-ethyl]-salicylimine (Hsaldmen), $[Zn_3(saldmen)_3(OH)](ClO_4)_2 \cdot 0.25H_2O$ is a trinuclear complex (Figure 1.7) in whichzinc(II) ions are penta-coordinated by two nitrogen atoms arising from the organic ligand, two phenoxo bridges and the μ_3-OH group [98].

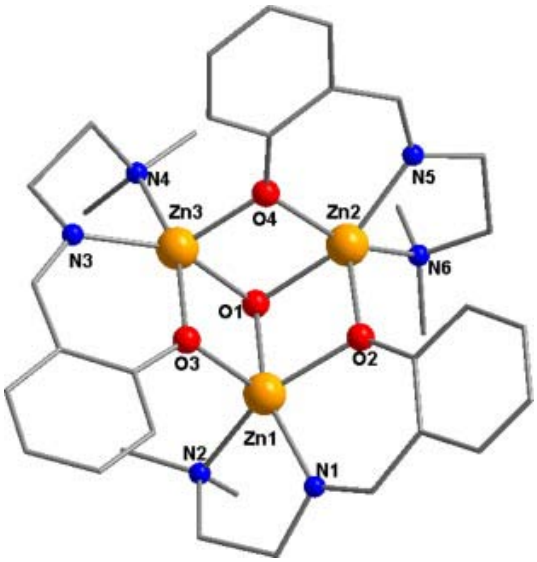

Figure 1.7 Structure of trinuclear $[Zn_3(saldmen)_3(OH)](ClO_4)_2 \cdot 0.25H_2O$

Reaction of $Zn(ClO_4)_2 \cdot 6H_2O$ with pentadentate 1,3-*bis*(salicylidenamino)propan-2-ol (H_2hsalpn) and the tridentate 4-methyl-2,6-*bis*(morpholinomethyl)phenol (Hbmmp) yielded the trinuclear zinc complex $[Zn_3(O_2CPh)_2(hsalpn)_2] \cdot 2MeOH$ (**A1**) and the hexanuclear zinc compound $[Zn_6(OH)_6(bmmp)_3][ClO_4]_3$(**A2**), respectively. The structures of both complexes were determined by single-crystal X-ray diffraction analysis. Complex **A1** consists of one central zinc ion which is octahedrally co-ordinated and two terminal metals surrounded by five donor atoms in the form of a square pyramid. The zinc ions are connected to the central metal atom *via* two phenolate oxygens of the dinucleating ligand and the oxygens of the benzoate ion. The six equivalent tetrahedrally co-ordinated zinc ions in **A2** are arranged in the form of a regular trigonal prism. Three dinuclear subunits are connected to each other by hydroxide groups [99].

Two NNS tridentate Schiff base ligands of 2-benzoylpyridine S-methyldithiocarbazate (HL1) and 2-benzoylpyridine S-phenyldithiocarbazate (HL2) and their zinc(II) complexes have been prepared and characterized by elemental analysis, IR, MS, NMR and single-crystal X-ray diffraction studies. $[Zn_2(L1)_2(ClO_4)_2]$ is a dimer in which each zinc atom

adopts a seven-coordinate distorted pentagonal bipyramidal geometry, while mononuclear $[Zn(L_2)_2]$ has octahedral coordination geometry [100].

1.6 Complexes with oxygen donor ligands

The common oxygen donor ligands capable of forming Zn(II) complexes include, H_2O, R-OH, acetyl group, carbamates, carboxylates and acetylacetonate [101-119]. In most of these compounds, zinc adopts a distorted tetrahedral geometry such as $[Zn(OPPh_3)_4](BF_4)_2$ [104]. However, in some cases it exhibits a distorted trigonal bipyramidal or octahedral coordination sphere. Chelating ethers also form stable complexes with zinc [115] but chelating β-diketones are much more effective [53,116-119].

Alkoxide (RO^-) and other similar oxygen donor ligands like aryloxides are hard σ donors which can also act as π donor due to their filled oxygen πp orbitals. These can stabilize metal atoms in higher oxidation states. As ancillary ligands, the alkoxide (RO^-) σ/ π donation depends upon the nature of R. The M-O-R groups are mostly bent [120,121]. Although the O-donor ligand chemistry of Zn with carboxylates is extensive [105-114], yet less work has been done with homoleptic aryloxides or alkoxides [102]. They are usually stabilized by the presence of alkali metal ions.

Zinc(II) complexes with carboxylates have been widely reported due to versatility of their structures and binding of carboxylate function of amino acid side chains to zinc in the enzyme [4-6,105-114]. In the compounds, the zinc atoms display a variety of geometries, such as tetrahedral, trigonal bipyramidal and octahedral, with the tetrahedral coordination most commonly found [4-6,106,107]. The carboxylate groups in these complexes exhibit monodentate terminal, monodentate bridging, bidentate bridging and bidentate chelating coordination modes [105-107].

1.6.1 Zinc(II)-acetylacetonate complexes

Three complexes have been isolated in the zinc-acetylacetonate system and their structures have been determined by X-ray crystallography [116-119]. The compound,

$[Zn(acac)_2(H_2O)_2]$ crystallizes in the monomeric form with the Zn atom on a centre of inversion. Zinc(II) adopts an octahedral geometry [116] as shown in Figure 1.8.

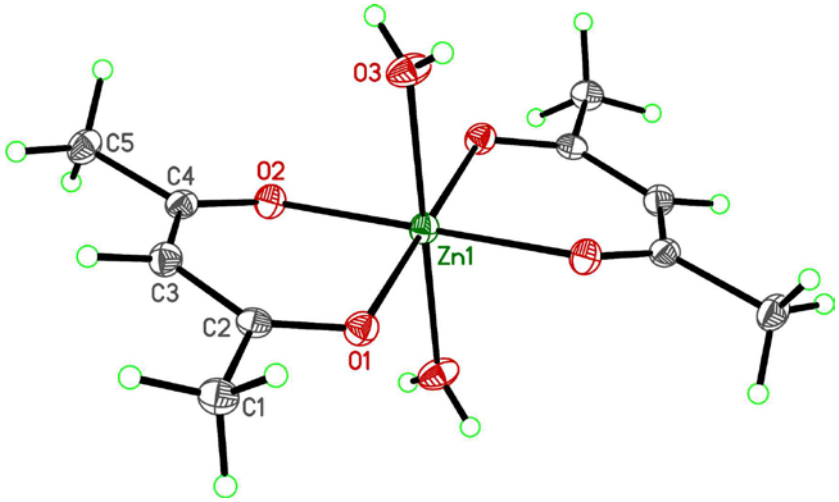

Figure 1.8 Structure of Zn-acetylacetonate dihydrate complex

The zinc acetylacetonate monohydrate, $[Zn(acac)_2(H_2O)]$ is five-coordinate and could have square pyramidal or trigonal bipyramidal geometry. X-ray analysis has shown the structure to be square pyramidal with some distortion toward a trigonal bipyramidal structure. The water molecule occupies the axial position. In the diaqua complex Zn adopts an octahedral geometry. The bond from Zn to the water molecule is significantly longer than the bonds to the acetylacetonate O atoms [117]. The structural formula is given below in Figure 1.9.

Figure 1.9 Structural arrangement of Zn-acetylacetonate monohydrate complex

The anhydrous acetylacetone complex of Zn(II), [Zn(acac)$_2$] is a trimer containing both 5- and 6-coordinate zinc. The X-rays structureshows that it contains one-six and two-five trigonal bipramidal zinc atoms in each molecule [118, 119] as shown in Figure 1.10.

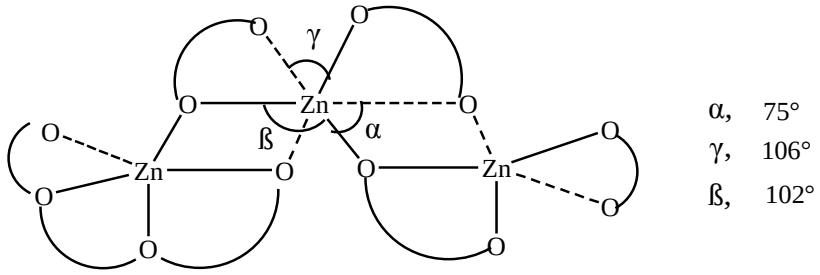

Figure 1.10 Structure of anhydrous [Zn(acac)$_2$] complex

1.7 Complexes with sulfur donor ligands

The main types of sulfur donor ligands for zinc(II) are dithiolenes [122-125], dithiocarbamates (R_2CNS_2) [126-135],thiones (>C=S) [136-150] and thiolates (RS^- and ArS^-) [88].

The 1,2-dithiolenes are a class of ligands, which have extended π systems, due to which delocalization of electrons onto the ligands occurs. It is the special characteristic of dithiolene type ligands. They form a wide variety of compounds with metals including zinc. For complexes containing only dithiolene ligands, four types of structures have been observed, which are square coordination (D_2h), five coordinate dimer (C*i*), trigonal prismatic (D_3h) and octahedral coordination (D_3) [53, 122-125]. A typical dithiolene complex in which zinc is surrounded tetrahedrally by S atoms is shown in Figure 1.11.

Figure 1.11 Structure of a typical [Zn(dithiolene)$_2$]$^{2-}$ complex

Zinc(II) complexes of dithiocarbamates are well known and have important industrial applications as antioxidants, antiabrasives in motor oils and vulcanization, accelerators in rubber as fungicides and for solvent extraction [53, 126-130]. Dithiocarbamate complexes are usually prepared from sodium salts like, NaS_2CNMe_2. They can also be made by insertion reactions of CS_2 with dialkylamides [53]. For example,

$$Ti(NR_2)_4 + 4CS_2 \rightarrow Ti(S_2CNR_2)_4$$

Several dialkyl thiocarbamate ($R_2NCS_2^-$) complexes have been examined structurally. When R = Me, a dimer is obtained with distorted four coordination about zinc [131]. The shape of dimethyl thiocarbamate (Me_2NCS_2-) complex with zinc metal is indicated in Figure 1.12. The Zn---Zn distance (3.97 Å) is sufficiently long to preclude metal-metal bonding. When R = Et, a different kind of dimerization leads to five coordinate zinc based on trigonal bipyramid geometry [132].

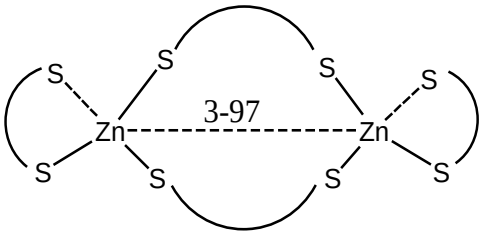

Figure 1.12 Structure of $[(Me_2NCS_2)_4Zn_2]$complex

Zinc(II) complex of pyrrolidinedithiocarbamate (PDTC) crystallizes in the form of a centrosymmetric dimer, $[Zn_2(PDTC)_4]$. The solid-state structure contains two crystallographically equivalent Zn^{+2} centers in a tetrahedrally distorted ion sphere as indicated in Figure 1.13. The dimeric structure is centrosymmetric and features an 8-membered, $[\text{-S-C-S-Zn-}]_2$ ring with a Zn-Zn separation of 3.73 Å [133]. The structure of butyl derivative is identical to $[Zn_2(PDTC)_4]$ [134]. The adducts of Zn-dithiocarbamates with amines are also known, *e.g.*, in the adduct $[Zn(S_2CNMe_2)_2(\text{pyridine})]$, zinc is five coordinated by one N and four S atoms [135].

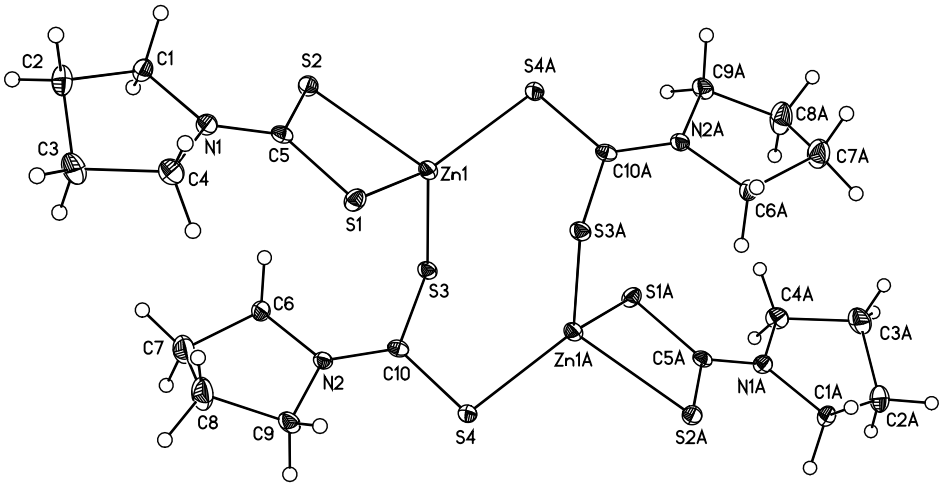

Figure 1.13 Centrosymmetricdimer of $[Zn_2(PDTC)_4]$

Zinc(II) complexes with simple N,S-ligands such as thiones (possessing a combination of soft sulfur and hard nitrogen donor atoms) provide suitable models for its coordination environment in the enzymes [1-6]. Several structural reports of zinc(II) complexes with thiones are available in the literature, which demonstrate that thiones coordinate with zinc(II) through sulfur atom in a tetrahedral environment [136-150]. In some cases, these units further aggregate to form the polymeric structures, for example, $[Zn(EBPT)_2Br_2]_n$where EBPT = *N*,*N*′-ethylene*bis*(pyrrolidine-2-thione [143].

The X-rays studies of thiourea complexes, $[Zn(thiourea)_2Cl_2]$ and $[Zn(thiourea)_2(acetate)_2]$ are known to have simple monomeric structures with a slightly distorted tetrahedral coordination about zinc and thiourea molecules are planar [136,137]. In the molecular structure of imidazolidine-2-thione (Imt) complex, $[Zn(Imt)_2(CH_3COO)_2]$ Zn(II) is bonded to two oxygen of acetate ions and two S atoms from Imt ligand coordinating *via* thione sulfur only [138].Similar structures have been found for the other thiourea derivatives, e.g. dimethylthiourea [139] and diethylthiourea [140].

Malik et al. (2011) reported the crystal structures of $[Zn(Tmtu)_2Cl_2]$ and $[Zn(Diaz)_2Cl_2]$ (Tmtu = tetramethylthiourea and Diaz = 1,3-diazinane-2-thione) [141]. Both complexesshow a tetrahedral coordination environment around the zinc atoms with the

bond angles ranging from 99.33(5)^{o} to 116.81(7)^{o}. The X-ray structure of [Zn(Diaz)$_2$Cl$_2$] is shown in Figure 1.14.

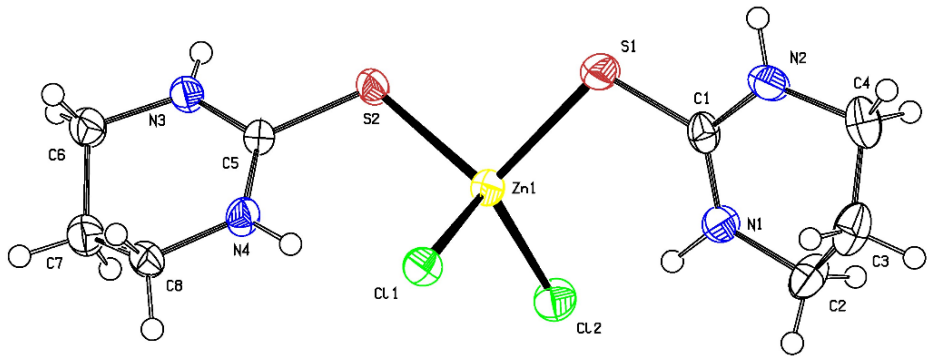

Figure 1.14 Molecular structure of [Zn(Diaz)$_2$Cl$_2$]

1.7.1 Zinc(II)thiolate complexes

Thiols are compounds that contain asulfhydryl group composed of anS bonded to aH atom. They are also called mercaptans. The term morcaptan is derived from the Latin "mercurium captans" meaning capturing mercury because the thiolate group forms strong bonds with mercury. So, thiols react with mercury to form mercaptides. Thiols are equivalent of alcohols in which S replacesO in the OH group of alcohol. They are better reducing agents than alcohols. Hence, thiolates are better electron donors as compared to alkoxides [151-154]. Thiols are more acidic than the corresponding alcohols, although oxygen is more electronegative than sulfur [155]. The higher acidity of thiols is due to the following reasons.

(i) The thiolate ions (R–S$^-$) possess a negative charge on sulfur which allows the charge to be delocalised over a larger region than that of alkoxide ion.

(ii) Large size of sulfur atoms in thiols

(iii) Sulfur is more polarizable than oxygen.

(iv) S–H bonds are weaker than O–H bonds. Hence S–H bond breaking is much easier.

Thiolates play a vital role in biological systems. These are used to prepare complexes of enzymatic models of different enzymes working in the living systems. The thiol group is a functional group of amino acid e.g. cysteine. When the thiol group of two cysteine residues approaches each other during protein folding, an oxidation reaction can produce a cystine unit with a disulphide bond (–S–S–). Hair straightening technologies are best example of cysteine-cystine equilibrium [156].

In the biological environment, the major part of thiols is carried by the tripeptide glutathione (GSH) whose cellular concentration is of the order of 1 mM. The high GSH concentration will generally protect the functional thiolates in cysteine zinc complexes against oxidizing agents. Glutathione which is a tripeptide containing thiol group acts as a mild reducing agent, detoxify peroxide and maintain the cysteine residue of hemoglobin in the reduced state. Glutathione can also detoxify alkylating agents. For example, the thiol of glutathione reacts with methyl iodide by SN_2 reaction, rendering the methyl iodide harmless and preventing its reaction with other molecules in the body [155].

Thiolates which are the conjugate bases resulting from thiols form stable complexes with several metal ions particularly qualified as soft [156]. Thiolates interact with metals to form coordinate bond in metal complexes. The ability of thiols to coordinate with heavy metals is useful in making antidotes to heavy metals poisoning. Scientists developed dimercaprol (2,3-dimercaptopropanol)as an effective antidote. Dimercaprol is useful against a variety of heavy metals including arsenic, mercury and gold [157].

Thiolates are very important in biological systems because they provide models for many enzymes and related natural sulfur compounds. Binding modes of thiolates, may be unidentate, bidentate and tridentate depending upon the nature of thiolate compounds [151].

Structures of some thiolate ligands and their resonance assignments used in this study are given in Scheme 1.2.

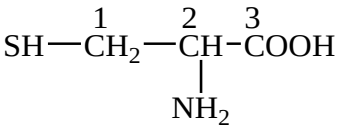

Cysteine (Cys)

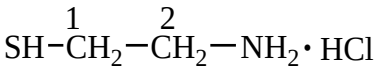

Aminoethanethiol hydrochloride (Cym)

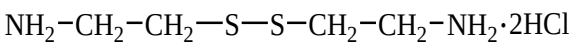

Cystamine dihydrochloride (Cym-Cym)

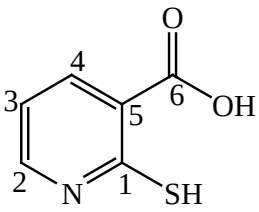

Mercaptonicotinic acid (Mnt)

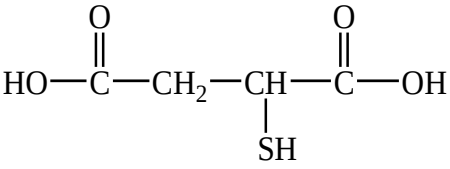

Mercaptosuccinic acid (Msa)

Scheme 1.2 Structures of some thiolate ligandsused in this study

Some of the representative complexes of zinc(II)containing thiolate ligands reportedin the literature are being discussed briefly as follows:

Casals et al. (1990) prepared the zinc(II) complex of 2-(dimethylamino)ethanethiol (Me_2AET) by electrochemical oxidation of zinc and simultaneous reduction of Me_2AET disulfide and determined its structure by single crystal X-ray diffraction. The structure consists of two crystallographically independent neutral monomeric units, which are optical isomers. Each zinc atom is bonded to two nitrogen atoms and two sulfur atoms adopting a distorted tetrahedral geometry [16].

Müller et al.(1999) reported that*bis*(pentafluorothiophenolato)zinc(II) and *bis*(2,4,6-triisopropylthiophenolato)zinc(II) could be combined with N-containing derivatives of benzyl alcohol and benzaldehyde to form (N,O-chelate) zinc thiolates. 2-Pyridylmethanol as well as 2-quinolylmethanol (HetMeOH) yieldedcorresponding complexes $[(HetMeO)Zn(SR)]_4$ having a cyclo-$Zn_4(\mu\text{-}O)_4$ backbone and only terminal SR. The zinc(II) ion lies in a tetrahedral $ZnNS_2O$, environment. Likewise, thiolate 1- and 2-(dimethylamino)benzyl alcohol form zwitterionic$[(dimethylammoniobenzylato)Zn(SR)_2]_2$ with bridging alkoxide and terminal thiolate [158].

Brand et al. (2001) prepared a series of pyrazolylborate-zinc-thiolate complexes $Tp^{Ph,Me}$Zn-SR and $Tp^{Me,Me}$Zn-SR, including two homocysteine derivatives, and structurally characterized them. Their reactions with methyl iodide in nonpolar media resulted in the formation of the thioethers MeSR, including two methionine derivatives, and $Tp^{R',\ Me}$Zn-I in all cases. The accumulated evidence indicates that the methylation occurs *intra*-molecularly, *i.e.*, at the zinc-bound thiolates [159].

Chiou et al. (2003) synthesized a series of mononuclear zinc(II) thiolate compounds of the type as shown in Figure 1.15. The reaction of the complexes with alkyl halides have been examined by kinetic methods. They observed that the reactions obeyed a second order rate law andactivation parameters were consistent with SN_2 attack of the zinc bound thiolate on electrophillic carbon in toluene solvent. They also reported quantitative assessment of the role of hydrogen bonding in changing the reactivity of a metal thiolate. Particularly, the nucleophlic character of the zinc thiolate, under study stabilized by an intra-molecular amide N--H--S is diminished relative to the other zinc thiolate[160].

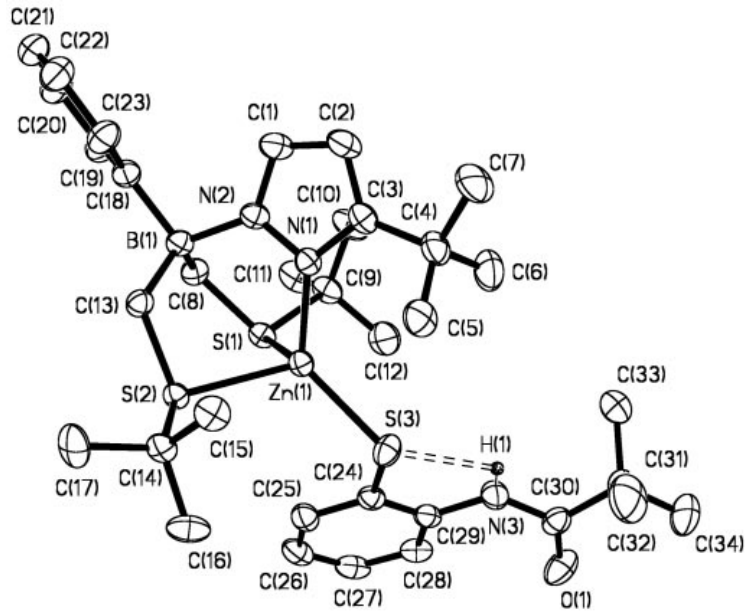

Figure 1.15 ORTEP diagram of a zinc(II) thiolate complex

Ibrahim et al. (2005) synthesized tris(thioimidazolyl)borate-zinc-thiolate complexes (Tti^{R}Zn-SR) to mimic the S_3ZnSR coordination of thiolate-alkylating enzymes such as the Ada DNA repair protein. One dozen new zinc(II) complexes were synthesized using four different borate (Tti^{R}) and nine diverse thiolate ligands[161].

Ji et al. (2005) alsosynthesized the zinc-thiolate complexes using the tripod ligands, *bis*(pyrazolyl)(3-*tert*-butyl-2-thioimidazol-1-yl)hydroborate and *bis*(pyrazolyl)(3-isopropyl-2-thioimidazol-1-yl)hydroborate. The ligands comprise aliphatic as well as aromatic thiolates and a cysteine derivative. Structure determinations have confirmed the tetrahedral ZnN_2S_2 coordination in the complexes. Upon reaction with methyl iodide, the species *bis*(pyrazolyl)(3-alkyl-2-thioimidazol-1-yl)hydroborate-Zn-SR are slowly converted to *bis*(pyrazolyl)(3-alkyl-2-thioimidazol-1-yl)hydroborate-Zn-I and the free thioethers, CH_3SR. A kinetic analysis has shown these alkylations to be about 1 order of magnitude slower than those of the tris(pyrazolyl)borate complexes $Tp^{Ph,Me}$Zn-SR described above [18].

Ji and Vahrenkamp (2005) prepared zinc thiolate complexes of three tridentate (N,N,S) ligands as models for the structure and function of thiolate alkylating zinc enzymes. The

first ligand,*N*-(2-Mercaptoisobutyl)(2-pyridin-2-yl-methyl)amine (**L_1**) forms isobutylthiolate-bridged dinuclear complexes with ZnN_2S_3 coordination. The second ligand,*N*-(2-Mercaptoisobutyl)(2-pyridin-2-yl-ethyl)amine (**L_2**) yields isobutylthiolate-bridged dinuclear complexes in which the pyridine donor is not coordinated to zinc, resulting in a $ZnNS_3$ coordination. Only the third ligand, *N*-(2-mercaptoisobutyl)(2-pyridin-2-yl-ethyl)methylamine (**L_3**) forms the desired mononuclear complexes with ZnN_2SCl coordination as shown in Figure 1.16 [17].

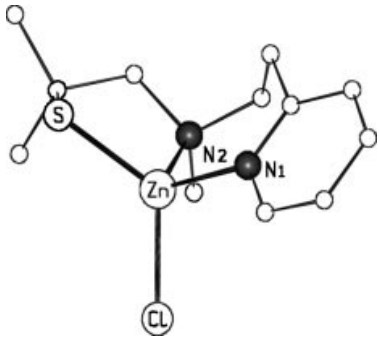

Figure 1.16 Structure of *N*-(2-mercaptoisobutyl)(2-pyridin-2-yl-ethyl)methylamine-Zn-Cl.

Fleischer and co-workers (2005) synthesized homoleptic complexes of cysteamine ligand (L), ML_2 in which the M-S bonds (M = Zn, Cd, Hg) were highly ionic in nature and S-M-S unit was called a three center four electron bond. It was observed that in addition to the size of M(II) ions, S-M-S angles in mononuclear ML_2 complexes and the energy required for their distortion are the main factors upon which coordination modes depend. A small S-Zn-S angle could make a substitution of Zn(II) by Cd(II) or Hg(II) from a $Zn(N_2S_2)$ environment unfavorable [14].

The same group (2006) also reported the structures of 1:1 complexesof cysteamine; $[Zn(SCH_2CH_2NH_2)Cl]$, $[Cd(SCH_2CH_2NH_2)Cl,]$ and $[Hg(SCH_2CH_2NH_2)Cl]$. These complexes displayed chelating N,S- coordination of $^-SCH_2CH_2NH_2$ ligand in which S donor atom acts as bridging ligand while Cl^- is coordinated at terminal position. Crystal structures of Zn and Cd compounds indicate that in both complexes, the asymmetric unit contains two molecules of [M(L)Cl], where M = Zn and Cd, having slightly different geometric parameters. The zinc and cadmium compounds show different coordination

modes at the metal ions as was found in ML_2 complexes. Zn^{2+} is tetrahedral $Zn(ClNS_2)$ configuration [15].

Ngan et al. (2007) prepared a series of zinc(II) diimine *bis*(thiolate) complexes with photochromic diarylethene-containing phenanthroline ligands, and their photophysical and photochromic properties were studied. The X-ray crystal structures of two of these complexes have been characterized [162].

The latter reacts with the alkylating agents CH_3I and $PO(OCH_3)_3$ in a two-step process. In the first step, the isobutylthiolate is methylated and its position in the ligand sphere of zinc is taken by I^- or $OPO(OCH_3)_2^-$, respectively.In the second step, the additional thiolate ligand is methylated and replaced by a second I^- or $OPO(OCH_3)_2^-$ [17]. The molecular structure of *N*-(2-mercaptoisobutyl)(2-pyridin-2-yl-ethyl)methylamine-Zn–SC_6H_5in ZnN_2S_2 coordnation modeis given in Figure 1.17.

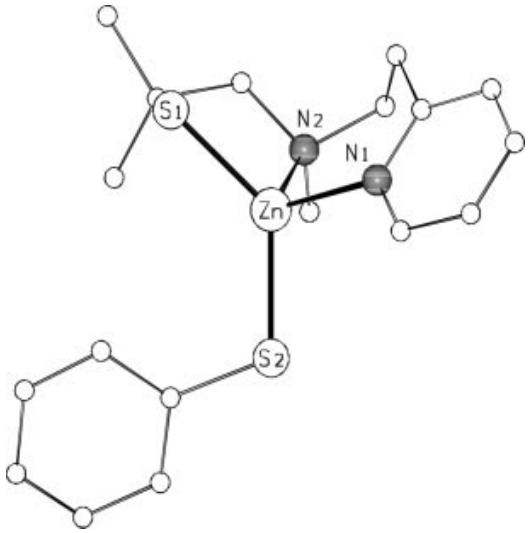

Figure 1.17 Molecular structure of *N*-(2-mercaptoisobutyl)(2-pyridin-2-yl-ethyl)methylamine-Zn–SC_6H_5.

Ohanessien and co-workers (2011) investigated the proton affinities of a series of mono- and polynuclear zinc-thiolate compounds, mimicking zinc finger protein and metallothioneins sites by density functional theory (DFT) calculations. The study allows to evaluate the intrinsic nucleophilicity of synthetic and natural zinc-bound thiolates and to compare their relative reactivities. The site specificity of the experimental thiolate

alkylation for the Zn_4Cys_{11} clusters in metallothioneins, as well as the relative reactivities of $ZnHis_2Cys_2$, $ZnHisCys_3$ and $ZnCys_4$ zinc finger sitesare well reproduced. The data indicated that thiolates in terminal position, coordinated to only one Lewis acid, were more reactive than bridging thiolates. Synthetic inorganic clusters and the $Zn_4Cys_9His_2$ cluster found in a cyanobacterial metallothionein are less reactive than Zn_4Cys_{11} and Zn_3Cys_9 clusters in metallothioneins [163].

Shaban (2011) synthesized two new zinc complexes containing dithiolate and diamine ligands, namely, $[\{Zn(N_2H_2S_2)\}_2]$and $[Zn(N_2Me_2S_2)]$, where $N_2H_2S_2^{2-}$ = *N*,*N*-*bis*(2-mercaptophenyl)ethylendiamine (2−) and $N_2Me_2S_2^{2-}$ = *N*,*N*′-dimethyl-*N*,*N*′-*bis*(2-mercaptophenyl)ethylendiamine) (2−) and structurally characterized by X-ray structure analysis [164]. The structure of $[\{Zn(N_2H_2S_2)\}_2]$ consists of a *bis*(μ-thiolato) binuclear unit in which each zinc resides in an N_2S_3 array between square pyramidal and trigonal bipyramidal environment. The complex, $[Zn(N_2Me_2S_2)]$ is mononuclear, where each zinc attains an N_2S_2 distorted tetrahedral environment.

1.8 Biological importance of zinc

Zinc plays an active role in the structural functions of proteins and in catalyzing the biochemical reactions. In addition to catalytic and structural functions, zinc(II) ions also take part in information transfer and cellular control [1-6].The active sites of more than 300 zinc-containing enzymes possess a zinc center connected to the protein backbone through three or four amino acid residues, the nature of which impacts the definite function of the enzyme. Generally, these amino acids include cysteine, histidine, aspartic acid and glutamic acid [1-10]. Zinc in proteins can either participate directly in chemical catalysis or be important for maintaining protein structure and stability. In all catalytic sites, the zinc ion functions as a Lewis acid [8].The thiolate group of cysteine has a particular affinity for Zn^{2+} cation and participates in the active center of enzymes, such as methionine synthase and metalloproteinase. The high affinity of thiolate for zinc allows it to link two zinc centers thus forming metal clusters as in metallothioneins (MT) [12,165,166]. A four-metal ion cluster in which two histidine residues participate in metal

ion coordination, resulting in a $Zn_4Cys_9His_2$ arrangement, has been described in a cyanobacterial MT [167,168]. Although the Zn^{2+}-cysteine complexes are critical mediators of protein structure, catalysis and regulation, traditionally, they perform structural roles in proteins.

The most abundant class of structural Zn^{2+}-cysteine complexes is the zinc finger. Zinc fingers are characteristically comprised $Zn(Cys)_4$ or $Zn(Cys)_2(His)_2$ coordination environments. Most of the zinc finger proteins act as transcription activators or suppressors [1-10,169]. A well-known example of a zinc finger acting as an active site is the $Zn(Cys)_4$ core of the DNA repair azodicarbonamide (Ada) proteinas shown in Figure 1.18.

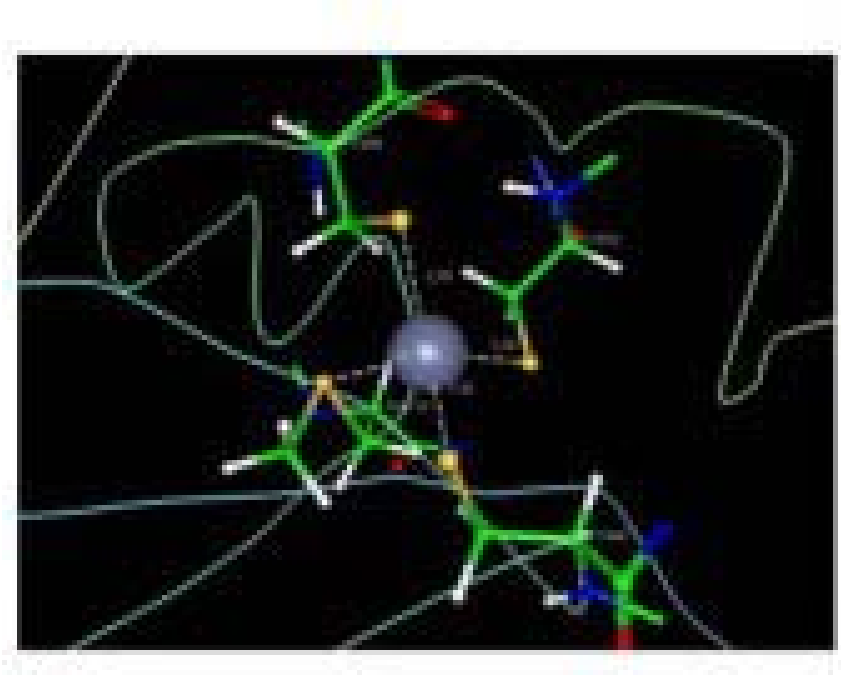

Figure 1.18 Structure of *E. Coli* Ada protein showing ZnS_4 environment.

The corresponding DNA repairing mechanism assists in the transfer of methyl groups from the DNA backbone phosphoesters to a zinc-complexed cysteine[5,170]. The effective strength of zincthiolate bond is dependent on the nature of the all four ligands in the complex, as indicated by the variation of the energy barrier for the alkylation of thiolate in various zincthiolate complexes [170].Along with cysteine, the amino acid, histidine, is also the frequently occurring ligand of zinc in the active centre of zinc containing enzymes.Substitution of cysteine by histidine also induces an increase in the magnitude of the reaction energy barrier.The energy barrier for the oxidation of zinc

fingers is strictly dependent on the type of ligands coordinated to zinc and on the protonation state of the complex [170].In order to understand, why different zinc enzymes utilize different amino acid residues at the active site, it is necessary to understand how the chemistry of zinc is modulated by its coordination environment.

While the structural zinc is coordinated by cysteinate, quite often in combination with histidine, the functional (catalytic) zinc is coordinated predominantly by histidine and to a lesser extent, aspartate and glutamate [1-6,171]. In the hydrolytic enzyme, carbonic anhydrase, the active site is composed of one zinc atom coordinated to three histidines. A fourth coordination site is occupied by a water molecule, which is loosely bonded through its oxygen as shown in Figure 1.19. Zinc activates its bound waterthat regulates pH *via* the following equilibrium:

$$CO_2 \rightleftharpoons HCO_3^-$$

The electronic properties of the histidines, as well as multiple non-bonded interactions provided by polar residues near the catalytic center (e.g., threonine residue abbreviated as Thr199), decrease the pKa of the Zn-bound water to about 7. The enzyme thus provides a nucleophilically “active” hydroxide at biological pH (about 7.4). The catalytic cycle is explained in Figure 1.19[172].

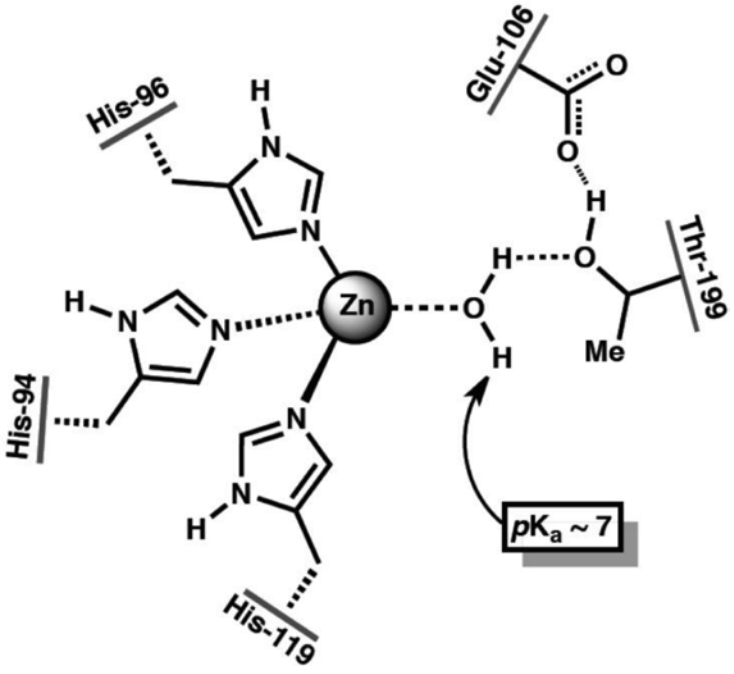

Figure 1.19 Active site of human carbonic anhydrase featuring a first coordination shell of three histidine residues and an activated water molecule.

Apart from the enzymes, with one zinc-binding site, such as carbonic anhydrase and carboxypeptidase A, the enzymes containing two or three zinc ions at the active sites are also known [3,105,172-174]. The most important and distinguishing feature in these enzymes is that the two zinc(II) ions are connected to each other through one solvent species (H_2O or OH^-) as well as the carboxylate function from amino acid side chains with the Zn…Zn distances from 3.0 to 3.5 Å [105,174]. In the enzymes, the zinc atoms display a variety of geometries, such as tetrahedral, trigonal bipyramidal and octahedral. Zinc(II) commonly exhibits tetrahedral geometry[3-7,106,175].

The ability of zinc to perform a variety of functions is due to the following reasons:
Firstly, the divalent zinc ion is exceptionally stable with respect to oxidation and reduction so it does not participate in redox reactions.

Secondly, zinc is an element of borderline hardness, so that nitrogen, oxygen and sulfur ligands can all be coordinated.

Thirdly, the d^{10} configuration of Zn^{2+} indicates that the coordination number and geometry of its complexes is only dictated by ligand size and charge. The flexibility in coordination geometry makes ligand exchange more facile and enhances the ability of zinc to effect a catalytic cycle.

Fourthly, when coordinated to zinc, anions such as OH^-, OR^- and SR^- still retain their nucleophilic character which plays an important role in group transfer. It is because of these characters that zinc has been adopted by nature to constitute many metal enzymes [1-6,175,176].

Chapter – 2
Binary Zinc(II) Complexes of Thiolates

2.1 Introduction

The zinc(II) complexes of thiolates are importantwith respect to the biological point of view since they act as structural models for metal binding sites in metallothioneins and metalloregulatory proteins [1, 2, 4-6, 165]. Zinc(II) often displays $Zn(N_2S_2)$ coordination modes by binding to two cysteine and two histidine residues in the biological systems [1-8, 12, 165, 169,175]. Therefore, the zinc(II) complexes containing N, S-donor ligands for instance cysteine, cysteamine may offerappropriate models for its coordination atmosphere in the enzymes. In some studies, simple multidentate ligands have been applied to model complexes relative to biological systems and to achieve higher reactivities of the complexes [13,17,176-180]. For example, Ji et al.reported the zinc thiolate complexes of (N,N,S)-tridentate ligands such as, *N*-(2-mercaptoisobutyl)(2-pyridin-2-yl-methyl)amine for the modeling of thiolate alkylating enzymes[17].

Notni et al. reported the synthesis of zinc thiolate complexes containing saturated macrocyclic polyamine ligands with the general formula $[Zn(Ln)(SR)]ClO_4$ (L*n*: *n*-dentate aza-macrocyclic ligand). Aza-macrocycles have been found to be suitable ligands to obtain stable, soluble thiolate complexes of Zn(II). They also studied theinfluence of the ligand, L*n* on the reactivity of zinc-bound thiolate for alkylation [178,179].

Zinc-bound thiolates have also been shown to promote alkyl group transfer in several zinc enzymes [11, 23, 180]. A rare aspect of these enzymes is the sulfur enriched zinc setting, which can classically be characterized as either NS_2ZnX or N_2SZnX, where N and S represent the side-chains of histidine as well as cysteine, while X is the coordination site of the substrate. When zinc behaves as a catalyst, one of the binding sites is usually occupied by a water molecule or a hydroxide ligand [1].

Zinc can coordinate to nitrogen, oxygen and sulphur containg ligands depending upon its coordination number. Zinc preferably coordinate with sulphur containg liagnds rather

than nitrogen containg liagnds when coordination number of Zn(II) complex is four [181].

Several structural reports onzinc(II) complexes with thiolates are available in the literature, which demonstrate that thiolates coordinate with zinc(II) through sulfur atom in a tetrahedral environment [13-15, 17, 19, 22-24, 166,170,176-185]. In these complexes, thiolates frequently act as bridging ligands and thus usually form polymeric complexes.
In the present study, we preparedthe binary zinc(II) complexes of four thiolate ligands, which include, cysteamine (Cym), cysteine (Cys), mercaptosuccinic acid (Msa) and mercaptonicotinic acid (Mnt). We also attempted to prepare the mixed ligand complexes of the type, [Zn(SR)(diamine)]Cl using cysteaminebut instead, we successfully isolated a new binary complex of cysteamine.

A tetranuclear complex, $[Zn_4(Cym)_4Cl_4]$ (**1**) was obtained in the presence of diamines, 1,2-diaminoethane (en), 1,3-diaminopropane (Dap) and tetramethylethylenediamine (TMEDA). In the reaction of cystamine (disulfide) in the presence of ethylenediamine (en),a new polymeric complex, $[Zn(Cym\text{-}Cym)Cl_2]_n$ (**2**) was obtained. The crystal structures of (**1**) and (**2**) were determined and a DFT based comparative spectroscopic investigation of both complexes is presented. The crystal structures of two other similar complexes in Zn^{2+}-cysteamine systems, $[Zn(Cym)_2]$ [14] and $[Zn(Cym)Cl]_4$ [15] have already been published, but the coordination environment is different in all cases.The reported X-ray structure of (**2**) demonstrated the stability of the disulfide bridges, which was not destroyed in order to increase the coordination ability of the ligand toward the metal ion. It also provides valuable information with a view to the lacking data for the metal complexes of cystamine (containing disulfide S-S bond), especially of the polymeric one.

The solid state simulation of the molecular structures of (**1**)and (**2**)accounts the intermolecular interactions and the crystal packing effect and thus holds out better structural model for frequency calculations, which were further compared to the experimental IR spectra measured in solid state. The combined experimental and theoretical vibrational analysis of cyclic $[Zn_4Cym_4Cl_4]$ (**1**) and polymeric $[Zn(Cym\text{-}Cym)Cl_2]_n$ (**2**) complexes as well as of the ligands was performed to select specific spectroscopic characteristics related to the different coordination polyhedron around the

Zn(II) ions. The vibrational spectra are calculated and interpreted in the solid state using a periodic model with the experimental unit cell parameters. The gas phase calculations of $[Zn_4Cym_4Cl_4]$ (**1**) and $[Zn(Cym)Cl]_4$ [15] at molecular level were also performed for comparison. The structural formulae of thiolate ligands employed in this study havealready been shown in Scheme 1.2.

2.2 Experimental

2.2.1 Chemicals

Zinc chloride ($ZnCl_2$) was supplied by Fluka Chemical Company, Switzerland.Thiolatesand cystaminedihydrochloride (Cym-Cym·2HCl)werepurchased from Acros Organics, Belgium. Diamines (en = 1,2-diaminoethane, Dap = 1,3-diaminopropane, TMEDA = *N*,*N*,*N´*,*N´*-tetramethylethylenediamine) were obtained from Merck Chemical Company.

2.2.2 Synthesis of complexes (1-5)

$[Zn_4(Cym)_4Cl_4]$ (1)

A solution of 0.12 g (1 mmol) of cysteamine hydrochloride in 10 mL methanol was added to 0.14 g $ZnCl_2$ (1 mmol) in 10 mL water contained in 100mL beaker. A colorless solution was formed on mixing. After stirring for 30 min (with 15 min heating), 1 mmol of diamines (en, Dap, TMEDA) in 10 mL methanol was added to this solution. The resulting colorless solution was stirred for 15 min and filtered. The filtrate was kept at room temperature to yield white crystals of complex (**1**).

$[Zn(Cym\text{-}Cym)Cl_2]$ (2)

To a solution of 0.14 g (1 mmol) $ZnCl_2$ in 10 mL water was added a 15 mL methanolic solution of 0.24 g (1 mmol)of cystaminedihydrochloride. The colorlesssolution was stirredfor 30 minutes and then 0.06 g (1 mmol) of 1,2-diaminoethane (en) in 10 mL

methanol was added to this solution.After stirring for 30 minutes,the solution was filtered.The filtrate was kept for crystallization at room temperature to result light brown crystals of complex (**2**).

[Zn(Cys)Cl]·0.5H_2O (3)

The complex(**3**) was prepared by adding 0.125 g (1 mmol) cysteine in 10 mL water to 0.14 g (1 mmol) of $ZnCl_2$ in 5 mL water. The reaction mixture was stirred for 30 minutes to produce a clear solution which was filtered. The water insoluble white crystals were obtained after 3-4 days.

[Zn(Msa)$_2$] (4)

The complex (**4**) was prepared by adding 0.32 g (2 mmol) 2-mercaptosuccinic acid (Msa) in 10 mL methanol to 0.14 g (1 mmol) of $ZnCl_2$ in 5 mL water.The mixture was stirred for 30 minutes. A clear solution was obtained, which was filtered and kept for crystallization. After 3-4 days, white crystals were obtained, which were washed with methanol and air-dried.

[Zn(Mnt)$_2$(H_2O)] (5)

For preparation of (**5**), 0.15 g (1 mmol) 2-mercaptonicotinic acid was dissolved in 25 mL water containing 0.06 g (1 mmol) ethylenediamine. The Mnt solution was then added to 0.14 g (1 mmol) of $ZnCl_2$ in 5 mL water. On addition light yellow precipitates formed immediately. The mixture was stirred for 30 minutes and then filtered. The product was washed with methanol and air-dried. When Mnt was dissolved in 50 mL 1:1 mixture of CH_3CN and methanol, no reaction occurred even with heating for 2 hours and only Mnt was recovered at the end.Elemental analysis of the complexes (1-5) and their melting points are in given in Table 2.1.

Table 2.1 Elemental analysis and melting points of zinc(II)-thiolate complexes

Complex	Found (Calculated)				M. P.
	C	H	N	S	(ºC)
$[Zn_4(Cym)_4Cl_4]$(**1**)	13.31	3.02	7.65	17.40	250-253
	(13.57)	(3.42)	(7.92)	(18.12)	
[Zn(Cym-Cym)Cl] (**2**)	16.41	4.43	9.58	21.53	193-195
	(16.65)	(4.19)	(9.71)	(22.22)	
$[Zn(Cys)Cl]\cdot 0.5H_2O$ (**3**)	16.21	2.90	6.73	14.15	230-233
	(15.67)	(3.07)	(6.09)	(13.94)	
$[Zn(Msa)_2]$ (**4**)	26.91	2.50	-	16.37	260-262
	(26.42)	(2.77)	-	(17.63)	
$[Zn(Mnt)_2(H_2O)]$ (**5**)	37.41	1.90	7.08	16.84	193-195
	(36.98)	(2.07)	(7.19)	(16.46)	

2.2.3 IR, NMRand thermal measurements

The FTIR spectra of the complexes were taken on PerkinElmer FT-IR 180 spectrophotometer using KBr pellets over the spectral range 4000-400 cm^{-1}. All NMR measurements were carried out on a Jeol JNM-LA 500 NMR spectrophotometer at 297K. The ^{1}H NMR spectra were recorded at a frequency of 500.00 MHz. The ^{13}C NMR measurementswere takenin DMSO at a frequency of 125.65 MHz (with ^{1}H broadband decoupling). TMS is used as reference for NMR measurements of samples. The NMR spectral conditions were32 k data points, 1.00 s pulse delay and 0.967 s acquisition time.The solid-state thermal gravimetric analysis (TGA) of complex (**3**) was performed on a Mettler Toledo TGA/SDTA 851e analyzer which is working under argon environment at 10 ºC min^{-1} as the heating rate.

2.2.4 X-ray structure determination

Single crystal data collection was performed at 296 K on a Bruker Kappa APEXII CCD diffractometer equipped with a four-circle goniometer and using MoKαgraphite mono-chromated radiation (λ = 0.71073 Å). The structures were solved by Direct Methods with SHELXS-97 [186] and refined by full-matrix least-squares procedures on F^2 using the program SHELXL-97 [187]. All non-hydrogen atoms were refined anisotropically. The H-atoms were positioned geometrically (C–H = 0.97, N–H = 0.97 Å) and refined as riding with U_{iso}(H) = xUeq(C, N), where x = 1.2 for other H-atoms. For molecular graphics, PLATON [188] was used. The crystals of complex (**2**)are twinned with Twin Law (0 0 1)[1 0 5] at 2.41 BASF 0.31. Crystal data and details of the data collection are summarized in Tables2.2 and 2.3.

2.2.5 Computational details

The polymeric $[Zn(Cym\text{-}Cym)Cl_2]_n$ complex in solid statewas simulated by using the periodic DFT calculations based on the Vienna *ab initio* simulation package (VASP 5.2.2) [189-191] performing a variational solution of the Kohn-Sham equations in a plane-wave (PW) basis with energy cut-off of 400 eV. All atomic positions in the Zn(II) complex were fully relaxed without symmetry restrictions in a fixed unit cell (taken from

the X-ray data) using a conjugate-gradient algorithm. GGA as parameterized by Perdew, Burke and Ernzerhof (PBE) functional are employed for treatment of electron exchange correlation (EXC) interactions [192]. The projector-augmented-wave (PAW) method wasemployed to elaborate electron-ion interactions [193]. 12valence electrons for each Zn ($3d^{10}4s^2$), 7 for Cl atom ($3s^23p^5$), 6 for S atom ($3s^23p^4$), 5 for N atom ($2s^22p^3$) and 4 for C atom ($2s^22p^2$) were treated explicitly and the remaining core electrons together with the nuclei were described by PAW pseudopotentials. The same approach was applied for calculations of$[Zn_4Cym_4Cl_4]$ and $[Zn(Cym)Cl]_4$ complexes in the solid state, where the intermolecular interactions and the crystal packing effect are taken into account. To describe correctly the strong Coulomb repulsion (*U*) between the localized *d* electrons of Zn, the DFT+*U* approach, adding a Hubbard-like term to the effective potential was applied in all calculations as implemented in VASP package. In the present work, the approach described by Dudarev et al. [194]was applied, where an effective Hubbard parameter $U_{eff}= U-J$ enters the Hamiltonian, with *U* and *J* being the Coulomb (of 4eV) and exchange interaction parameter (of 1 eV), respectively.

In addition, thegeometryoptimizationsandfrequencycalculationsof$[Zn_4Cym_4Cl_4]$ (**1**) and$[Zn(Cym)Cl]_4$ complexes inC_i symmetry wereperformedin gas phase at DFT level with the one-parameter hybrid PBE1PBE functional, containing themodifiedPBE (Perdew, Burke, Ernzerhof) exchangeandcorrelationfunctional[192,195]combinedwith 6-311+G(d) basis set for Zn, Cl, S, N and C atoms and 6-31G(d) basis set for H atoms. The combined basis set is called **B1**. The initial geometries of the Zn(II) complexes were taken from single crystal X-ray diffraction analysis [15]. All calculations at molecular level were used with the Gaussian 09 software [196]. The prognosis of the internal coordinates onto each normal mode in terms of percentage relative weights was computed as implemented in Gaussian09. Each normal mode is described on the basis of the largest percentage value of the total displacement vector magnitude. In addition, the vibrational modes have been analyzed by visual inspection of the modes animated using the ChemCraft program [197]. The calculated gas phase frequencies of the $[Zn_4Cym_4Cl_4]$ complex were comparedwith the corresponding frequencies obtained from the periodic solid state calculations.

The ^1H and ^{13}C NMR chemical shift calculations of the Cym-Cym and Cym (zwitterionic form) ligands, and $[Zn(Cym\text{-}Cym)Cl_2]_n$ and $[Zn_4Cym_4Cl_4]$ complexes were performed in

DMSO solution at PBE1PBE/**B1** level. The absolute isotropic magnetic shielding constants (σ_i) were used to obtain the chemical shifts ($\delta_i = \sigma_{TMS} - \sigma_i$) for C and H atoms by referring to the standard tetramethylsilane (TMS). The σ_{TMS} values were calculated at the same theoretical value. The NMR spectra calculations in DMSO were fulfilled for the optimized geometries in the same solvent. A non-equilibrium implementation of the polarisable conductor calculation model (CPCM) was applied to simulate the solvent [198]. For the polymeric complex (**2**), a neutral cluster involving three Zn ions was chosen for calculation in solution and the chemicalshifts for inner C and H (between two metal ions) atoms were estimated.

2.2.6 Antimicrobial activities

The antimicrobial activities (average of triplicate measurements) of free thiolates, their zinc(II) thiolate complexes and Amoxil medicineas a standard drug were appraised by minimum inhibitory concentrations (MIC; μg mL^{-1}) as givenin the literature [141]. Standard culture media of bacteria such as *E. coli*, (ATCC 13706) and *P. aeruginosa* (MTCC 424); molds such as *A. niger*(MTCC 1349) and *P. citrinum* (MTCC 5215); and yeast such as*C. albicans* (MTCC 183) and *S. cerevisiae* (MTCC 463) were procured from Qingdao YijiaHuuyi Co. China.

Bacteria were injected into 5 mL of liquid SCD (soybean, casein and digest) medium and cultured for 24 h at 35.5 ^oC. The cultured solutions were diluted and adjusted to a concentration of 105-106microorganisms per mL which areemployed for inoculation in the antimicrobial test. In the case of mold culture, the agar slant containing mixture of polypeptoneand dextrose (PD) medium for one week cultivation at 27 ^oC was gently washed with saline containing 0.05% Tween 80. The spore suspension obtainedwas adjusted to the concentration of 105 microorganisms per mL that is applied for inoculation in the antimicrobial test. Yeast were injected into 5 mL of solution containing glucose and polypeptone (GP) medium and cultured for 48 h at 30 ^oC. The cultured solutions were diluted and adjusted to a concentration of 106–107 mL, which were used for inoculation in the antimicrobial test.The complexes were halted in water. For bacteria, solutions were then diluted with SCD medium. For mold and yeast, solutions were then diluted with GP. These solutions were dilutedtwo times. Resultantly, the dilute solutions

with concentration of 1000 to 10 mg mL^{-1} were ready for antimicrobial studies. Each 1 mL of culture medium containing various concentrationof zinc(II) thiolate complexes was inoculated with 0.1 mL of the microorganism suspension. Bacteriawere cultured for 1 day at 35.5^{o}C, mold for 7 days at 25 ^{o}C and yeast for 2 days at 30 ^{o}C. The proliferation of the microorganisms was checked for the stipulated time. When there is no more significant proliferation of microorganism in the medium containing the lowest concentration of the complexes. At this point, the concentration of zinc(II) thiolate complexes is considered as minimum inhibitory concentrations (MIC) in μg mL^{-1}.

Table2.2Crystal data and refinementdetailsforcompound(**1**)

Formula	$C_8H_{24}N_4S_4Zn_4Cl_4$
Formula Weight	707.84
Crystal system	Monoclinic
Space Group	*P*-21/n
a, *b*, *c* (Å)	8.4359(5), 8.4471(5), 16.6530(9)
β (deg)	100.907(3)
V (Å^3)	1165.24(12)
Z	2
ρ_{calc} (g cm^{-3})	2.017
μ(MoKα) (mm^{-1})	4.885
F(000)	704
Crystal size (mm)	0.32 x 0.28 x 0.16
Temperature (K)	296(2)
λMoKα (Å)	0.71073
2 θ range (deg)	2.491 - 26.997
h, k, l limits	-10:10, -10:7, -21:21
Reflections; collected/ Uniq.	9391 / 2526 [R(int) = 0.0305]
Reflections: observed [$I > 2\sigma(I)$]	2126
T_{min}, T_{max}	0.304, 0.509
Data / restraints / parameters	2256 / 0 / 109
R_1, wR_2, S [$I > 2\sigma(I)$]	0.0422, 0.1157, 1.129
Largest diff. peak, hole (e Å^{-3})	1.364, -0.458

$w = [\sigma^2(F_o^2) + (0.0414P)^2 + 6.4623P]^{-1}$ where $P = (F_o^2 + 2F_c^2)/3$

Table 2.3Crystal data and refinementdetailsforcompound(**2**)

Formula	$C_4H_{12}N_2S_2ZnCl_2$
Formula Weight	288.55
Crystal system	Monoclinic
Space Group	*P*21/c
a, *b*, *c* (Å)	5.1201(3), 20.0319(18), 10.4282(9)
β (deg)	93.221(4)
V (Å^3)	1067.88(15)
Z	4
ρ_{calc} (g cm^{-3})	1.795
μ(MoKα) (mm^{-1})	3.136
F(000)	584
Crystal size (mm)	0.44 x 0.22 x 0.18
Temperature (K)	296(2)
λMoKα (Å)	0.71073
2 θ range (deg)	2.822 - 27.000
h, k, l limits	-6:6, -25:25, 0:13
Reflections; collected/ Uniq.	2293/1743 (Rint = 0.0489)
T_{min}, T_{max}	0.340, 0.603
Data / restraints / parameters	2293 / 0 / 113
R_1, wR_2, S [$I > 2\sigma(I)$]	0.0447, 0.0871, 1.124
Largest diff. peak, hole (e Å^{-3})	0.514, -0.667

$w = [\sigma^2(F_o^2) + (0.0167P)^2 + 1.9056P]^{-1}$ where $P = (F_o^2 + 2F_c^2)/3$

2.3 Results and discussion

In most of the cases, the binary zinc(II) complexes of thiolates were synthesized by the addition of 1 or 2 mmol of ligand solution to 1 mmol of $ZnCl_2$.

$$ZnCl_{2(H2O)} + 2RSH_{(MeOH/Water)} \rightarrow Zn(SR)_2 + 2HCl$$

It has been observed that zinc(II) prefers to bind suphur donor ligand rather than nitrogen donor ligand owing to border line hardness [175, 176] as given in the following reactions. In the reaction of $ZnCl_2$ and Cym-H·HCl in the presence of diamines (en, Dap and TMEDA), a tetranuclear zinc-cysteaminate complex was obtained as explained below.

$$ZnCl_2 + 2\ \text{Cym-H·HCl} + \text{en, Dap or TMEDA} \rightarrow [Zn_4(Cym)_4Cl_4]\ (\mathbf{1}) + (\text{en-}H_2)Cl_2$$

Similarly, $ZnCl_2$ reacts with cystamine dihydrochloride (Cym-Cym·2HCl) in the presence of 1,2-diaminoethane (en) to yield a polymeric complex, $[Zn(Cym\text{-}Cym)Cl_2]_n$(**2**).

$$ZnCl_2 + \text{en} + \text{Cym-Cym·2HCl} \rightarrow [Zn(Cym\text{-}Cym)Cl_2]_n(\mathbf{2}) + (\text{en-}H_2)Cl_2$$

The structural information for both of these complexes was obtained by X-ray crystallography. Their vibrational analysis was also carried out using DFT modeling studies.

A similar reaction of $ZnCl_2$ with TMEDA (tetramethylethylenediamine) and 2-mercaptosuccinic acid (Msa) led to an ionic chlorido complex (**10**).

$$ZnCl_2 + \text{TMEDA} + \text{Msa} \rightarrow (\text{TMEDA-}H_2)^{2+}[ZnCl_4]^{2-}$$

2.3.1 Spectroscopic characterization

The important FTIR frequencies of free ligands and their corresponding complexes (**1-5**)are recorded in Table 2.4. In the FTIR spectra, the absence of the S-H peak around 2550-2500 cm^{-1} indicates that the S-H bonds in the coordinated ligands have been substituted by the S-Zn moiety in zinc(II) thiolate complexes (**1-5**). It shows the

anticipated high attraction of sulfur towards zinc(II). As given in Table 2.4, anoteworthy change in the C-S stretching bands of the complexes in comparison of free ligands also approves the suggested Zn-S coordination. The FTIR spectra of complexes (**1**) and (**3**)displaythe existence of N-H stretching bands around 3400 cm^{-1} and 3100 cm^{-1}. The peak at 1576 cm^{-1} for (**1**) can be assigned to NH_2 bending.Sharp bands around 1600 cm^{-1} and 1700 cm^{-1} were observed for carboxylate vibration in complexes (**3-5)**. The IR spectrum of complex (**3**) is shown in Figure 2.1.

Table 2.4 Selected IR absorptions (cm^{-1}) of thiolates and theirzinc(II) complexes

Species	ν(C-S)	ν(N-H)	δ(N-H)	ν(C=O)
Cym-H·HCl	785	-	1594, 1500	-
(1)	840	3288, 3245, 3131	1576	-
Cys-H	692	3179	1576	1627
(3)	650	3420, 3254	1595, 1506	1595
Msa	611	-	-	1715
(4)	677	-	-	1698
Mnt-H	638	-	-	1675
(5)	661	-	-	1593, 1558

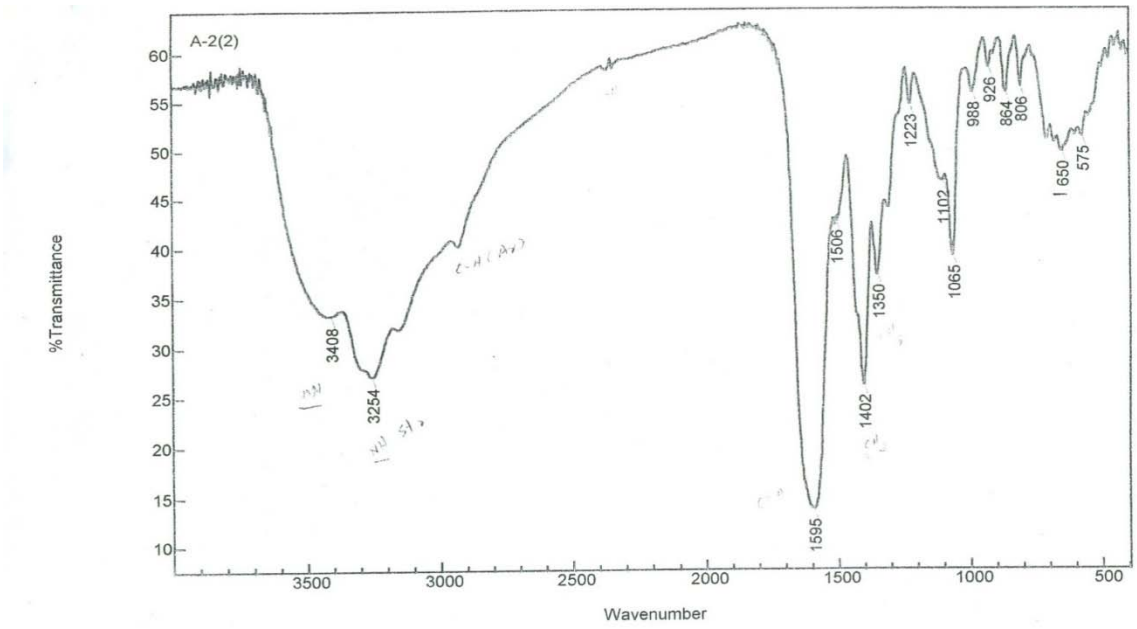

Figure 2.1 IR spectrum of Zn-Cysteine complex (**3**)

The ^{1}H and ^{13}C NMR chemical shifts of the CymH and Cym-Cym ligands and theirZn(II) complexes(**1**&**2**)are summarized in Table 2.5.The proton NMR spectraof Cym-Cym ligand and complex (**2**)are shown in Figure2.2. In the proton NMR spectrum of $[Zn(Cym\text{-}Cym)Cl_2]_n$ (**2**), a small upfield shift for the methylene protons attached to sulfur is observed with respect to the free ligand. The S-S bond of disulfide possesses a barrier of rotation [199] and due to hindered rotation, the CH_2 protons attached to sulfur are diastereotopic and appeared as a doublet of two identical triplets at 2.91 and 3.03 ppm (3.09 ppm in cystamine). The difference of inner lines in both triplets is 0.0146 ppm (7.3 Hz) and of outer lines is 0.0135 ppm (6.75 Hz). The NCH_2 protons in complex **2**were also shifted upfield in comparison with the free ligand (2.74 *vs* 3.02 ppm). Appearance of the resonance at 8.38 ppm in the ^{1}H NMR spectrum of ligand Cym-Cym·2HCl indicates hydrogen-bonded NH_3 groups. Similar peaks were observed in the ^{1}H NMR spectrum of CymH ligand. Therefore, the methylene protons upfield shifts could not be simply related to the nitrogen binding to Zn(II) in structure **2**. The N-H peaks in the complexes were not observed due to rapid exchange with traces of water present in the solvent.

The ^{1}H NMR spectrum of free Msa ligand shows an ABX system consisting of a doublet of doublets for methyne protons and two doublets of doublets for geminal protons (^{a}H and

^{b}H) of the neighboring methylene group. The chemical shift of methyne proton is ~3.8 ppm, while the methylene protons resonate at ~3.0 and 2.9 ppm respectively [200].In [$Zn(Msa)_2$],the –CH signals are shifted upfield by 1 ppm, whereas the chemical shifts of methylene protons are almost unchanged. This observation suggests that thiolate is binding to zinc(II) through sulfur atom. The H-3, H-4 and H-5 protons of free ligand Mnt-H are detected at 8.15, 7.13 and 8.51 ppm, respectively that is in the form of doublets of doublets. In the spectrum of Mnt-H-derived zinc(II) complex, these signals appear as multiplets at 8.11, 7.09 and 8.25 ppm respectively.

A comparison of ^{13}C signals of complexes (**1**) and (**2**) provide a deeper comprehension of their NMR behavior as given in Table 2.5. The^{13}C NMR spectrum of cyclic complex (**1**) shown in Figure 2.3 showed downfield shift of ~1.4 ppm in C-Nresonance. At the same time, the downfield shift of C(-S) signal for (**1**) is higher by 7 ppm as compared to that observed for complex (**2**)at ~1 ppm. This result indicates the formation of S-bridge in complex (**1)** in contrast to complex (**2**). In the ^{13}C NMR spectrum of (**2**) (Figure 2.4) downfield shifts were observed for the C-S and C-N resonances with respect to those of free ligand (38.7 *vs* 37.8 ppm and 35.1 *vs* 33.7 ppm respectively) and the larger shift for C(-N) resonance. The ^{13}C peak assignments and the trends found were supported by the calculated ^{13}Cchemical shifts for the model compounds and they are in accordance withthe coordination of cystamine to the metal center through nitrogen atom. The downfield shift of C(-N) signal in (**2**) is in agreement with the observed elongation of C-N bond upon nitrogen binding to Zn(II). It should be mentioned that in polymeric complex (**2**), the C-(S) resonance (38.7 ppm) is upfield shifted with respect to C-(N) resonance (35.1 ppm), whereas in the cyclic complex (**1**), C-(S) signal (at 28.4 ppm) is downfield shifted as compared to C-(N) one (43.3 ppm).

The ^{13}CNMR spectrum of uncoordinated Msa ligand shows four resonances due to two carboxyl carbons around 180 ppm, methylene carbon at ~42 ppm and methyne carbon at ~39 ppm [48]. Upon complexation with zinc(II), the C=O and C-H signals are shifted upfield (Table 2.6). Two weak signals due to disulfide were also observed around 48 ppm.In [$Zn(Mnt)_2(H_2O)$], downfield shifts were observed in the resonances on coordination. The ^{13}C chemical shifts of the free ligands and their corresponding complexes are listed in Table 2.6.

The insolubility of complex (**3**)in DMSO prevented the measuring of its NMR spectra. As a result, complex (**3**) was characterized by TGA that shows a good agreement between the calculated and found weight loss values for the suggested empirical formula of the complex, [Zn(Cys-H)Cl]·0.5H_2O (Figure 2.5).In addtion to this, TG studies were also carried out to asses the thermal stability of the complex, [Zn(Cys-H)Cl]·0.5H_2O (**3**). The thermal decomposition starts at 50°C with the initial weight loss of 3.90 % (calculated 3.91 %) that indicates the removalof half of water molecule per mole of [Zn(Cys-H)Cl]. The next weight loss of 55.63 % in the temperature range of 200-630°C corresponds to the removal of one Cys-H ligand (calculated 52.20 %). The decomposition seems incomplete untill 1000^{o}C.However, it can be theoretically expected that the remaining material may be $[ZnCl]^{+}$ ionwhich is equal to 40. 47% (calculated 43. 64 %) in weight of [Zn(Cys-H)Cl]·0.5H_2O.

Table 2.5 Experimental ^{1}H NMR and ^{13}C NMR data of ligands;CymH, Cym-Cym and Zn(II) complexes; **1** and **2**, recorded in DMSO-d_6 and calculated (at PBE1PBE/**B1** level) ^{13}C chemical shifts (δ_i) of the model compounds in DMSO

^{1}H NMR signals in ppm, peak multiplicity[a]			
Compound	H(-CN)	H(-CS)	H(-N)
(CymH·HCl)	2.71 t	2.94 t	8.32
$[Zn_4Cym_4Cl_4]$ (**1**)	2.70	2.85	Not observed
Cym-Cym·2HCl	3.00, 3.02, 3.04	3.07, 3.09, 3.1	8.38 s
$[Zn(Cym\text{-}Cym)Cl_2]_n$ (**2**)	2.74 s	3.03 t, 2.91 t	Not observed
^{13}C NMR signals in ppm, peak multiplicity			
	C-N	C-S	
(CymH.HCl)	41.9 s	21.3 s	
	(41.0**)**	(23.7)	
$[Zn_4Cym_4Cl_4]$ (**1**)	43.3 s ↑	28.4 s ↑	
	(45.9)	(35.5)	
Cym-Cym.2HCl	33.9 s	37.8 s	
	(34.9)	(39.0)	
$[Zn(Cym\text{-}Cym)Cl_2]_n$ (**2**)	35.1 s ↑	38.7 s ↑	
	(41.7**)**	(44.1**)**	

[a]The calculated ^{1}H chemical shifts are not in good relation to the experimental ^{1}H NMR data and additional methodological calculations may be needed.

Table 2.6 ^{13}C chemical shifts (δ, ppm) of RSH ligands and theirzinc(II) complexes

Species	C1	C2	C3	C4	C5	C6
Msa	38.9, 41.9	177.1, 178.9	-	-	-	-
(4)	35.8, (47.6,48.2)	172.1, 173.7 (171.7, 172.0)				
Mnt-H	173.2	129.4	143.1	115.0	143.9	165.1
(5)	170.85	135.0	141.0	118.4	148.6	166.3

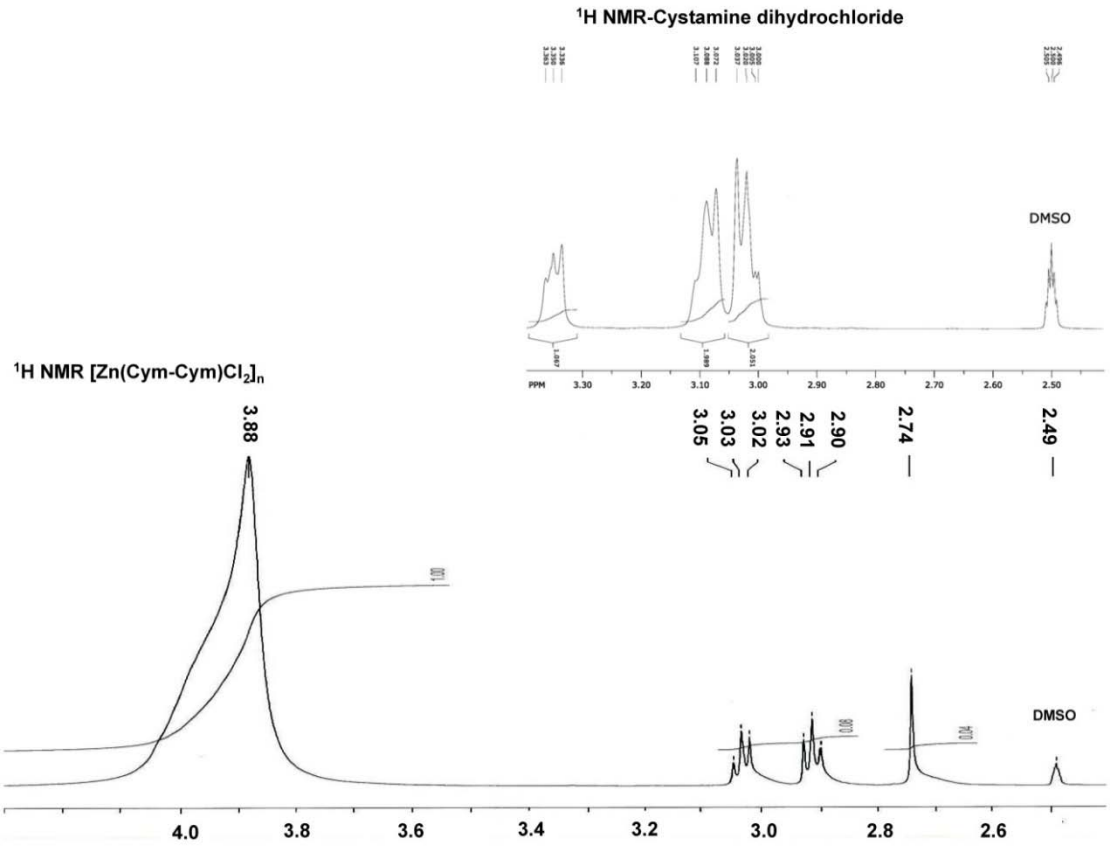

Figure 2.2 ^{1}H NMR data of cystamine dihydrochloride and its $[Zn(Cym\text{-}Cym)Cl_2]_n$ complexes in DMSO.

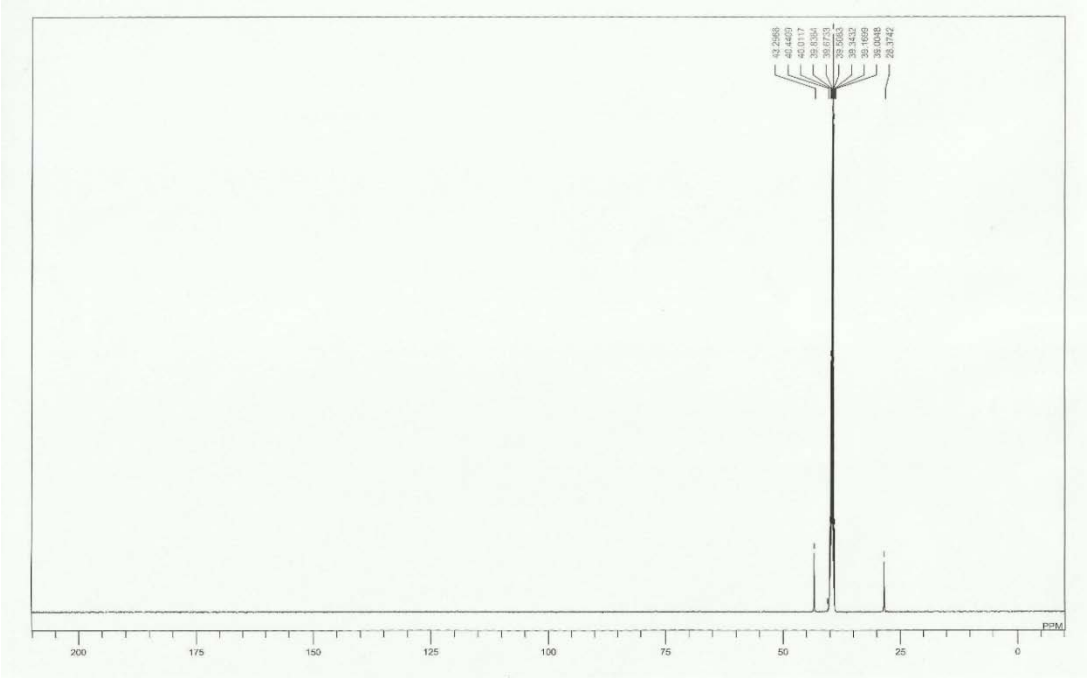

Figure 2.3 The $^{13}C\{^{1}H\}$ NMR spectrum of complex (**1**) in DMSO

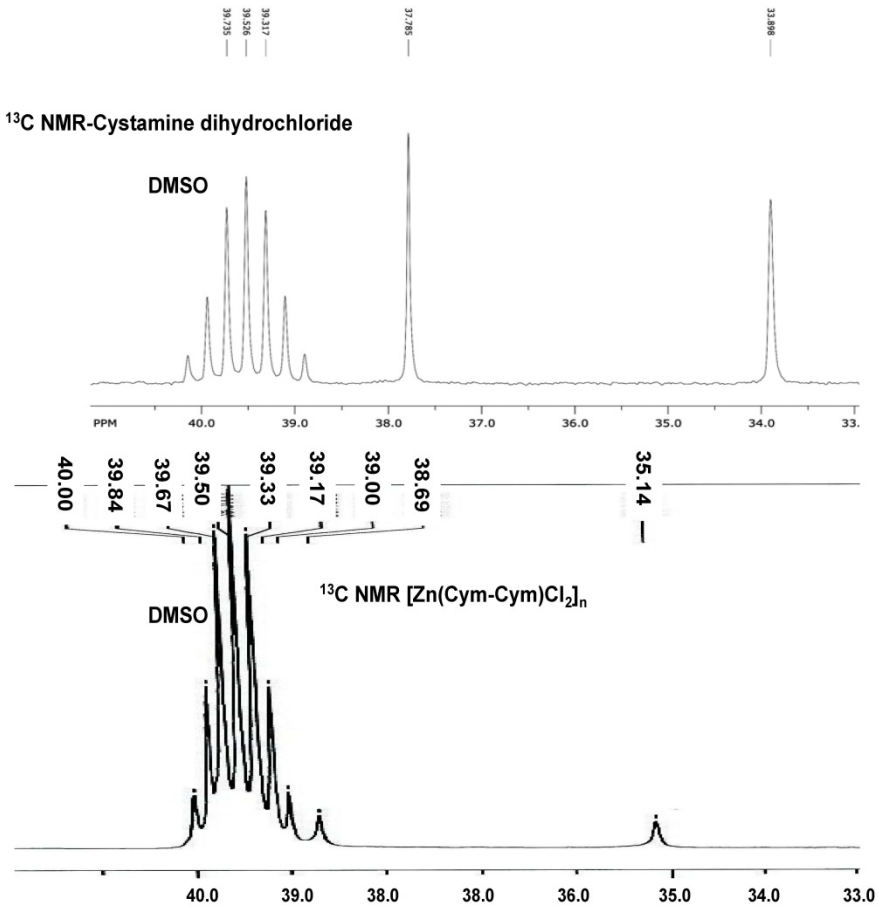

Figure 2.4 ^{13}C NMR data of cystamine dihydrochloride and its $[Zn(Cym\text{-}Cym)Cl_2]_n$ complex (**2**) in DMSO.

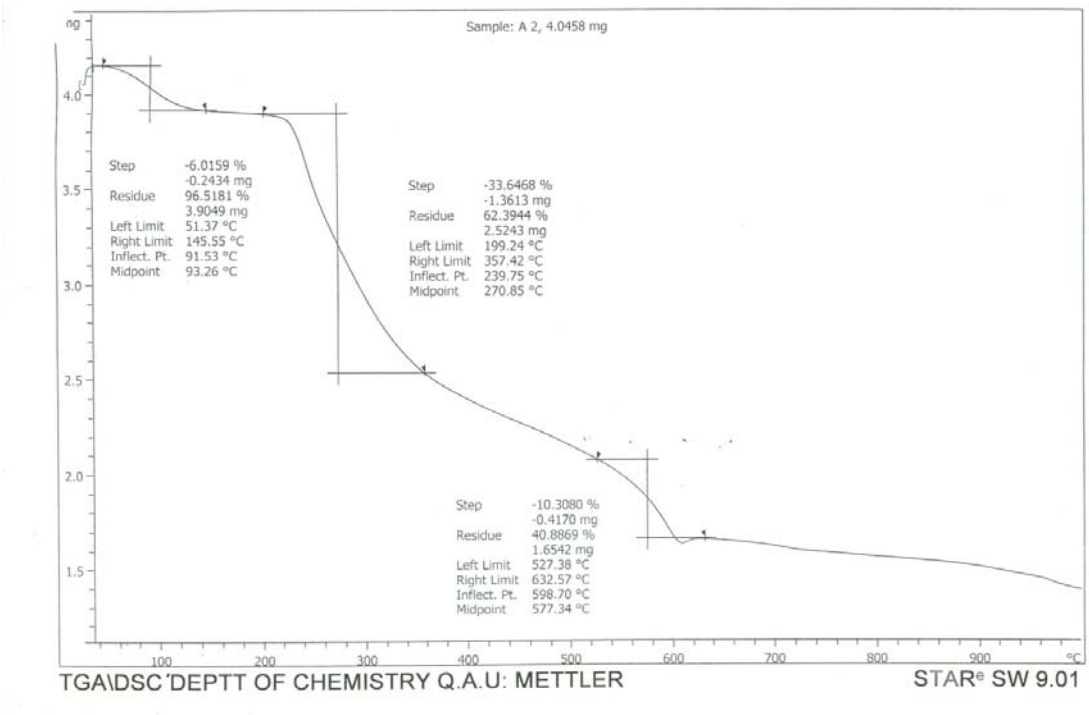

Figure 2.5 Thermogravimetric curve of complex [Zn(Cys-H)Cl].0.5H_2O (**3**).

2.3.2 Description of X-ray structures

The molecular structure of (**1**)is shown in Figure 2.6. The chosen bond lengths (Å) and bond angles (˚) for (**1**) are given in Table 2.7. The complex (**1**) is tetranuclear, $[Zn_4Cym_4Cl_4]$ consisting of two crystallographically independent Zn(II) ions. Zn1 and a symmetry related ion are coordinated with two sulfur atoms and two nitrogen atoms of Cym, while Zn2 and a symmetry related ion exhibit a ZnS_2Cl_2 setup. Zn1 atom shows significant distortion from tetrahedral geometry as the S-Zn1-S/N angles (around 90 and 122^o) are significantly smaller or larger than the tetrahedral value of 109.5^o. The N1-Zn1-S1 with a value of 90.27(15)° shows the largest deviation from the ideal value. The coordination environment around Zn2 is close to regular tetrahedral geometry (∠S-Zn-S/Cl = 105.21(6)^o- 113.49(6)^o). The Cym ligand binds in the chelating mode. The zinc atoms are bridged by S atoms of Cym forming an eight-membered ring. The bridging S atoms exhibit tetrahedral environment. The Zn-L distances are in accordance with those found in other zinc(II) complexes such as, $[Zn(Cym)Cl]_4$ [15]. The compound (**1**) is somewhat similar to the known isomeric zinc(II) complex, $[Zn(Cym)Cl]_4$ [15] but with different coordination environment. The compound $[Zn(Cym)Cl]_4$ is also tetranuclear but in that all four zinc atoms are equivalent, each being coordinated bytwo bridging sulfur atoms, one nitrogen and one chlorine [15].The compound (**1**) on the other hand consists of two crystallographically independent Zn(II) ions, Zn1 and Zn2.The compound$[Zn(Cym)_2]$ exists in the form of a mononuclear chelate having sulfur atom of thiolate bound in a terminal mode [14].

The crystal structure of (**1**) is stabilized by N-H and non-classical intramolecular hydrogen bonding interactions involving methyl H atoms with S and Cl atoms (Table 2.8).H-bonding interactions can clearly be seen in a crystal packing (Figure 2.7). Apart from these relatively strong hydrogen bonds there exist also some weak C–H…S and C–H…Cl bonds. The N–H…Cl are stronger than the C–H…Cl bonds on the basis of polarity.

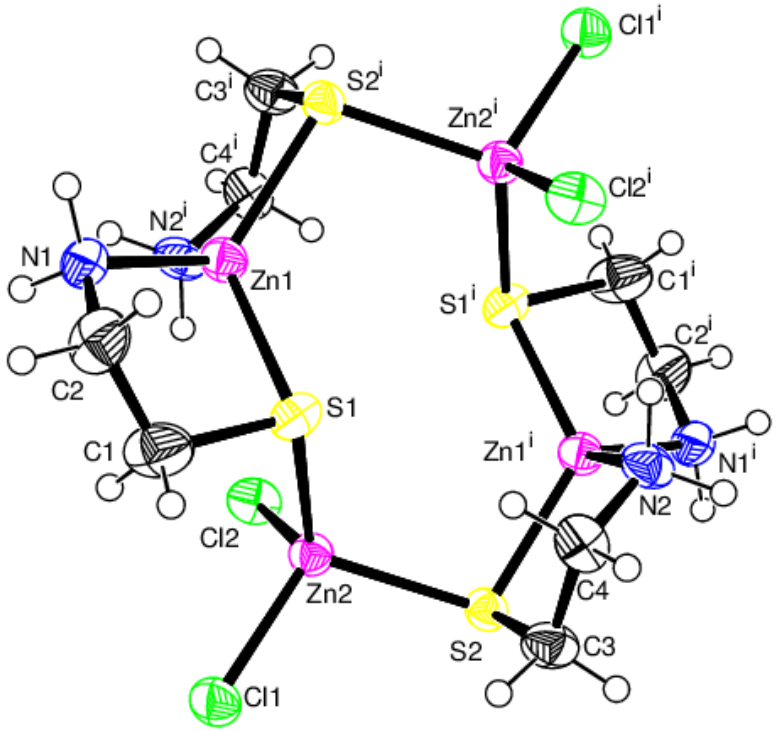

Figure 2.6 Molecular structure of compound (**1**), including the atomic numbering scheme(i = -x,-y,-z)

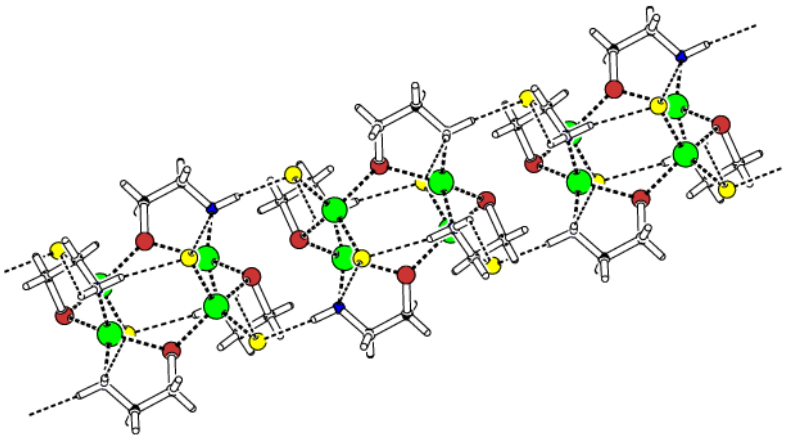

Figure 2.7 Crystal packing diagram of (**1**) showing hydrogen bonding interactions

Table 2.7 Selected bond distances (Å) and bond angles (˚) for (**1**)

Bond Distance		Bond angles	
Zn(1)-N(1)	2.038(5)	N(1)-Zn(1)-N(2)	110.4(2)
Zn(1)-N(2)	2.019(5)	N(1)-Zn(1)-S(1)	90.27(15)
Zn(1)-S(1)	2.3006(16)	N(1)-Zn(1)-S(2)	121.24(15)
Zn(1)-S(2)	2.3087(15)	N(2)-Zn(1)-S(1)	123.28(15)
Zn(2)-Cl(1)	2.2596(16)	N(2)-Zn(1)-S(2)	91.36(14)
Zn(2)-Cl(2)	2.2768(17)	S(1)-Zn(1)-S(2)	122.57(6)
Zn(2)-S(1)	2. 3503(16)	S(1)-Zn(2)-Cl(1)	105.21(6)
Zn(2)-S(2)	2.3369(15)	S(1)-Zn(2)-Cl(2)	113.49(6)
C(1)-S(1)	1.847(8)	S(2)-Zn(2)-Cl(1)	107.49(6)
C(3)-S(2)	1.833(7)	S(2)-Zn(2)-Cl(2)	105.80(6)
C(2)-N(1)	1.450(8)	Cl(1)-Zn(2)-Cl(2)	112.14(6)
C(4)-N(2)	1.459(8)	S(1)-Zn(2)-S(2)	112.68(6)
		Zn(1)-S(1)-Zn(2)	111.24(7)
		Zn(1)-S(2)-Zn(2)	104.62(6)

Table 2.8 Hydrogen bonds in complex (**1**) (Å, º)

Donor-H···Acceptor	D-H	H···A	D···A	∠Δ–H&A
N1-H1A…Cl1^{i}	0.97	2.39	3.335(5)	163.5
N1-H1B…Cl2^{ii}	0.97	2.62	3.495(6)	150.2
N2-H2A…Cl1^{iii}	0.97	2.71	3.359(5)	125.1
N2-H2A…Cl2^{iii}	0.97	2.94	3.416(5)	111.4
N2-H2B…Cl2^{iv}	0.97	2.48	3.381(5)	155
C3-H3A…Cl1	0.97	2.98	3.638(7)	126
C4-H4A…S1	0.97	2.85	3.721(7)	150.5
C4-H4B…Cl^{iii}	0.97	2.99	3.632(7)	125

Symmetry codes: (i) *x*+1/2, −*y*+1/2, *z*+1/2; (ii) −*x*, −*y*, −*z*+1; (iii) *x*, *y*+1, *z*; (iv) −*x*, −*y*+1, −*z*+1.

The asymmetric unit of compound(**2**) shown in Figure 2.8, consists of a zinc(II) ion bound to two cystamine ligands and two chloride ions. The coordination sphere around Zn1 is a distorted tetrahedron that consists of two Cl donor atoms and two N donor atoms of cystamine. The sulfur atoms of cystamine retained the disulfide linkage with S-S bond distance of 2.0304(19) Å and did not participate in coordination. The particular bond distance (Å) and bond angles (˚) are given in Table 2.9. The asymmetric units are linked in the form of one-dimensional polymeric chains extending along the crystallographic *b*-axis (Figure 2.9). The Zn1-$S2^{i}$ [i = -x, y+1/2, -z+1/2] and Zn1-S1 distances are 5.1706(16) and 5.1890(15) Å, respectively. In these polymeric chains, the Zn-Zn distance is 10.5434(13) Å. The bond angles about the zinc atom are qualified for tetrahedral geometry (Table 2.9). The Zn–N [2.041(4) and 2.032(4) Å] and Zn–Cl [2.2301(14)–2.2569(13) Å] distances are equivalent to the values given for other like complexes [14,15]. The R-S-S-R unit is not linear as the angles around sulfur are in the range of tetrahedral geometry. A similar binding of disulfide has been observed in the structure of dichloro[*bis*(1-methylimidazole-2)disulfidozinc] [201].

The composition of compound (**1**) and the related complex, $[Zn(Cym)Cl]_4$[15] is same andthe Zn:Cym ratio in both compounds is 1:1. Both of them exist in the form of cyclic and tetranuclear complexes through sulfur bridging but with different coordination environments. On the other hand, the compound (**2**) is a linear polymer that containsZn-Cym-Cymin the ratio of1:1.

In the crystal packing of the complex, the polymeric chains are inter-linked due toD—H--S and D—H—Cl(D = C, N) hydrogen bonds.The H-bonding interactions are illustrated in Figure 2.10 and Table 2.10. A 2D network structure was formed throughH-bonding interactions as shown in Figure 2.10.

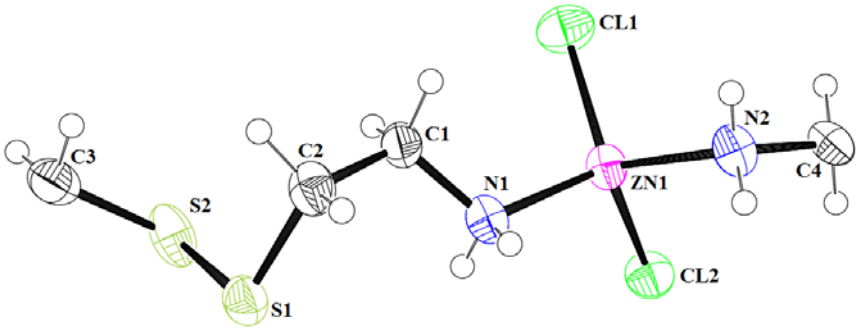

Figure 2.8 The asymmetric unit of (**2**)with thermal ellipsoids drawn at 50 % probability level

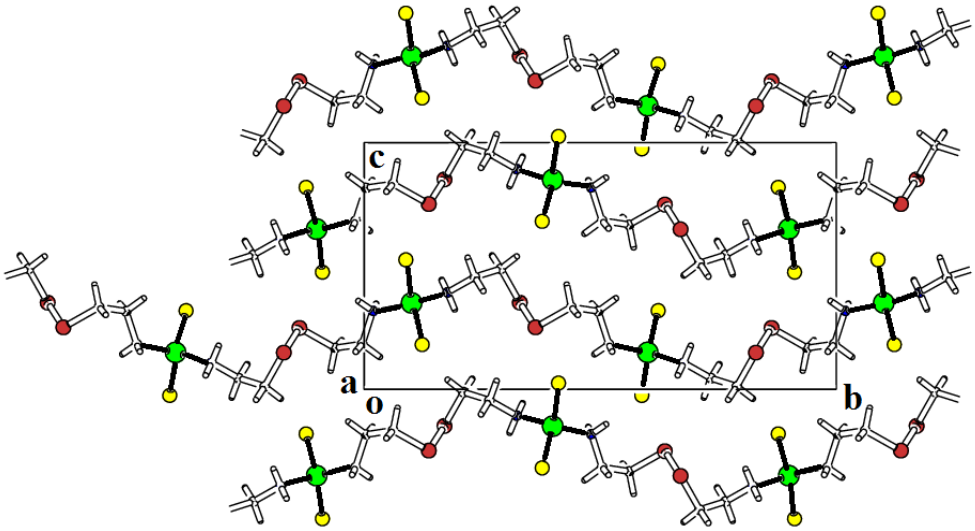

Figure 2.9 A projection perpendicular to ***b*** axis showing theformation of one dimensional polymeric chains along the ***a***axis in (**2**)

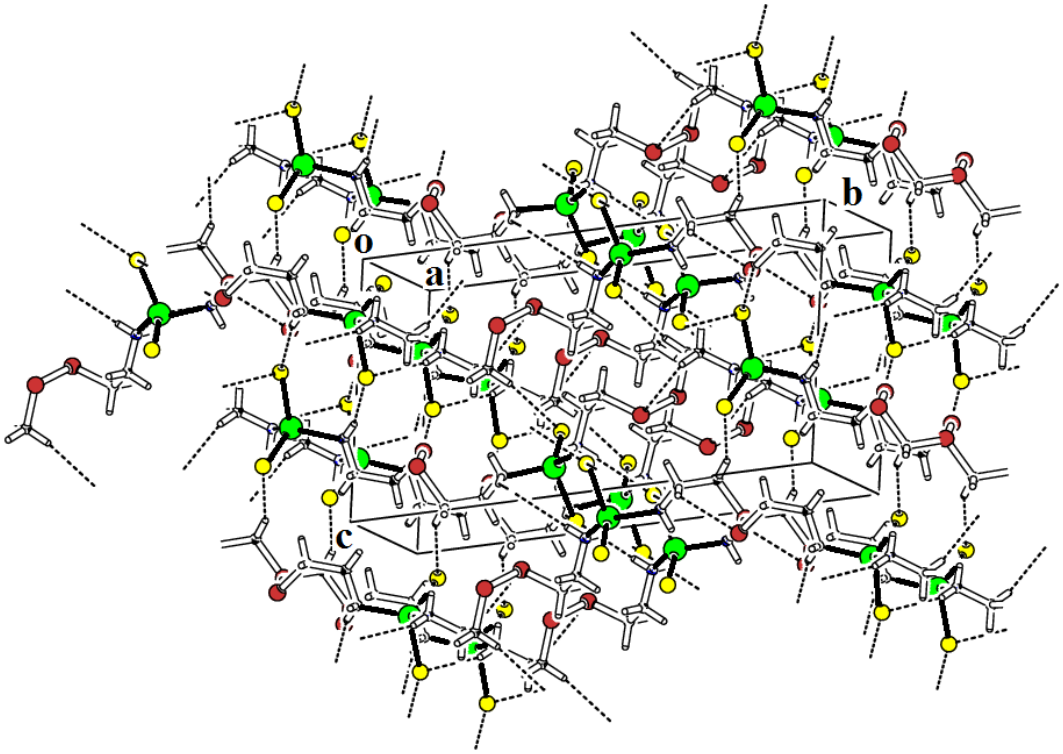

Figure 2.10 Crystal packing diagram of (**2**) showing H-bonding interactions

Table 2.9 Selected bond distances (Å) and bond angles (˚) for (**2**)

Bond Distance		Bond angles	
Zn(1)-N(1)	2.041(4)	N(1)-Zn(1)-N(2)	106.82(17)
Zn(1)-N(2)	2.032(4)	N(1)-Zn(1)-Cl(1)	110.94(13)
Zn(1)-Cl(1)	2.2301(14)	N(1)-Zn(1)-Cl(2)	112.12(13)
Zn(1)-Cl(2)	2.2569(13)	N(2)-Zn(1)-Cl(1)	112.56(14)
S(1)-C(2)	1.802(5)	N(2)-Zn(1)-Cl(2)	105.58(13)
S(2)-C(3)	1.812(5)	Cl(1)-Zn(1)-Cl(2)	108.73(5)
S(1)-S(2)	2.0304(19)	S(1)-S(2)-C(3)	102.38(18)
C(1)-N(1)	1.470(6)	S(2)-S(1)-C(2)	103.89(18)

Table 2.10 Hydrogen bonds in complex (**2**) (Å, º)

Donor-H···Acceptor	D-H	H···A	D···A	∠Δ–H&A
N1-H1C…Cl2	0.8	2.67	3.431(4)	160
N1-H1D…Cl2	0.81	2.95	3.697(5)	154
N2-H2C…S2	0.85	2.89	3.290(4)	111
N2-H2D…Cl2	0.88	2.56	3.390(5)	156
C1-H1B…Cl1	0.97	2.92	3.595(5)	127.5
C3-H3A…Cl1	0.97	2.82	3.729(5)	156.3
C4-H4A…S1	0.97	2.82	3.341(5)	114.7
C4-H4B…S1	0.97	2.94	3.672(5)	133.5

2.3.3 Comparative geometrical analysis of the ligands (CymH and Cym- Cym) and the corresponding Zn(II) complexes

Selected experimental and calculated bond lengths of the ligands, cysteamine (zwitterionic tautomer form), cystamine (Cym-Cym·2HCl) and the corresponding Zn(II) complexes; $[Zn_4Cym_4Cl_4]$ (**1**)(Figure 2.6),$[Zn(Cym\text{-}Cym)Cl_2]_n$ (**2**) (Figure 2.8)and $[Zn_4Cym_4Cl_4]$ (**1A**) (Figure 2.11),are summarized in Table 2.11 and they allowto trace the bond length changes in the ligands and their complexes **1**, **2** and **1A**. It is expected that the deduced trends help the assignment of the IR vibrational modes of the compounds studied. Firstly, the comparison of the C-S, C-C and C-N bond lengths of the CymH and Cym-Cym ligands showed that they increase in the cystamine due to S-S bond formation and this change is larger for C-N and C-C bonds (by ~0.1 Å).

A survey of the experimental bond lengths of CymH ligand and its Zn(II) complexes,**1** and **1A**revealedthe following trends. The C-S bond length (at 1.823 Å) was found to increase in the cyclic $[Zn_4Cym_4Cl_4]$ and $[ZnCymCl]_4$ complexes (by 0.1-0.2 Å). The C-N bond length decreases in the $[Zn_4Cym_4Cl_4]$ complex (by ~0.03 Å) and it is only slightly changed in $[ZnCymCl]_4$. The result obtained reflects the N,S-bidentate binding of Cym to Zn(II) in **1** and **1A**, where the sulfur atom is bridging the two Zn(II) ions as shown Figure 2.6 and 2.11. The C-N bond changes in the complexes**1** and **1A** are unrepresentative as regards the ligand coordination to Zn(II) through the N atom. One explanation is the zwitterionic form of the Cym ligand, where the $–C\text{-}NH_3^+$ group exists and an elongated C-N bond is expected. In summary, the significant increase of the C-S bond lengths (in complexes **1** and **1A**) could be indicative for the bridging coordination through the S atom. The coordination of the ligand studied through the N atom (complexes **1**, **2** and **1A**), however, does not produce explicit C-N bond length changes as the isolated ligand forms differ from the coordinated ones in the complexes.

Tracing the bond length variation going from Cym-Cym ligand to the polymeric Zn(II) complex (**2**), a decrease for all ligand bonds was observed. The C-N bond length showed significant decrease by 0.12 Å and the extent of the bond length change diminishes in the following order: C-C, C-S, S-S. The result obtained could be related to the bridging binding of the Cym-Cym ligand to two Zn(II) ions through the nitrogen atoms of the two

amino groups(Figure 2). At first sight, the decrease of the C-N bonds due to coordination of the ligand N atom to Zn(II) is unusual. However, it should be taken into account, that Cym-Cym crystallizes with two HCl and hydrogen bonds network (NH···Cl) exists in the solid state [202]. The calculated geometry of the isolated Cym-Cym ligand and the obtained shorter C-N and C-C bond lengths (Table 2.11) as compared to that of the solid state experiment confirmed the suggestion made above.

A comparison of the experimental Zn-ligand bond lengths for the three complexes shows that the Zn-Cl, Zn-N and Zn-S (for **1** and **1A**) distances vary in the region 2.230 – 2.277 Å, 2.019 – 2.045 Å and 2.301 – 2.368 Å, respectively. The Zn-N bond lengths were elongated in the following order: $[Zn_4Cym_4Cl_4]$ (**1**), $[Zn(Cym\text{-}Cym)Cl_2]_n$ (**2**) and $[ZnCymCl]_4$ (**1A**). Shorter C-S bonds were also found in complex **1** in comparison with the complex **1A**. Apparently, the bidentate binding of the two Cym ligands to Zn(II) (in $[Zn_4Cym_4Cl_4]$) leads to shorter Zn-N and Zn-S bond lengths than that in $[ZnCymCl]_4$, Figure 2.11. The Zn-Cl bond distances are similar and shorter for $[Zn(Cym\text{-}Cym)Cl_2]_n$ and $[ZnCymCl]_4$ than these for $[Zn_4Cym_4Cl_4]$ complex. It is expected that the comparative analysis of the geometrical parameters of ligands and their Zn(II) complexes studied to help the reliable interpretation of their vibrational data and to derive relation between the ligand coordination behavior, bond length changes and vibrational analysis.

A comparison of the geometrical parameters of $[Zn_4Cym_4Cl_4]$ complex calculated in gas phase and in solid state showed that the last ones better approach the experimental structural data. For $[ZnCymCl]_4$complex the calculated bond lengths in gas phase and in solid state are similar. As it is seen, the calculated bond lengths of the Zn(II) complexes **1**, **2** and **1A** are in good agreement with the experimental ones, the deviations from the experimental Zn-S/N/Cl bonds are up to ~0.03 Å. Larger C-S (by ~0.03 Å) and S-S (by ~0.10 Å) bond lengths were calculated for $[Zn(Cym\text{-}Cym)Cl_2]_n$ complex in solid state.The trends observed for the experimental bond lengths in the complexes are well reproduced from the solid state calculations and this finding is a good prerequisite for the reliable assignment and interpretation of the vibrational frequencies.

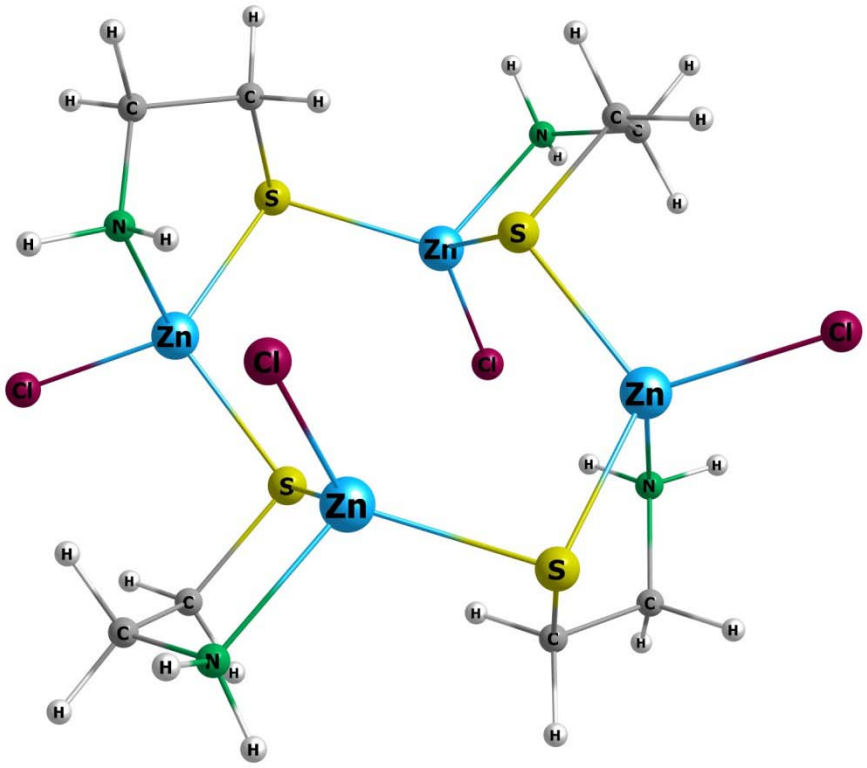

Figure 2.11 Optimized geometry structure of $[ZnCymCl]_4$ (**1A**) in gas phase at DFT/PBE1PBE/**B1** level.

Table 2.11 Selected experimental and calculated bond lengths (Å) of polymeric $[Zn(Cym\text{-}Cym)Cl_2]_n$, cyclic $[Zn_4Cym_4Cl_4]$ and $[ZnCymCl]_4$ complexes, compared to the cystamine (Cym-Cym·2HCl) and cysteamine (Cym, zwitterionic tautomer) ligands parameters

Bonding	$[Zn(Cym\text{-}Cym)Cl_2]_n$.(**2**)		Cym-Cym·2HCl		$[Zn_4Cym_4Cl_4]$ (**1**)			$[ZnCymCl]_4$(**1A**)			Cym
	exp [this work]	calc	exp[a]		exp[b]	calc		exp[c]	Calc		exp[d]
		solid[e]		gas[f]		solid[e]	gas[f]		solid[e]	gas[f]	
Zn-Cl	2.257	2.241			2.277	2.292	2.264	2.241	2.249	2.242	
	2.230	2.231			2.260	2.279	2.231	2.234		2.227	
Zn-N	2.041	2.074			2.038	2.050	2.144	2.045	2.070	2.100	
	2.032	2.042			2.019	2.039	2.070	2.043	2.065	2.135	
Zn-S	-	-			2.350	2.360	2.454	2.368	2.377	2.366	
					2.337	2.343	2.410	2.312	2.320	2.338	
					2.309	2.324	2.291	2.360	2.377	2.385	
					2.301	2.311	2.298	2.323	2.358	2.353	
C-S	1.812	1.844	1.83(10)	1.83	1.847	1.846	1.837	1.843	1.841	1.842	1.823
	1.803	1.843	1.87(5)		1.833	1.844	1.833	1.830		1.834	
C-C	1.506	1.511	1.56(7)	1.52	1.508	1.523	1.521	1.502	1.516	1.518	1.500
	1.505	1.510	1.62(9)		1.500	1.521	1.515			1.515	
C-N	1.470	1.485	1.56(9)	1.45	1.459	1.478	1.480	1.495	1.477	1.475	1.487
			1.62(6)		1.451	1.477	1.478	1.473		1.468	
S-S	2.030	2.127	2.06(4)	2.07	-	-	-				-

[a] ref [202],
[b] ref. [14],
[c] ref. [15],
[d] this work.
[e] optimized structure in solid state with DFT/PAW-PBE method (VASP program).
[f] optimized structure in gas phase at DFT/PBE1PBE/**B1** level (**B1** is a combined basis set, seeComputational Details).

2.3.4 Vibrational analysis of $[Zn_4Cym_4Cl_4]$ (1) and $[Zn(Cym\text{-}Cym)Cl_2]_n$ (2)

The vibrational spectroscopy is a finger print tool able to provide information on the coordination polyhedron around the metal ion in solid state. Our study is directed to reliable interpretation of the measured IR spectral data of $[Zn_4Cym_4Cl_4]$ (**1**) and the novel $[Zn(Cym\text{-}Cym)Cl_2]_n$ complex (**2**) by means of DFT modelling and IR spectra simulations in solid state and in gas phase for comparison. In addition, the measured IR spectral data of [Cym-Cym·2HCl] ligand and available vibrational data for cysteamine negative form [203] are used to trace the ligand frequency shifts upon coordination to the Zn(II) ion. The experimental IR spectra of cysteamine and $[Zn_4Cym_4Cl_4]$ complex are compared in Figure 2.12. The experimental IR spectra of the region 2000-400 cm^{-1} of Cym-Cym·2HCl, cyclic $[Zn_4Cym_4Cl_4]$ complex (**1**) and polymeric $[Zn(Cym\text{-}Cym)Cl_2]_n$ cmplex (**2**) areshown in Figure 2.13. The IR spectra of the region 4000-2000 cm^{-1} are presented in Figure 2.14. The experimental and calculated vibrational frequencies, and their assignments for complexes **1** and **2** are given in Tables 2.12 and 2.13, respectively.

Nuclear site group analysis and vibrational assignment

The nuclear site group analysis (symmetry analysis carried out on every atom in the primitive unit cell based on space group and occupied Wyckoff positions) is useful tool to predict the type, number and symmetry of the normal modes for compounds **1** and **2**. The $[Zn_4Cym_4Cl_4]$ (**1**) crystal, which is in monoclinic $P2_1/c$ (Z=4) space group and point group C_{2h} (2/m) shows total 288 normal modes as follow: $\Gamma_{optic} = 72A_g + 71A_u + 72B_g + 70B_u$ (including $3A_g$ unit cell rotation modes) and $\Gamma_{acoustic} = A_u + 2B_u$. The ungerade A_u and B_u modes should be IR active and the gerade A_g and B_g modes – Raman active. The $[Zn(Cym\text{-}Cym)Cl_2]_n$ (**2**) crystal is in monoclinic $P2_1/c$ (Z=4) space group and point group C_{2h} (2/m) and all atoms are in 4e Wyckoff positions. Complex (**2**) in C_{2h} point group displays total 276 normal modes, which belong to A_g, A_u, B_g and B_u symmetry as follow: $\Gamma_{optic} = 69A_g + 68A_u + 69B_g + 67B_u$ (including $3A_g$ unit cell rotation modes) and $\Gamma_{acoustic} = A_u + 2B_u$ (unit cell translation modes). The "*ungerade*" A_u and B_u normal modes are IR active modes and *"gerade"* A_g and B_g are Raman active modes.

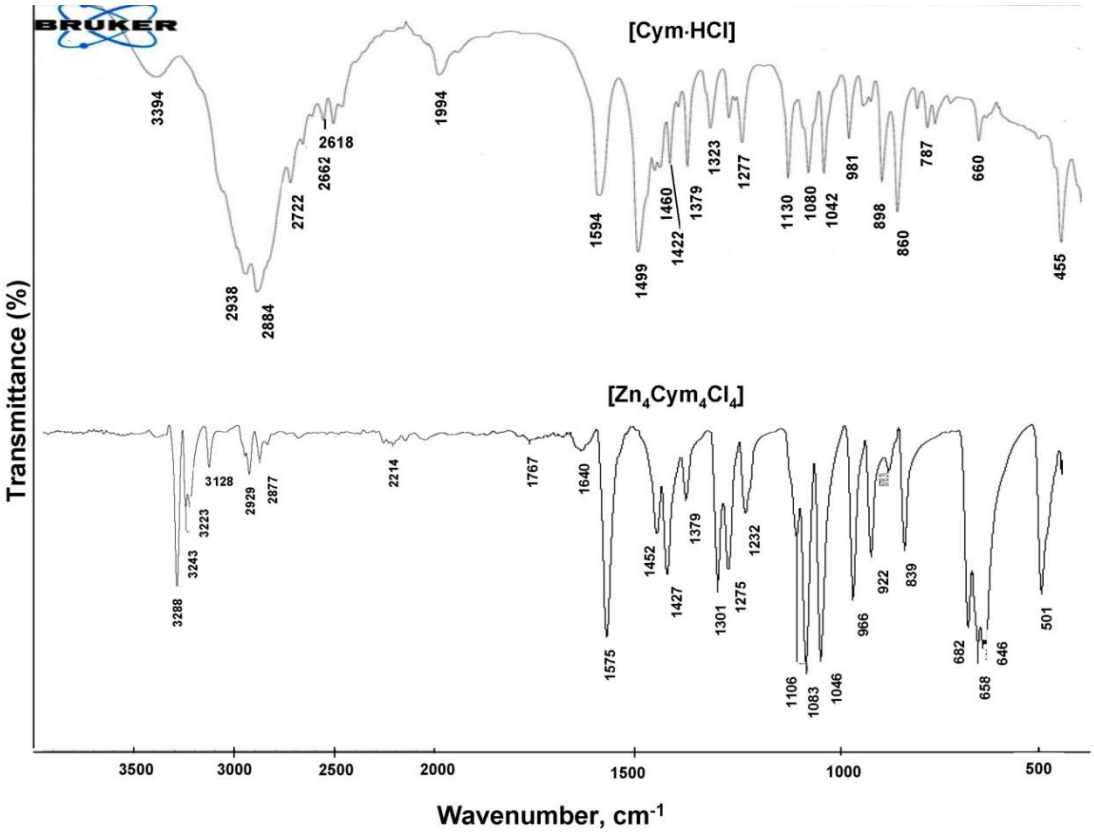

Figure 2.12 Experimental IR spectra of [Cym·HCl] ligand and cyclic $[Zn_4Cym_4Cl_4]$ (**1**) complex

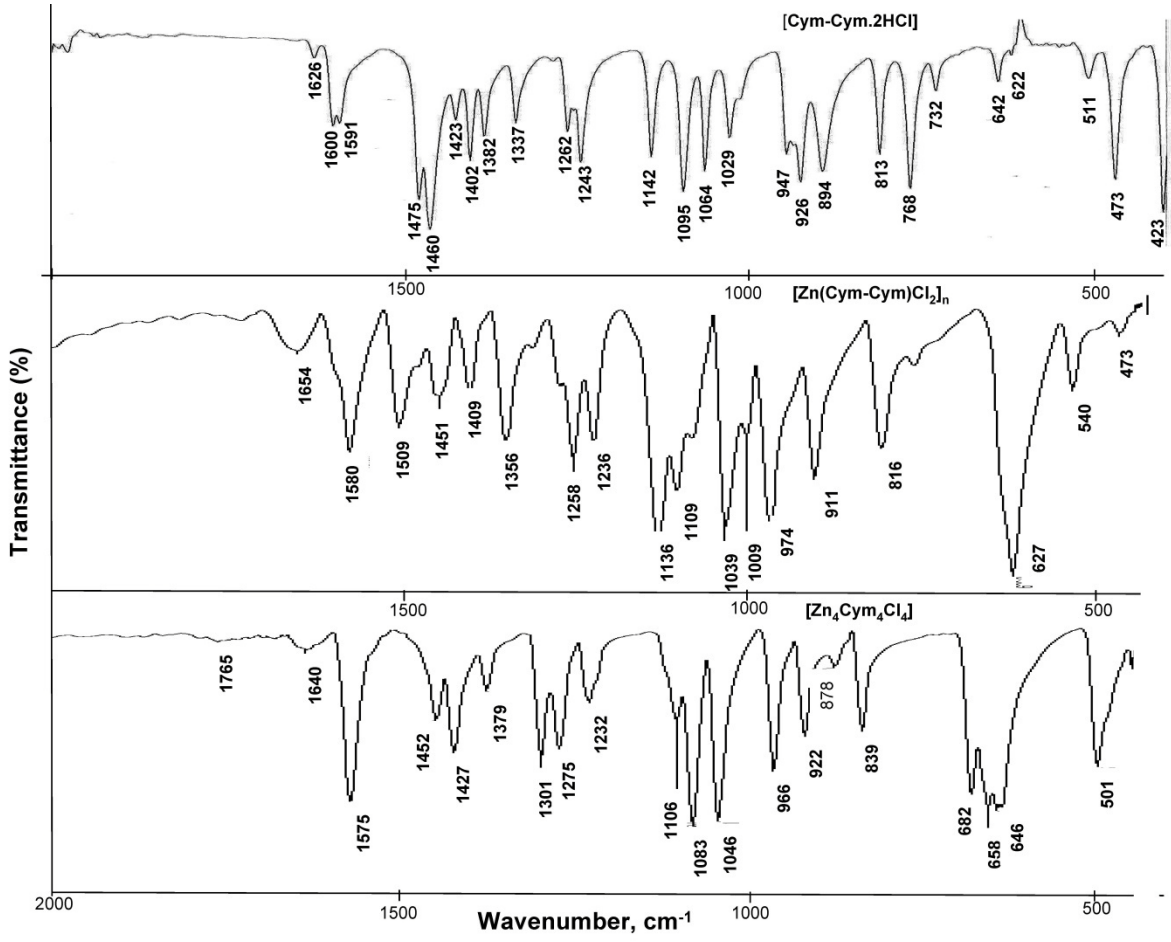

Figure 2.13 Experimental IR spectra (2000-400 cm^{-1}) of [Cym-Cym·2HCl], cyclic $[Zn_4Cym_4Cl_4]$ (**1**) and polymeric $[Zn(Cym\text{-}Cym)Cl_2]_n$ (**2**) complexes.

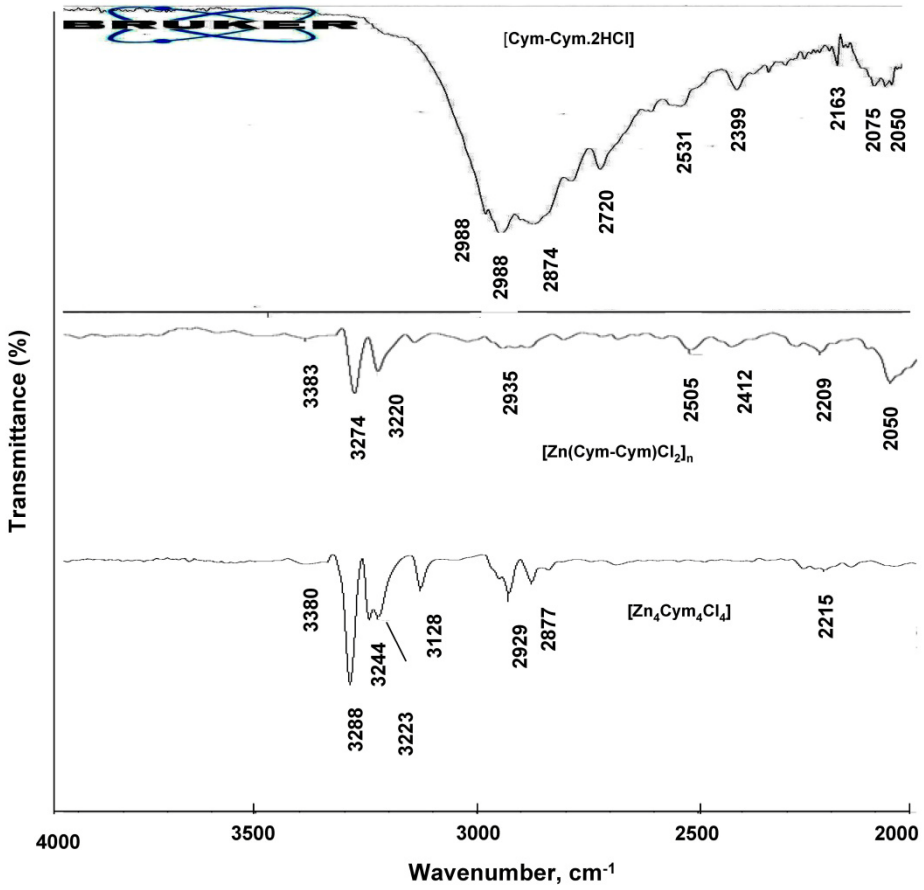

Figure 2.14 Experimental IR spectra (4000-2000 cm^{-1}) of [Cym-Cym·2HCl] ligand, cyclic $[Zn_4Cym_4Cl_4]$ (**1**) and polymeric $[Zn(Cym\text{-}Cym)Cl_2]_n$ (**2**) complexes.

Table 2.12 Experimental IR and calculated harmonic frequencies (cm^{-1}) of cyclic $[Zn_4Cym_4Cl_4]$ complex (Z = 4). Comparison with the experimental (Raman) frequencies of deprotonated cysteamine and CymH·HCl ligand in the solid state.

$[Zn_4Cym_4Cl_4]$						Cysteamine	
exp.	calc.					exp.	
	gas phase (C_i)		Solid		Assignments		
	A_u (IR int.)	A_g (Ra int.)[b]	freq (IR_{int})	freq (IR_{int}=0)		Ra [a] (deprot.form)	IR (CymH·HCl)
3380 w	3595 (40)	3595 (257)	3377 (0.35), 3377 (0.22)	3376 *	$\nu_{as}(NH_2)$	3365 m-w,sh	3394 w
3288 s	3559 (53)	3559 (435)	3353 (0.44), 3353 (0.44)	3353 *	$\nu_{as}(NH_2)$		2937 s
3244 m	3514(20)	3514 (644)	3303 (0.14), 3300 (0.50)	3302, 3299	$\nu_{s}(NH_2)$	3301 vs	2884 vs
3223 m	3354 (652)	3352 (961)	3252 (0.09), 3249 (1.0)	3252, 3251	$\nu_{s}(NH_2)$		
	3161 (1)	3161 (479)	3065 (0.002) *	3065 *	$\nu_{as}(CH_2)$		2722 w
3128 m	3157 (2)	3157 (353)	3057 (0.01) *	3057 *	$\nu_{as}(CH_2)$	2950 m	2663 w
	3138 (2)	3138 (647)	3044 (0.002) *	3044 *	$\nu_{as}(CH_2)$		2618 w
	3132 (18)	3132 (576)	3030 (0.01), 3030 (0.03)	3030 *	$\nu_{as}(CH_2)$		2561 w
	3093 (19)	3093 (859)	3004 (0.01), 3004 (0.002)	3004 *	$\nu_{s}(CH_2)$		2511 w
2929 m	3074 (111)	3074 (2706)	2992 (0.02), 2992 (0.01)	2992 *	$\nu_{s}(CH_2)$	2920 vs	
2877 w	3064 (37)	3064 (940)	2990 (0.03), 2990 (0.01)	2990 *	$\nu_{s}(CH_2)$	2872 s	
	3060 (83)	3060 (2209)	2983 (0.06), 2983 (0.004)	2983 *	$\nu_{s}(CH_2)$	2845 s	

2215 d,w	overtone						1994 m
1640 m	1696 (40)	1696 (33)	1584 (0.01), 1584 (0.04)	1585, 1583	$\delta(NH_2)_b$		
1575 vs	1686 (108)	1685 (164)	1578 (0.13), 1578 (0.02)	1576, 1575	$\delta(NH_2)_b$	1596 m	1594 s
	1511 (5)	1510 (298)	1450 (0.004), 1450 (0.01)	1450 *	$\delta(CH_2)_b$	1463 m	1499 vs
1452 s	1506 (21)	1506 (307)	1440 (0.06), 1440 (0.01)	1440 *	$\delta(CH_2)_b$	1436 s	1459,1423 d,w
1427 s	1482 (17)	1482 (359)	1425 (0.01), 1425 (0.003)	1425 *	$\delta(CH_2)_b$		
	1476 (25)	1476 (205)	1414 (0.07), 1414 (0.01)	1414 *	$\delta(CH_2)_b$		
1379 s	1431 (2)	1431 (84)	1374 (0.004) [2]	1374 *	$\delta(CH_2)_{wag}$	1384 w	1379 m
	1425 (5)	1425 (28)	1369 (0.02)	1369 *	$\delta(CH_2)_{wag}+(NH_2)_{tw}$	1354 m	1323 m
1301 s	1353 (22)	1352 (257)	1292 (0.02)[2],1292 (0.01)	1292	$\delta(NCH)+\delta(CH_2)_{wag}$		
	1346 (33)	1346 (126)	1287 (0.03), 1287 (0.01)	1287 *	$\delta(NCH)$		
1275 s	1322 (19)	1322 (148)	1267 (0.03), 1267 (0.01)	1267 *	$\delta(CH_2)_{wag}+(NH_2)_{tw}$	1271 vs	1278 w
1232 m	1315 (30)	1317 (134)	1259 (0.07)	1259 *	$\delta(CH_2)_{wag}^{g}/\delta(CH_2)_{tw}^{s}$	1234 m	1244 s
	1280 (20)	1279 (146)	1220 (0.05)	1220 *	$\delta(CCH)+\delta(SCH)^{g}/$ $\delta(CH_2)_{wag}+\delta(NH_2)_{wag}^{s}$		
	1274 (15)	1275 (204)	1209 (0.02), 1207 (0.001)	1209 *	$\delta(SCH)+\delta(CCH)^{g}/$ $\delta(CH_2)_{wag}^{s}$		
	1165 (74)	1163 (367)	1116 (0.01), 115 (0.001)	1116 *	$\delta(CH_2)_{tw}+\delta(NH_2)_{tw}$	1130 w	1130 s
1106 m	1137 (63)	1137 (104)	1103 (0.004), 1103(0.002)	1103 *	$\delta(SCH)+\delta(CH_2)_{tw}^{g}/$		

					$\nu(CN)+\delta(CH_2)_r^s$		
	1131 (49)	1131 (213)	1095 (0.03), 1092 (0.01)	1095 *	$\delta(CH_2)_{tw}+\delta(NH_2)_{tw}$		
1083 vs	1097 (197)	1096 (333)	1073 (0.25), 1069 (0.002)	1075, 1069	$\delta(NH_2)_{wag}$	1063 m	1080 s
	1086 (23)	1086 (99)	1060 (0.02), 1060 (0.002)	1055 *	$\nu(CN)+\nu(CC)$		
1046 vs	1082 (31)	1081 (78)	1054 (0.004), 1053 (0.17)	1053 *	$\nu(CN)+\nu(CC)$	1016 w	1042 s
	991 (1)	990 (256)	968 (0.001), 966 (0.001)	967, 966	$\delta(CH_2)_r$		
966 m	980 (71)	980 (94)	952 (0.08), 950 (0.003)	953 *	$\delta(CH_2)_r$	896 w	981 m
922 m	950 (20)	950 (181)	921 (0.001), 920 (0.02)	921, 920	$\nu(CC)$		946 w
876 w	947 (43)	947 (201)	919 (0.02), 919 (0.04)	919 *	$\nu(CC)$		898 s
839 m	857 (13)	858 (245)	836 (0.01), 835 (0.03)	834 *	$\delta(CCH)+\delta(CH_2)_r$	824 m	860 s
	856 (18)	856 (96)	834 (0.001), 833 (0.001)	834, 833	$\delta(CH_2)_r$		812 w
	690 (17)	690 (2014)	705 (0.05), 704 (0.10)	706, 703	$\delta(NH_2)_r^s\,(\nu(CS)^g)$		730 vw
682 s	685 (14)	685 (499)	671 (0.01), 670 (0.18)	671, 669	$\delta(NH_2)_r^s\,(\nu(CS)^g)$	656 vs	660 m
658 s	667 (52)	667 (462)	650 (0.04)	650 *	$\nu(CS)^s\,(\delta(NH_2)_r^g)$		787 w
646 s	605 (47)	604 (326)	641 (0.01), 638 (0.05)	639, 638	$_/\nu(CS)^s\,(\delta(NH_2)_r^g)$		768 w
501 m	494 (32)	494 (217)	498 (0.02),497 (0.07)	498, 496	$\delta(CCN)$		455 s
428 w,d	463 (5)	463 (87)	484 (0.02), 484 (0.004)	484 *	$\delta(CCN)$	401 m	~ 400 m
412 w	411 (42)	410 (410)	425 (0.004), 424 (0.02)	428,425	$\nu(ZnN)$		
405 w	385 (19)	382 (1444)	413 (0.01), 412 (0.01)	411 *	$\nu(ZnN)$		

344 (127)	343 (977)	319 (0.003), 316 (0.02)	317, 315	skel (ν(ZnCl)^{g})
326 (63)	325 (501)	315 (0.06), 314 (0.10)	315, 314	ν(ZnS)
310 (43)	308 (158)	292 (0.01), 291 (0.09)	293, 291	skel
290 (62)	290 (1148)	281 (0.05), 280 (0.05),	283, 277	skel
285 (48)	283 (1647)	274 (0.04), 271 (0.23)	274, 273	ν(ZnCl) (skel^{g})
		264 (0.02), 263 (0.05),	263, 261	δ(SZnS)
		254 (0.03), 253 (0.03)	257, 256	
		242 (0.01), 242 (0.03)	238, 236	

[a]ref. [41], the Raman measurements were in solution

[b] T =298.15 K, incident laser intensity, 10000 cm^{-1}.

*Double-repetitive frequency.

Molecular vibrations: b, bending; wag, wagging; tw, twisting; r, rocking; s, solid; g, gas phase.

Table 2.13 Experimental IR and calculated harmonic frequencies (cm^{-1}) of polymeric $[Zn(Cym\text{-}Cym)Cl_2]_n$ complex (Z = 4) compared to the experimental IR data of [Cym-Cym·2HCl] ligand.

$[Zn(Cym\text{-}Cym)Cl_2]_n$				[Cym-Cym·2HCl]
exp.	calc.[a]			exp.
	freq (IR_{int})[b]	freq[c] (IR_{int}=0)	Assignments	
3383 w	3377 (0.06) *	3377 *	$\nu_{as}(NH_2)$	2988sh
3274 m	3371 (0.44), 3370 (0.35)	3365 *	$\nu_{as}(NH_2)$	2950 s
3220 m	3236 (1.0), 3236 (0.07)	3240, 3239	$\nu_s(NH_2)$	
~3130 w	3177 (0.91), 3177 (0.62)	3180, 3179	$\nu_s(NH_2)$	
	3039 (0.01), 3039 (0.03)	3039 *	$\nu_{as}(CH_2)$	2874 s
2990 w	3028 (0.004), 3026 (0.6)	3028, 3027	$\nu_{as}(CH_2)$	2720 w
	3019 (0.001), 3019 (0.02)	3021, 3020	$\nu_s(CH_2)$	
	3014 (0.003),314 (0.07)	3014 *	$\nu_s(CH_2)$	
2935 w	2850 (0.29), 2850 (0.02)	2850 *	$\nu(CH_2)$	
	2847 (0.39), 2847 (0.002)	2847 *	$\nu(CH_2)$	
	2707 (0.01), 2707 (0.02)	2707 *	$\nu(CH_2)$	
	2699 (0.03), 2699 (0.01)	2699 *	$\nu(CH_2)$	2531w
2505 w		Overtone		2399 w
2412 w		Overtone		2163 w

2209 w		Overtone		2075 m
2050 m		Overtone		2050 m
1654 m	1594 (0.10), 1594 (0.001)	1616, 1615	$\delta(NH_2)_b$	1626 w
1580 s, br	1566 (0.01), 1566 (0.10)	1566 *	$\delta(NH_2)_b$	1600, 1591 d,m
1509 s	1422 (0.04), 1422 (0.02)	1422 *	$\delta(CH_2)_b$	1475, 1460 d,s
1451 m	1418 (0.02), 1418 (0.08)	1418 *	$\delta(CH_2)_b$	1423 m
1409 m	1396 (0.004), 1396 (0.12)	1401 *	$\delta(CH_2)_b$	1402 m
	1374 (0.03), 1373 (0.10)	1374, 1373	$\delta(CH_2)_b$	
1356 s	1360 (0.01), 1358 (0.003)	1359, 1357	$\delta(CH_2)_{wag}+\delta(NH_2)_{tw}$	1382 m
	1357 (0.02), 1356 (0.05)	1352 *	$\delta(NCH)$	
	1331 (0.01), 1331 (0.04)	1332 *	$\delta(CH_2)_{wag}+\nu(CC)$	
1300 vw	1326 (0.003), 1326 (0.07)	1326 *	$\delta(CH_2)_{wag}$	1337 m
1258 s	1257 (0.06), 1257 (0.04)	1257 *	$\delta(CH_2)_{wag}+\delta(NH_2)_{tw}$	1262 s
	1250 (0.01), 1246 (0.09)	1248, 1246	$\delta(CH_2)_{wag}+\delta(NH_2)_{wag}$	
1236 s	1243 (0.08), 1242 (0)	1244, 1241	$\delta(CH_2)_{wag}$	1243 s
	1226 (0.02), 1226 (0.03)	1231, 1230	$\delta(CH_2)_{tw}+\nu(CC)$	
1136 vs	1153 (0.16), 1145 (0.02)	1155, 1145	$\delta(NH_2)_{wag}$	1142 s
	1130 (0.05), 1129 (0.10)	1126, 1126	$\nu(CC)+\nu(CN)$	
1109 vs	1111 (0.15), 1111 (0)	1111 *	$\delta(CNH)$	1095 s

~ 1070 m	1100 (0.08), 1096 (0.25)	1095 *	$\nu(CC)+\delta(CH_2)_{tw}$	1064 s
	1067 (0.03)	1066 *	$\nu(CC)$	
1039 vs	1062 (0.11), 1062 (0.01)	1063, 1060	$\nu(CN)$	1029 m
1009 m	986 (0.06), 984 (0.05)	987, 984	$\nu(CN)$	~1000 w
974 s	970 (0.13), 968 (0.12)	968, 965	$\delta(CH_2)_r$	947 w
	908 (0.02), 907 (0.01)	908, 907	$\nu(CC)$	926 m
911 s	905 (0.09), 904 (0.17)	902, 901	$\delta(CCS)$	894 s
816 m	822 (0.01), 821 (0.003)	823, 820	$\delta(CH_2)_r$	813 vs
			$\delta(CH_2)_r+\delta(NH_2)_{wag}$	768 vs
780 w	805 (0.003), 804 (0.003)	806, 805	$\nu(CS)+\delta(CCS)$	732 w
627 vs	658 (0.31), 657 (0.05)	661, 660	$\delta(NH_2)_r+\delta(ZnNH)$	642 w
	629 (0.07), 628 (0.004)	628, 627	$\delta(NH_2)_r+\nu(CS)$	
	625 (0.14), 624 (0.05)	626, 624	$\delta(NH_2)_r+\nu(CS)$	
540 m	621 (0.004), 620 (0.03)	622 *	$\nu(SS)$	511 w
	556 (0.02), 555 (0.001)	556, 555	$\delta(CCN)$	
473 w	532 (0.03), 532 (0.01)	529 *	$\delta(CCS)+\delta(CCN)$	473 s
	406 (0.01)	406, 404	$\delta(CSS)$	423 vs
	395 (0.002), 395 (0.01)	395 *	$\delta(CSS)$	
	386 (0.03), 385 (0.02)	385, 384	$\nu(ZnN)+\delta(CCS)$	

322 (0.05), 322 (0.004)	319, 316	ZnCl+δ(CCS)
313 (0.16)	315, 314	ZnCl
309 (0.01), 307 (0.04)	306 *	
297 (0.2), 296 (0.002)	296 *	
253 (0.02), 249 (0.01)	251, 250	
241 (0.01), 238 (0.003)	239, 238	
225 (0.02), 215 (0.001)	221, 211	
204 (0.003), 201 (0.002)	206, 201	
179 (0.05), 177 (0.13)	182, 179	
162 (0.01), 158 (0.01)	156, 154	
146 (0.01), 139 (0)	148 *	
137 (0.03), 131 (0.12)	136, 130	δ(ClZnCl)

Molecular vibrations: b, bending; wag, wagging; tw, twisting; r, rocking.

[a]Periodic DFT/PAW-PBE calculations.

[b] $[Zn(Cym\text{-}Cym)Cl_2]_n$is a monoclinic crystal system, point group 2/m (C_{2h}) and according to the nuclear site group analysis the IR active normal modes belong to $A_u(45)$ and $B_u(45)$ symmetry.

[c]The calculated frequencies are with IR intensity = 0 and according to the nuclear site group analysis,these frequenciesshould be Raman active belonging to $A_g(45)$ and $B_g(45)$ normal modes.

*Double-repetitive frequency.

According to the calculations, in the IR spectrum of **1**, the NH_2 stretching vibrations appear at similar band position at 3288, 3244/3223d, 3128 cm^{-1} (Table 2.12). The infrared 3400-3000 cm^{-1} and 3000-2700 cm^{-1} frequency ranges of **2** contain bands due to the N-H (3274, 3220, 3130 cm^{-1}) and C-H (2990, 2935 cm^{-1}) stretching modes, respectively (Table 2.13). In both complexes the cyst(e)amine NH_2 group is coordinated to the Zn(II) ion. In complex **1,** the ν(N-H) frequencies are shifted to lower frequencies refer to that of deprotonated ($NH_2CH_2CH_2S^-$) ligand (3365, 3301 cm^{-1}) in solution, indicating an elongation of the N-H bond lengths when ligand NH_2 group coordinates to the Zn(II), Table 2.12. At the same time, the ν(N-H) frequencies of **1** are blue-shifted as compared to that of CymH·HCl ligand in solid state, where the NH···Cl interactions exist (Table 2.12 and Figure 2.14). For complex **2**, these frequencies are blue-shifted referred to that of the corresponding ligand, Table 2.13. As discussed above, the elongated N-H bonds and the lower ν(N-H) frequencies in the ligand are due to the existing NH··Cl hydrogen bonding in the Cym-Cym·2HCl ligand pattern.

Four bands are observed in the 2900 -2000 cm^{-1} IR region of $[Zn(Cym\text{-}Cym)Cl_2]_n$ (at 2505, 2412, 2209 and 2050 cm^{-1}) and they probably originate by a Fermi resonance between the above CH_2 stretching fundamental and the overtone or combination bands of the CH_2 bending modes. In $[Zn_4Cym_4Cl_4]$ complex, the IR overtone bands observed at ~2215 cm^{-1} arevery weak. Hence, the vibrational behavior in the discussed IR region is different for the polymeric $[Zn(Cym\text{-}Cym)Cl_2]_n$ and cyclic $[Zn_4Cym_4Cl_4]$complexes. It should be mentioned that for the cyclic $[ZnCymCl]_4$ complex (**1A**) a medium overtone bands at 2599 and 2399 cm^{-1} have been reported [14].

Generally, in the 1700-1550 cm^{-1} frequency range, the asymmetric and symmetric NH_2 bending modes are observed. According to the calculations the two intense bands at 1640 and 1575 cm^{-1} observed in the IR spectrum of $[Zn_4Cym_4Cl_4]$ were assigned to the bending δ(NH_2) vibrations. In the $[Zn_4Cym_4Cl_4]$ IR spectrum, these modes appear at 1654 and 1580 cm^{-1}.The intense band in the complex **1** (or **2**) at 1575 (1580) cm^{-1} is shifted to lower frequencies (~20 cm^{-1}) in relation to the corresponding ligand and could be indicative of vibrational characteristic for the coordination of the Cym (or Cym-Cym) ligand to Zn(II)

through the amino N atom (Tables 2.12 and 2.13). The strong bands observed at at 1083 cm^{-1} for **2** and 1136 cm^{-1} for **1** are assigned to the wagging $\delta(NH_2)$ vibrations. A strong band at 682 cm^{-1} for the cyclic complex **1** and the band at 627 cm^{-1} for the polymeric complex **2** are attributed to the rocking $\delta(NH_2)$ vibrations. In summary, the comparative vibrational analysis of the ligands and their Zn(II) complexes revealed that the $\delta(NH_2)$ vibrations of the coordinated NH_2 group in the two Zn(II) complexes are shifted to lower frequencies.

In both complexes (**1** and **2**), the bands of the bending vibrational modes of $(CH_2)_2$ chain are in the 1510-1400 cm^{-1} frequency range, the wagging vibrational modes are in the 1380-1230 cm^{-1} range; the bands due to the twisting vibrational modes appear in the 1230-1070 cm^{-1} range and the rocking CH_2 vibrations appear at lower frequencies, 1000-750 cm^{-1} (Tables 2.12 and 2.13). It should be noted that a strong band at 1509 cm^{-1} due to $\delta(CH_2)_b$ was observed only in the IR spectrum of the polymeric complex (**2**), but not in the IR spectrum of (**1**). According to the calculations such a vibartional mode should also be observed for (**1**)**,** but its intensity is low. Therefore, $\delta(CH_2)_b$ at 1509 cm^{-1} is IR active in the polymeric complex **2** and it is IR silent in the cyclic complex (**1**) and this vibrational characteristic could be used to distinguish the two complexes. For comparison, in the IR spectrum of the cyclic $[ZnCymCl]_4$ complex (**1A**) the bands due to the $\delta(CH_2)_b$ modes have been observed at lower frequencies (1477, 1461 and 1422 cm^{-1}) [15]. The bands of the C-C stretching modes were observed in the 1130-900 cm^{-1} infrared spectral region and in the alkylene chain they are mixed with the CH_2 wagging modes.

According to the performed frequency calculations, the two strong IR bands observed at 1039 (1009) cm^{-1} for the polymeric complex and the band at 1046 cm^{-1} observed for the cyclic complex were assigned to the C-N stretching vibrations. The lower ν(CN) frequency in the polymeric complex (**2**) is consistent with the longer C-N bond lengths (1.470 Å) as compared to those (~1.455 Å) of the cyclic Zn(II) complex (**1**), Table 2.11. The ν(CN) band is blue-shifted toward the corresponding frequency of the deprotonated ligand Cym (in solution) and almost unchanged in relation to that of CymH·HCl ligand (in solid state), Table 2.12. For complex (**2**), the ν(CN) band of (**1**) is shifted to higher

frequencies relative to that at 1029 cm^{-1} for Cym-Cym (Table 2.13, 1.59 Å), which is in agreement with the shorter C-N bond length in the complex. Since the ionic form is the active one for coordination, we suggest that amino coordination of Cym in the cyclic Zn(II) complex produces a C-N shortening and blue-shift of the ν(CN) frequency. The vibrational analysis mode revealed that the comparative approach of the vibrational data for the ligands and their Zn(II) complexes is not routine and the vibrational behavior of the different ligand forms, deprotonated active ligand form in solution or hydrogen-bonded solid state ligand should be taken into account.

The analysis of the C-S stretching mode deserves attention because of its different type in the two Zn(II) complexes: in the cyclic complex (**1**), the (C)S atom is a bridging one, linking two Zn ions and in the polymer complex **2**, the CS groups are connected by S-S bond. In principle, the ν(C-S) normal modes possess low IR intensity and these bands are weak. For complex (**1**), the C-S vibration is found at lower frequencies at 658 and 646 cm^{-1} in agreement with its larger C-S bond lengths (by ~0.035 Å) (Figure 2.13, Table 2.11).

In the IR spectrum of (**2**), a weak band at 780 cm^{-1} was assigned to ν(C-S) normal mode. The ν(CS) bands in the IR spectrum of **1** showed significant IR intensity. The ν(C-S) frequency of (**2**) is blue-shifted (shorter C-S bond) in relation to this at 732 cm^{-1} for Cym-Cym ligand, although the CS groups do not take part in the coordination to Zn(II) ion. The ν(C-S) bands at 787 (732) cm^{-1} for CymH ligand was found to shift to lower frequencies at 658 and 646 cm^{-1} for complex (**1**). Therefore, the S bridging coordination to two Zn(II) in the cyclic complex (**1**) produce elongation and polarization of C-S bonds resulting in red-shift and IR intense ν(C-S) bands. The bands at 501 cm^{-1} in Cym-Cym and at 504 cm^{-1} for complex (**2**) were assigned to the ν(S-S) stretching vibration, are in agreement with the calculations and the literature data [204].

The frequency calculations of (**2**) predicted IR frequencies for the ν(Zn-N) and ν(Zn-Cl) vibrational modes at 386 and 313 cm^{-1}, respectively**.** Unfortunately, this IR frequency range was not experimentally available. For complex(**1**), theν(Zn-N) mode should appear

at higher frequencies ~425/413 cm^{-1} and the ν(Zn-Cl) mode - at lower frequencies ~270 cm^{-1}, according to the observed Zn-N and Zn-Cl bonds lengths in (**1**) and (**2**), Table 2.11. The ν(Zn-S) band in (**1**) was suggested to be at ~ 315 cm^{-1}. The calculated frequencies at ~120 cm^{-1} and ~ 130 cm^{-1} for (**1**) and (**2**), respectively were assigned to δ(ClZnCl) mode.

2.3.5 Antimicrobial activities

Antimicrobial activities (average of triplicate measurements) of the zinc(II) thiolate complexes (**1-5**) and Amoxil as a standard drug, gauged by minimum inhibitory concentrations (MIC; μg mL^{-1}). The data of antimicrobial activities are given in Table 2.14. The complex (**3**) showed outstanding activity against all the organisms. The compound (**1**) also displayed substantial activity against the gram-negative bacteria such as *E. coli*and *P. aeruginosa*; but the activities against the molds such as *A. niger* and *P. citrinum*; and yeasts such as *C. albicans* and *S. cerevisiae;* were moderate. The complex (**4**) inhibited the growth of bacteria and molds significantly but it was almost inactive against the yeasts.

Astraight interaction of the metal ions with bio-ligands for instance proteins, enzymes and membranes proteins is responsible for biological activities. [205]. The Zinc(II) complexes are generally labile due to the absence of crystal field stabilization energy. The activities of the zinc(II) thiolate complexs (**1-5**) may be credited to their ability to undertake further ligand substitution reactions with the bio-ligands like proteins and DNA. The least activity of complex (**4**) displays due to high stability so the ligands could not be removed easily by biomolecules.

Table 2.14: Antimicrobial activities of zinc(II) complexes evaluated by minimum inhibitory concentration (MIC: μg mL^{-1})

Complexes	Microbial Activity (in terms of (MIC: μg mL^{-1})					
	Escherichia coli	*Pseudomonas aeruginosa*	*Aspergillus niger*	*Penicillium citrinum*	*Candida albicans*	*Saccharomyces cerevisiae*
Amoxil	8	12	890	870	660	580
Cym.HCl	220	180	670	720	>1000	>1000
$[Zn(Cym)Cl]_4$ (**1**)	140	190	820	780	240	480
Cys	220	230	470	590	710	>1000
[Zn(Cys)Cl]. $0.5H_2O$ (**3**)	80	100	270	220	390	310
Msa	100	130	250	300	470	650
$[Zn(Msa)_2]$ (**4**)	320	330	510	600	770	>1000

Conclusions

The present study describes the preparation, spectroscopic, structural and theoretical characterization ofzinc(II) complexes of thiolates. The crystal structure of a new tetranuclear complex, $[Zn_4Cym_4Cl_4]$ (**1**) was determined in which zinc possesses two types of environments, ZnS_2Cl_2 and ZnS_2N_2. In addition, a novel polymeric Zn-cystamine complex, $[Zn(Cym\text{-}Cym)Cl_2]_n$ (**2**) was obtained by reaction of $ZnCl_2$ and cystaminedihydrochloride (Cym-Cym·2HCl) in the presence of 1,2-diaminoethane (en). In the polymeric complex, the cystamine ligand retained the disulfide S-S linkage and the sulfur atoms did not participate in coordination to Zn(II). The structure of the complex demonstrated that the the disulphide bridge is retained during course of the the complex formation reaction.

Combined experimental (IR, ^1H, and ^{13}C NMR) and theoretical (DFT) studies of the isolated ligands cysteamine (CymH, zwitterionic tautomer)and cystamine (Cym-Cym·2HCl), and their complexessuch as cyclic $[Zn_4Cym_4Cl_4]$ and $[ZnCymCl]_4$; and polymeric $[Zn(Cym\text{-}Cym)Cl_2]_n$) revealed structure-spectra correlations which are able to distinguish the complexes on the basis of their IR and NMR spectral characteristics. DFT-based theoretical analysis showed that due to the polymeric nature of $[Zn(Cym\text{-}Cym)Cl_2]_n$ complex, the model calculations at molecular level are not capable to give a reliable explanation of the structural and vibrational properties. The periodic-DFT calculations performed with the experimental unit cell parameters give excellent agreement with the experimental structural parameters and assured reliable calculations and interpretations of the IR parameters. The C-S stretching vibration is the characteristic mode able to distinguish different binding type of the CS donor group in the complexes (**1**) and (**2**). The downfield shift for ^{13}C(-N) signal in (**2**), is consistent with C-N elongation upon N binding to Zn(II) and the smaller downfield shift for ^{13}C(-S) signal are indicative NMR characteristics for the ligand coordination to Zn(II) through N atom and for uncoordinated S atom.

Some of the Zinc-thiolate complexes exhibited a wide range of activitiesquantitatively against gram-negative bacteria (*E. coli* and *P. aeruginosa*), while moderate activity was observed against molds, *A. niger and P. citrinum*.

Chapter – 3
Zinc(II)Complexes of Diamines

3.1 Introduction

Zinc is essential for many cellular processes and plays an active role in catalyzing the biochemical reactions [1, 2, 5, 10]. The most effective biological catalytic function is to catalyze condensation and (in reverse) hydrolysis reactions at physiological pH by polarizing the substrates. Such reactions include polymerization of RNA (condensation) and the cleavage of peptides, proteins or esters (hydrolysis) [1,2]. Several zinc(II)-diamines complexes find promising applications in catalysis due to their minimal toxicity [25, 27, 28]. In view of this importance, zinc(II) complexes of diamines have been studied extensively [8-16]. There are also numerous reports on the crystal structure of zinc SCN^- amine systems [17-22]. The crystal structures of neutral dithiocyanato zinc(II) complexes with ethylenediamine (en) and its methyl derivatives bearing tetrahedral geometry were determined with an idea to study the intermolecular H-bonding interactions [17]. Although, thiocyanate can function as an ambidentate ligand [23-25], in its discrete complexes with Zn(II) it appears to coordinate exclusively through the N atom [17,26]. The extraordinarily active hydrogen-bonding behavior allows this anion to act as a powerful bridge between different molecular fragments [26].On the other hand, in $Zn(NCS)_2$, half the Zn atoms are bonded exclusively to the N and the other half exclusively to the S atoms of the anion [27]. In this study, the spectroscopic characterization,crystal strucures or DFT studies of eightzinc(II) complexes of diamines, which include;$[Zn(Dach)_2][ZnCl_4]$ (**6**), $[Zn(Dach)(NCS)_2]_n$ (**7**), $[Zn(Dap)(NCS)_2][Zn(Dap)(NCS)_2]_n$ (**8**),$[Zn(TMEDA)(NCS)_2]$ (**9**), $(TMEDA\text{-}H_2)^{2+}[ZnCl_4]^{2-}$ (**10**),$[Zn(en)(Mnt\text{-}Mnt)].H_2O$ (**11**), [Zn(Dap)(Mnt)]Cl (**12**) and $[Zn(en)(NCS)_2]$ (**13**) are reported. The compound (**10**) was prepared unpredictably while attempting to synthesize a mixed-ligand containing *N,N,N´,N´*-tetramethylethylenediamine and 2-mercaptosuccinic acid zinc(II) complex. The crystal structure of $[Zn(en)(NCS)_2]$ (en = 1,2-diaminoethane) has already been reported [17]. The structural characterization of $[Zn(TMEDA)(NCS)_2]$ (**9**) was attempted earlier but the

proper refinement could not be done due to disorder [17]. Therefore, the spectral data of the compound (**9**) is presented here.

3.2 Experimental

3.2.1 Chemicals

$ZnCl_2$, ethylendiamine, propylenediamine, *N,N,N',N'*-tetramethylethylenediamine and potassium thiocyanate were purchased from Merck Chemical Co., Germany. *Cis*-1,2-diaminocyclohexane was obtained from Aldrich Chemicals, Germany.

3.2.2 Synthesis of Complexes (6-13)

Preparation of $[Zn(Dach)_2][ZnCl_4]$ (6)

A solution of 0.12 g (1 mmole) *cis*-1,2-diaminocyclohexane in 15 mL methanol was added to 0.14 g $ZnCl_2$ (1 mmol) in 5 mL distilled water. A clear solution was obtained on mixing. After stirring for 15 min, the light yellow solution was filtered and the filtrate was kept for crystallization at room temperature. After 24 hours light yellow crystals were obtained.

Preparation of $[Zn(Dach)(NCS)_2]$ (7)

A solution of 0.14 g (1 mmol) $ZnCl_2$ in 5 mL of water was added slowly to a 15 mL methanolic solution of 0.12 g (1mmol) of diamine (Dach) in a 100 mL beaker. The solution was magnetically stirred for 15 minutes to obtain a clear solution. At this point 0.20 g (2 mmol) KSCN in 10 mL of water were added and stirred for 30 minutes. The solution was filtered and the filtrate was kept at room temperature to result brownish yellow crystals of (**7**).The complexes, $[Zn(TMEDA)(NCS)_2]$ (**9**) and $[Zn(en)(NCS)_2]$ (**13**) were prepared by the same procedure and separated as white crystals.

Preparation of $[Zn(Dap)(NCS)_2][Zn(Dap)(NCS)_2]_n$ (8)

A solution of 0.14 g (1 mmol) $ZnCl_2$ in 5 mL of water was added slowly to a 15 mL methanolic solution of 0.12 g (1mmol) of diamine (Dap) in a 100 mL beaker. The solution was magnetically stirred for 15 minutes to obtain a clear solution. White precipitates were obtained. The solution was filtered and to the filtrate, 0.20 g (2 mmol) KSCN in 10 mL of water were added and stirred for 30 minutes. The solution was filtered and the filtrate was kept at room temperature to result white crystals of complex (**8**).

Preparation of $(TMEDA\text{-}H_2)^{2+}[ZnCl_4]^{2-}$ (10)

A solution of 0.14 g (1 mmol) $ZnCl_2$ in 5 mL of water was added slowly to a 15 mL methanolic solution of 0.12 g (1mmol) of tetramethylethylenediamine (TMEDA) in a 100 mL beaker. The slightly turbid solution was magnetically stirred for 15 minutes. At this point 0.16 g (1 mmol) 2-mercaptosuccinic acid (Msa) in 15 mL of methanol was added and stirred for 30 minutes. The solution was filtered and the filtrate was kept at room temperature to result white crystals of complex (**10**).

Preparation of $[Zn(Mnt\text{-}Mnt)(en)]\cdot H_2O$ (11)

A solution of 0.14 g (1 mmol) $ZnCl_2$ in 5 mL of water was added slowly to a 15 mL methanolic solution of 0.06 g (1mmol) of ethylenediamine in a 100 mL beaker. The solution was magnetically stirred for 15 minutes to obtain a clear solution. At this point 0.16 g (1 mmol) 2-mercaptonicotinic acid in 25 mL water was added to the above solution. The solution was stirred for 30 minutes and then filtered. The filtrate was kept at room temperature to result white crystals of complex (**11**).The complex [Zn(Dap)(Mnt)]Cl (**12**) was prepared by the same procedure using 1,3-diaminopropane instead of ethylenediamine.

The elemental analysis of the complexes and their melting points are given in Table 3.1.

3.2.3 IR and NMR measurements

The IR spectra were recorded on a Nicolet 6700 FTIR spectrophotometer using KBr pellets in the 4000-400 cm^{-1} range. The spectra were collected from 16 scans at a spectral resolution of 2 cm^{-1}. NMR measurements were carried out in DMSO on a Jeol JNM-LA 500 NMR spectrophotometer at 297K. The ^{1}H NMR spectra were recorded at a frequency of 500.00 MHz. The ^{13}C NMR spectra were obtained at the frequency of 125.65 MHz with ^{1}H broadband decoupling and referenced relative to TMS. The spectral conditions were: 32 k data points, 0.967 s acquisition time and 1.00 s pulse delay.

Spectroscopic data

IR (ν, cm^{-1}): $[Zn(Dach)_2][ZnCl_4]$ (**6**), 3388, 3245, 3131 (N−H), 2933, 2863 (C-H), 1100 (C−N);$[Zn(Dach)(NCS)_2]$ (**7**), 3326, 3237, 3145 (N−H), 2930, 2863 (C-H), 2088 (SCN), 1008 (C−N); Dach, 3363, 3288 1591, 1092; $[Zn(Dap)(NCS)_2][Zn(Dap)(NCS)_2]_n$(**8**), 3282, 3208 (N−H), 3130 (C−H), 2087 (SCN), 1002 (C−N); Dap, 3357, 3282, 1070; $[Zn(TMEDA)(NCS)_2]$ (**9**), 2998, 2975, 2862 (C−H), 2110 (SCN), 1006, 1024, 1040 (C−N); TMEDA, 2970, 2943, 2860, 1043, 1033; $[Zn(en)(Mnt\text{-}Mnt)]\cdot H_2O$ (**11**), 3240 (N-H), 1096 (C-N), 677 (C-S), 1604, 1561(C=O),$[Zn(Dap)(Mnt)]Cl$(**12**), 3182 (N-H), 1096 (C-N), 681 (C-S), 1697 (C=O); $[Zn(en)(NCS)_2]$ (**13**), 3400 (N−H), 2920 (C−H), 2089 (SCN), 1060 (C−N); en, 3393, 1033.

^{1}H NMR (500 MHz, DMSO, 297 K, TMS, ppm): $[Zn(Dach)_2][ZnCl_4]$ (**6**), δ = 1.26, 1.45. 1.51, 2.84; $[Zn(Dach)(NCS)_2]$ (**7**), δ = 1.26, 1.37, 1.46, 1.52, 2.77; Dach, δ = 1.12, 1.28, 1.69, 1.85, 2.23; $[Zn(Dap)(NCS)_2][Zn(Dap)(NCS)_2]_n$(**8**), δ = 1.59, 2.79; Dap, δ = 1.94, 2.98; $[Zn(TMEDA)(NCS)_2]$ (**9**), δ = 2.25, 2.42; TMEDA, 2.13, 2.29; $[Zn(en)(NCS)_2]$ (**13**), δ = 2.58; en, δ = 3.2.

^{13}C NMR (125.65 MHz, DMSO, TMS, ppm): $[Zn(Dach)_2][ZnCl_4]$ (**6**), δ = 50.48, 27.43, 20.48; $[Zn(Dach)(NCS)_2]$ (**7**), δ = 20.46, 27.75, 49.59, 134.20; Dach, δ = 26.36, 35.26,

58.20; [Zn(Dap)$(NCS)_2$][Zn(Dap)$(NCS)_2$]$_n$(**8**), δ = 28.30, 41.92, 135.04; Dap, δ = 25.69, 37.47; [Zn(TMEDA)$(NCS)_2$] (**9**), 46.13, 55.25, 134.95; TMEDA, 46.01, 57.83; [Zn(en)$(NCS)_2$] (**13**), δ = 40.22, 135.34; en, 37.67.

3.2.4. Theoretical (DFT) calculations

Theoretical studies were performed for the fivecompounds; [Zn(Dach)Cl_2] (**6**), [Zn(Dach)$(NCS)_2$] (**7**), [Zn(Dap)$(NCS)_2$][Zn(Dap)$(NCS)_2$]$_n$ (**8**),[Zn(TMEDA)$(NCS)_2$] (**9**) and [Zn(en)$(NCS)_2$] (**13**) and their analogues. In all cases, as the starting geometry in the optimization procedures, the fragments of the crystallographic structurewere used.For example, during the optimization of [Zn(Dach)$(NCS)_2]_8$ (**7_8**), the positions of the all atoms of the central [Zn(Dach)$(NCS)_2$] complex were relaxed, while the positions of the atoms of the other seven complex molecules were frozen. With respect to the all complexes studied the optimizations with frozen position of the sulfur atoms were performed. The calculations were performed with B3LYP-D3 [213] method (B3LYP functional corrected with the original D3 damping function) and combined basis sets LanL2DZ [214] for Zn and S atoms in conjunction with the D95V(d,p) [215]basis set for all other atoms.

The interaction energies between selected ligands and the rest of the complexes were calculated as a difference between electronic energies of the whole complex and the sum of selected ligand energies and the rest of the complex. BSSE corrections of the interaction energies were performed using the counterpoise method [216]. Natural bond orbital (NBO) analysis provides a detailed understanding of the nature of electronic structure and bonding in the molecules. In this work, the atomic charges and second-order interaction energies were calculated with DFT method using version 5.0 of the NBO program [217, 218]. All computations were carried out with Gaussian 09 set of programs [196].

3.2.5 X-ray structure determination

Single crystal data collection was recorded at 296 K on a Bruker Kappa APEXII CCD diffractmeter equipped with a four-circle goniometer and employing MoKα(for **6** CuKα) graphite mono-chromated radiation. All further calculations including refinement were accomplished using SHELXL-2014 [186, 187]. All H atoms were positioned in calculated locations with C—H = 0.97- 0.98 Å, N—H = 0.89 Å which were further refined as riding with $U_{iso}(H) = 1.2U_{eq}(C, N)$. PLATON software was used for molecular graphics [188]. Crystal data including data collection are shortened in Tables 3.2-3.5.

Table 3.1 Elemental analysis and melting points of zinc(II) complexes with diamines

	Found (Calculated)				M. P.
	C	H	N	S	(ºC)
$[Zn(Dach)_2][ZnCl_4]$ (**6**)	28.91	5.16	10.60	-	261-263
	(28.75)	(5.63)	(11.18)	-	
$[Zn(Dach)(NCS)_2]$ (**7**)	32.20	4.82	18.82	21.06	173-175
	(32.48)	(4.77)	(18.95)	(21.68)	
$[Zn(Dap)(NCS)_2]$ (**8**)	22.98	3.78	22.12	24.26	180-182
	(23.48)	(3.94)	(21.91)	(25.08)	
$[Zn(TMEDA)(NCS)_2]$ (**9**)	31.80	4.87	18.71	21.96	152-155
	(32.25)	(5.37)	(18.81)	(21.50)	
$[Zn(Mnt\text{-}Mnt)(en)]\cdot H_2O$	37.93	3.23	12.58	14.64	250-253
(**11**)	(37.38)	(3.59)	(12.46)	(14.26)	
[Zn(Dap)(Mnt)Cl] (**12**)	32.05	3.92	12.17	9.13	232-235
	(32.84)	(4.29)	(12.74)	(9.74)	
$[Zn(en)(NCS)_2]$ (**13**)	20.19	3.08	22.72	26.26	188-190
	(19.88)	(3.31)	(23.19)	(26.54)	

Table 3.2 Crystal data and refinement details for compound (**6**)

Formula	$C_{12}H_{28}N_4Cl_4Zn_2$
Formula Weight	900.92
Crystal system	Orthorhombic
Space Group	Pna21
a, b, c (Å)	18.8332(6), 10.3741(3), 10.0453(3)
α, β, γ (deg)	90, 90, 90
V (Å^3)	1962.63(10)
Z	4
ρ_{calc} (g cm^{-3})	1.695
μ(MoKα) (mm^{-1})	8.016
F(000)	1024
Crystal size (mm)	0.3 x 0.1 x 0.1
Temperature (K)	120(2)
λ CuKα (Å)	1.54184
2 θ range (deg)	4.867 - 65.999
h, k, l limits	-22:22, -7:12, -11:11
Reflections; collected/ Uniq.	6310 / 2822 (R_{int} = 0.0369)
T_{max}, T_{min}	1.00000, 0.66186
Data / restraints / parameters	2822 / 9 / 224
Goodness of fit on F^2	1.035
R_1, wR_2([$I > 2\sigma(I)$])	0.0288, 0.0665
R_1, wR_2(all data)	0.0314, 0.0680
Largest diff. peak, hole (e Å^{-3})	0.338, -0.317

Table 3.3 Crystal data and refinement details for compounds (**7**) and (**8**)

Formula	$C_8H_{14}N_4S_2Zn$	$C_5H_{10}N_4S_2Zn$
Formula Weight	295.72	255.66
Crystal system	Orthorhombic	Orthorhombic
Space Group	Pbca	Pbca
a, b, c (Å)	8.4826(5), 16.6335(15), 18.2753(16)	7.6966(2), 22.9258(7), 23.0156(7)
$\alpha\beta\gamma$ (deg)	90, 90, 90	90, 90, 90
V (Å^3)	2578.6(4)	4061.1(2)
Z	8	16
ρ_{calc} (g cm^{-3})	1.524	1.673
μ(MoKα) (mm^{-1})	2.204	2.784
F(000)	1216	2080
Crystal size (mm)	0.40 x 0.24 x 0.18	0.44 x 0.34 x 0.28
Temperature (K)	296(2)	296(2)
λ MoKα (Å)	0.71073	0.71073
2 θ range (deg)	2.229 - 25.500	1.777 - 28.398
h, k, l limits	-10:9, -20:20, -13:22	-10:6, -30:19, -30:28
Reflections; collected/ Uniq.	10253 / 2405	24277 / 5054
Reflections: observed [$I > 2\sigma(I)$]	1167	4184
T_{min}, T_{max}	0.695, 0.476	0.380, 0.510
Data / restraints / parameters	2405 / 0 / 136	2405 / 12 / 241
R_1, wR_2, S [$I > 2\sigma(I)$]	0.0438, 0.0979, 0.922	0.0354, 0.0631, 1.042
Largest diff. peak, hole (e Å^{-3})	0.381, -0.325	0.346, -0.326

Table 3.4 Crystal data and refinement details for compound (**10**)

Formula	$C_6H_{18}N_2ZnCl_4$
Formula Weight	325.39
Crystal system	Triclinic
Space Group	*P*-1
a, *b*, *c* (Å)	6.893(4), 8.257(6), 13.330(10)
α, β, γ (deg)	72.78(3), 87.44(3), 69.42(3)
V (Å^3)	676.9(8)
Z	1
ρ_{calc} (g cm^{-3})	1.596
μ(MoKα) (mm^{-1})	2.568
F(000)	332
Crystal size (mm)	0.95 x 0.44 x 0.08
Temperature (K)	293(2)
λ MoKα (Å)	0.71073
2 θ range (deg)	3.16 - 25.57
h, k, l limits	-8:8, -9:9, -15:16
Reflections; collected/ Uniq.	9440 / 2466 [R(int) = 0.0413]
Reflections: observed [$I > 2\sigma(I)$]	1806
T_{min}, T_{max}	0.194, 0.821
Data / restraints / parameters	2466 / 6 / 154
R_1, wR_2, S [$I > 2\sigma(I)$]	0.0551, 0.675, 1.048
Largest diff. peak, hole (e Å^{-3})	0.400, -0.538

$w = [\sigma^2(F_o^2) + (0.0336P)^2 + 0.0660P]^{-1}$ where $P = (F_o^2 + 2F_c^2)/3$

Table 3.5 Crystal data and refinement details for compound (**11**)

Formula	$C_{14}H_{16}N_4O_5S_2Zn$
Formula Weight	449.80
Crystal system	Triclinic
Space Group	*P* -1
a, b, c (Å)	10.3201(3), 10.3251(3), 10.9132(4)
β (deg)	92.886(2), 113.5960(10), 118.5660(10)
V (Å^3)	892.70(5)
Z	2
ρ_{calc} (g cm^{-3})	1.673
μ(MoKα) (mm^{-1})	1.644
F(000)	460
Crystal size (mm)	0.34 x 0.30 x 0.16
Temperature (K)	296(2)
λ MoKα (Å)	0.71073
2 θ range (deg)	2.568 - 26.000
h, k, l limits	-11:12, -12:12, -13:11
Reflections; collected/ Uniq.	3475/3054 (Rint = 0.0311)
T_{min}, T_{max}	0.5878, 0.7457
Data / restraints / parameters	3475 / 0 / 243
R_1, wR_2, S [$I > 2\sigma(I)$]	0.0258, 0.0685, 1.025
Largest diff. peak, hole (e Å^{-3})	0.284, -0.260

$w = [\sigma^2(F_o^2) + (0.0400P)^2 + 0.2097P]^{-1}$ where $P = (F_o^2 + 2F_c^2)/3$

3.3 Results and discussion

Treatment of $ZnCl_2$ (aqueous solution) directly with diamines and KSCN in a mole ratio of 1:1:2 resulted in complexes of the composition, [Zn(Diamine)$(NCS)_2$].

3.3.1 IR studies

The IR data of the complexes is listed in section 3.2.3. In IR spectra of the complexes, the ν(N−H) and ν(C−N) frequencies of diamines were found near 3300 and 1000 cm^{-1} respectively. The ν(SCN) band was observed near 2100 cm^{-1}, which for KSCN appears at 2140 cm^{-1}. The δ(N-H) vibrations of [Zn(Dach)$(NCS)_2$] (**7**), [Zn(en)$(NCS)_2$] (**13**), [Zn(Dap)$(NCS)_2$][Zn(Dap)$(NCS)_2]_n$(**8**) and [Zn(Dap)(Mnt)]Cl (**12**) were observed at 1585, 1602 & 1635, 1605 and 1591 cm^{-1} respectively. TheC-H stretching bands were observed between 3000 and 2900 cm^{-1} with weak intensity of signals, attributed for all zinc(II) complexes. The presence of these bands in the IR spectra indicates the complexation of both the diamine and thiocyanate ligands to the metal center. In the IR spectrum of complex (**8**)shown in Figure 3.1,the peak at 1580 cm^{-1} was assigned to NH_2 bending (1599 cm^{-1} for free DAP). The C-H stretching was detected as a weak signal at 3130 cm^{-1}. This value is greater than the normal value of around 2950 cm^{-1} [219]. The C-H stretching frequencies can be shifted to higher values when they are involved in hydrogen bonds as observed for (**8**) (*vide infra*). The appearance of these bands indicates the coordination of Dap ligand to the metal center. The IR spectrum of [Zn(TMEDA)$(NCS)_2$] (**9**) is shown in Figure 3.2 that displays the ν(C−H), ν(SCN) andν(C−N) bands at 2998, 2110 and 1058 cm^{-1} respectively.

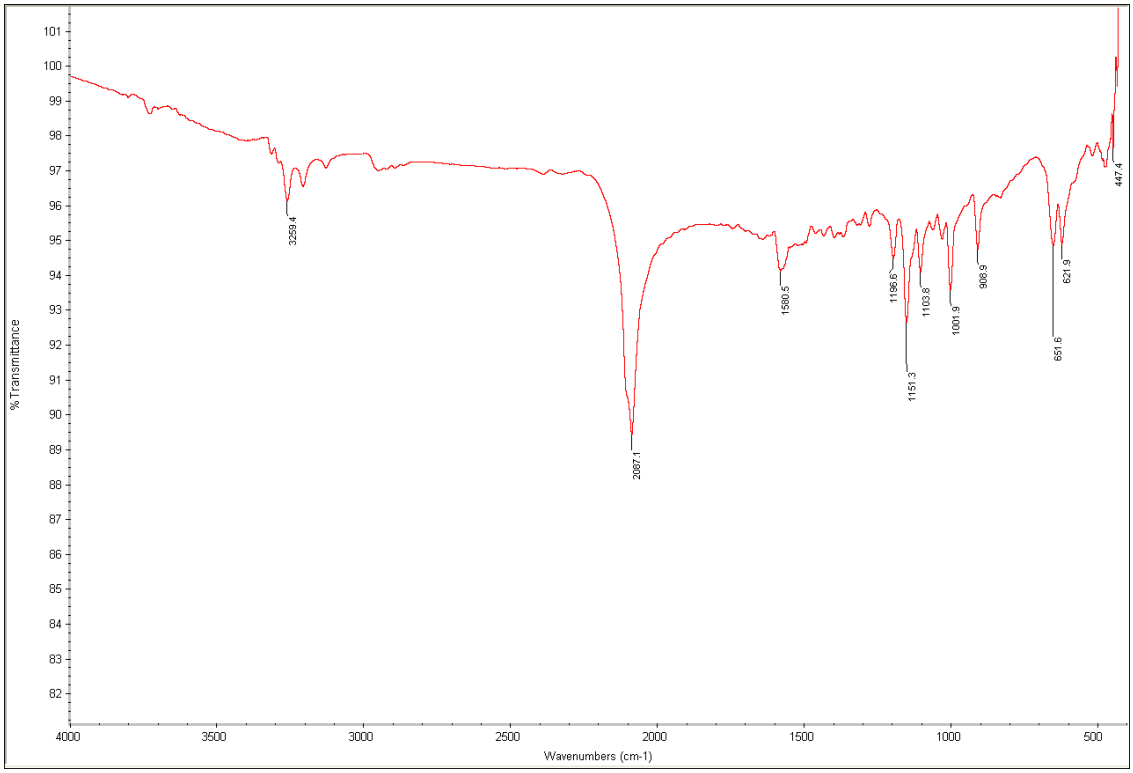

Figure 3.1 IR spectrum of $[Zn(Dap)(NCS)_2][Zn(Dap)(NCS)_2]_n$ (**8**)

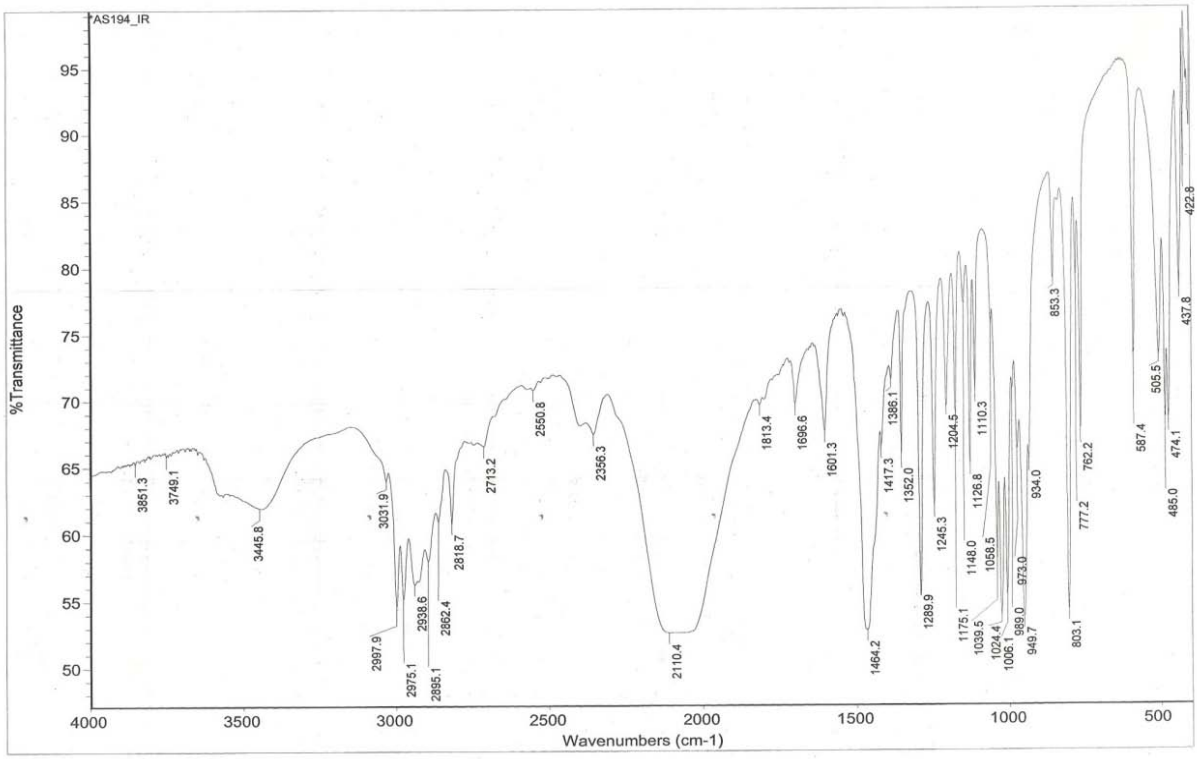

Figure 3.2 IR spectrum of $[Zn(TMEDA)(NCS)_2]$ (**9**)

3.3.2 NMR studies

In the ^{1}H NMR spectrum of (**8**), the Dach protons were identified as two sets of signals, a singlet at 2.77 ppm and a multiplet between 1.26 and 1.52ppm. The hydrogen atoms attached to C-N carbon are diastereotopic due to the presence of prochiral carbon atoms and therefore appeared as multiplets. In the proton NMR spectrum of $[Zn(Dap)(NCS)_2][Zn(Dap)(NCS)_2]_n$(**8**) shown in Figure 3.3, the methylene protons attached to nitrogen and carbon are observed at 2.73 and 1.56 ppm respectively. In $[Zn(TMEDA)(NCS)_2]$ (**9**), the methylene and methyl protons appear at 2.42 and 2.25 ppm respectively. The N-H protons of Dach, en and Dap were not detected. The signals of C-H protons of Dach shifted towards downfield position compared to those in free ligand.On the other hand, the C-H protons of en and Dap in complexes appeared a slight upfield in comparison of the free ligand.

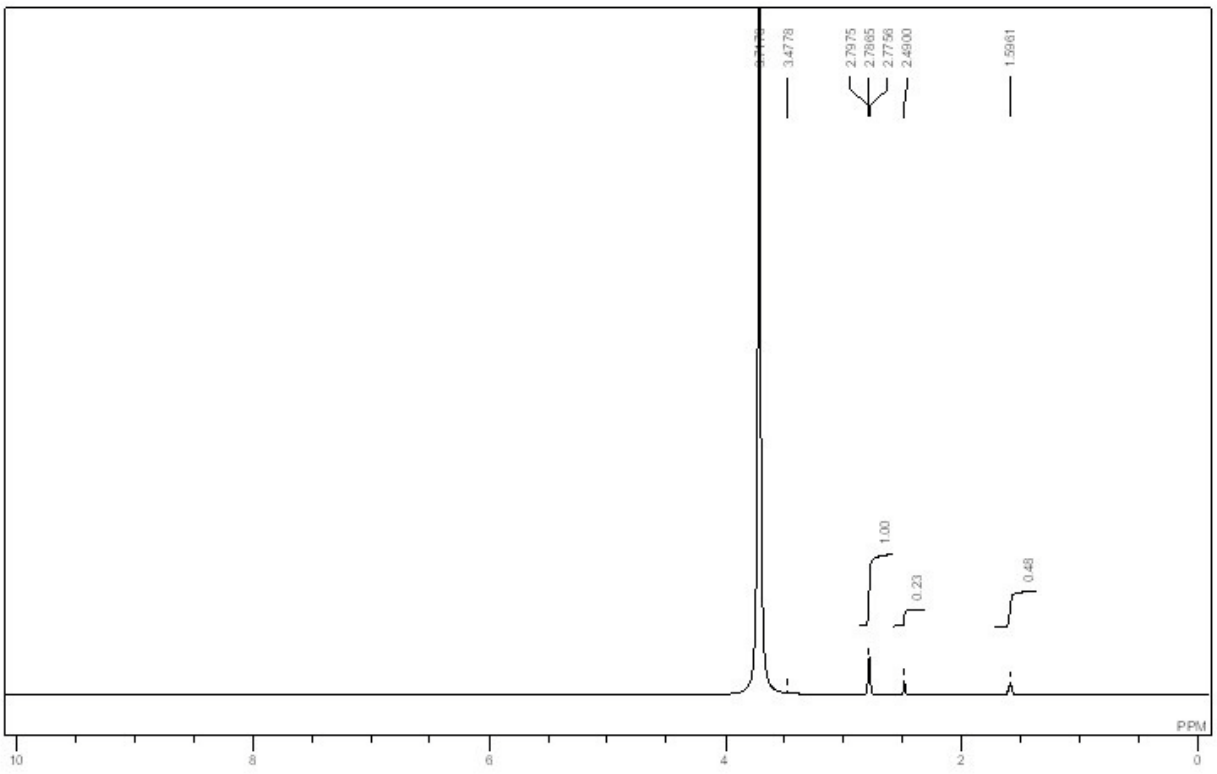

Figure 3.3 ^{1}H NMR spectrum of $[Zn(Dap)(NCS)_2][Zn(Dap)(NCS)_2]_n$(**8**)

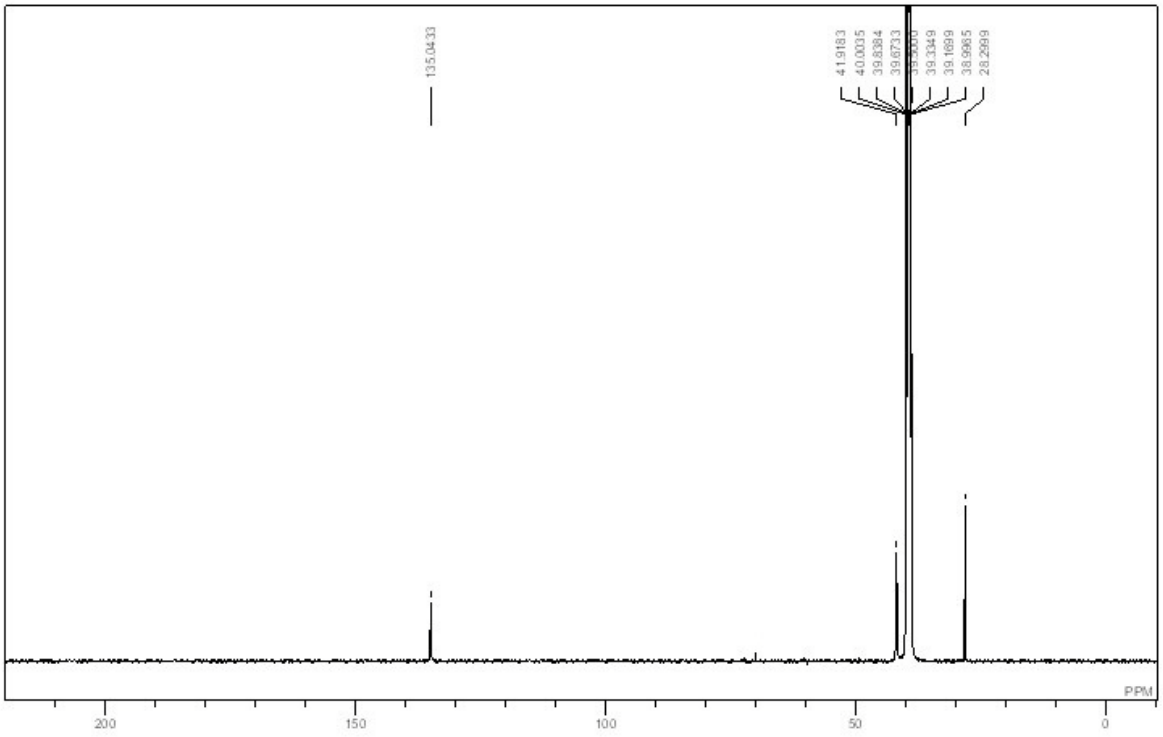

Figure 3.4 $^{13}C\{^{1}H\}$ NMR spectrum of $[Zn(Dap)(NCS)_2][Zn(Dap)(NCS)_2]_n$(**8**)

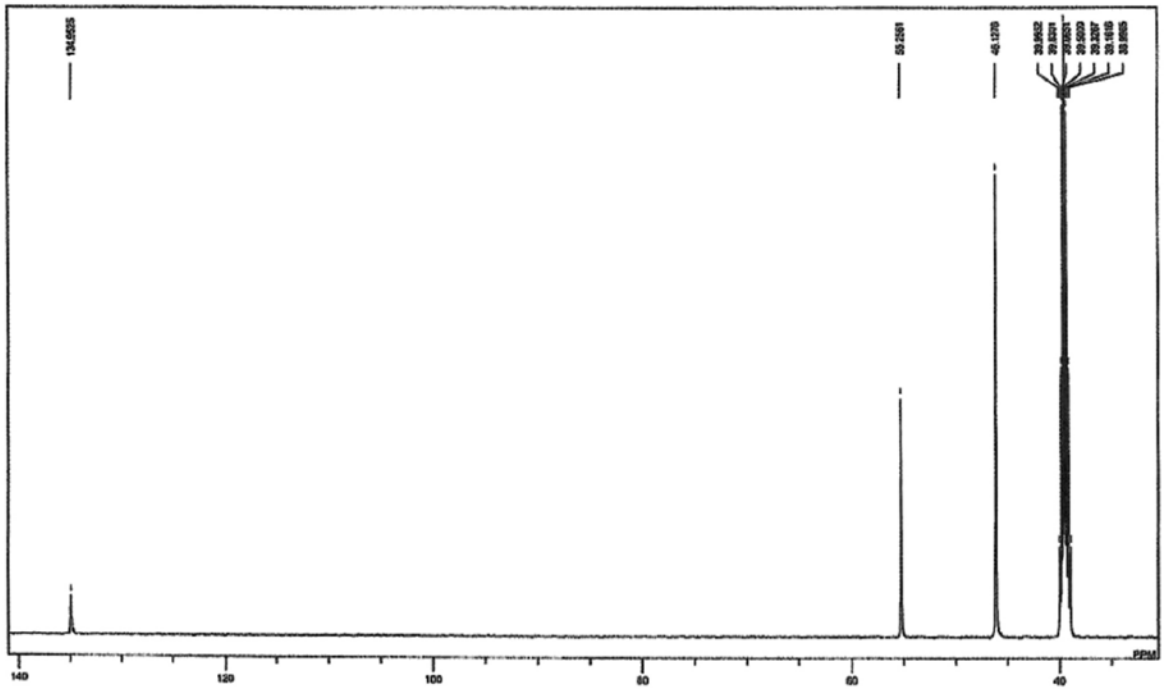

Figure 3.5 $^{13}C\{^{1}H\}$ NMR spectrum of $[Zn(TMEDA)(NCS)_2]$ (**9**)

In the ^{13}C NMR spectrum of **7** the C-N, **C**-CN and **C**-CC carbons of Dach are observed at 49.59, 27.75 and 20.56 ppm, respectively. For $[Zn(Dap)(NCS)_2]$ (**8**) the resonances of methylene carbons attached to nitrogen and carbon atoms are observed at 41.76 and 29.11 ppm respectively. In $[Zn(TMEDA)(NCS)_2]$ (**9**), the methylene and methyl signals appear at 55.25 and 46.13 ppm respectively. In ^{13}C NMR of $[Zn(Dach)(NCS)_2]$ and $[Zn(TMEDA)(NCS)_2]$ (**9**), an upfield shift was observed for the carbon atoms of Dach and TMEDA respectively, whereas, for $[Zn(en)(NCS)_2]$ (**13**) and $[Zn(Dap)(NCS)_2][Zn(Dap)(NCS)_2]_n$(**8**), downfield shifts were observed in the $–CH_2$ resonances of diamine ligand. The SCN resonances are observed around 135 ppm. The ^{13}C NMR spectrum of $[Zn(Dap)(NCS)_2][Zn(Dap)(NCS)_2]_n$(**8**) and $[Zn(TMEDA)(NCS)_2]$ (**9**) are shown in Figures 3.4 and 3.5 respectively.

In [Zn(DAP)(Mnt)]Cl(**12**), the C1 to C5 resonances of Mnt are observed at 171.6, 132.2, 140.1, 117.6 and 148.5 ppm, while in free Mnt, these resonances appear at 173.2, 129.4, 143.1, 115.0, 143.9 ppm respectively. The C6 resonance could not be detected. The methylene carbon atoms CH_2-C and CH_2-N of Dap moiety resonated at 30.30 and 42.50 ppm respectively.

3.3.3 DFT calculations

$[Zn(Dach)_2][ZnCl_4]$ (6)

Fully DFT-optimized structure of $[Zn(Dach)_2][ZnCl_4]$ (**6**) in the gas phase is illustrated in Figure 3.6. As the starting geometry in the optimization procedures the fragment of the crystallographic structure was taken. As shown in this figure, full optimization in the gas phase leads to the final structure different from the experimental one. In this model, the first coordination sphere of the Zn(II) cation is distorted. As is seen in Figure 3.6, differently than in the crystal (*vide infra*), one of the chlorine atoms of $ZnCl_4^{2-}$ is located in the first coordination sphere of the metal cation.

To avoid the artificial interactions, the larger model was built. In this model the $[Zn(Dach)_2][ZnCl_4]$ (**6**) complex was surrounded by additional two $[Zn(Dach)_2][ZnCl_4]$ (**6**) complexes, as shown in Figure 3.7. The external complexes were also taken in the

geometry as in the solid state. Moreover, these external complexes were frozen during the optimization procedure. Therefore, during the optimization the crystal packing effects were covered. As shown in Figure 3.7, the optimized structure of the central $[Zn(Dach)_2][ZnCl_4]$(**6**) complex is similar to that obtained in the experiment.

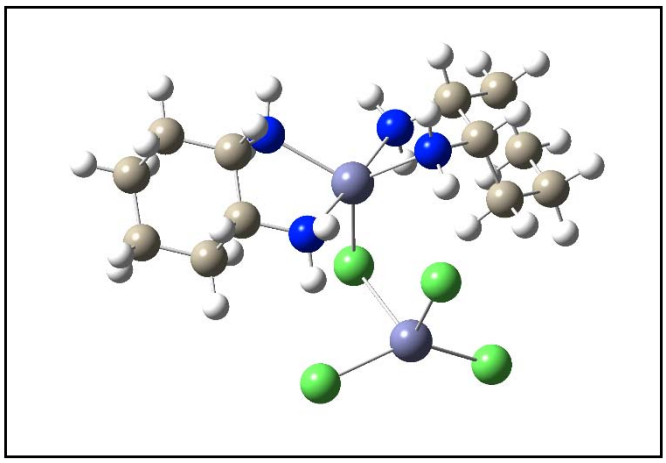

Figure 3.6 Fully DFT optimized structure of the $[Zn(Dach)_2][ZnCl_4]$ (**6**) complex in the gas phase.

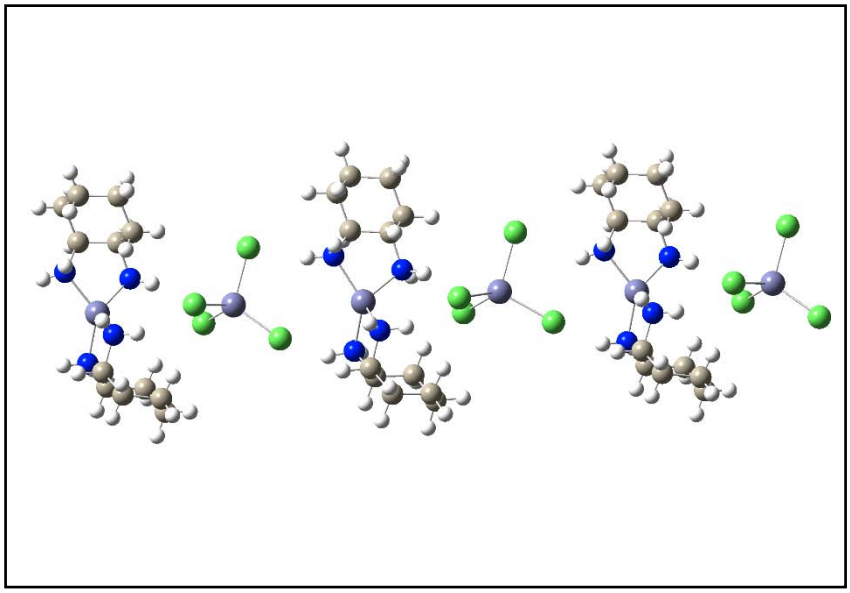

Figure 3.7 Optimized structure of the central $[Zn(Dach)_2][ZnCl_4]$ complex surrounded by two frozen units in the $\{[Zn(Dach)_2][ZnCl_4]\}_3$complex $(\mathbf{6})_3$.

The selected, experimentally determined and B3LYP-D3 calculated interatomic distances, and bond angles of the $\{[Zn(Dach)_2][ZnCl_4]\}_3$ (**6**)$_3$ complex are collected in Table 3.6. As follows from this table, in the theoretical model of complex**6**, the calculated bond distances between the Zn(1) cation and the nitrogen atoms are slightly over-estimated with respect to the corresponding experimental X-ray data. The differences range from 0.044 to 0.075 Å for Zn(1)-N(4) and Zn(1)-N(3), respectively. With respect to the bond distances between the Zn(2) and the chlorine atoms, the differences between the calculated and the experimentally determined values are about twice larger and range from 0.081 to 0.176 Å for Zn(2)-Cl(4) and Zn(2)-Cl(3), respectively. In the cases of the others bond distances collected in Table 4, the corresponding differences are smaller than 0.017 Å.

In the optimized structure of the $\{[Zn(Dach)_2][ZnCl_4]\}_3$ complex, the tetrahedron surroundings around the Zn(1) ion is slightly more distorted than that found from the X-ray diffraction. The N(2)-Zn(1)-N(3) and N(1)-Zn(1)-N(4) bond angles are 117.87° and 113.54°, respectively, whereas they are 126.94° and 117.27° in the crystal. Simillar situation has been found with respect to the surroundings around the Zn(2) ion. In (**6**)$_3$ complex, the calculatedCl(1)-Zn(2)-Cl(4) and Cl(2)-Zn(2)-Cl(3) bond angles are 104.88° and 100.56°, while in the crystal they are 112.09° and 106.03°, respectively

With respect to the zinc(II) complex with *cis*-1,2-diaminocyclohexane and the chlorine anions ligands, studied in this work, the question arises, which of the complex is more stable: dinuclear $[Zn(Dach)_2][ZnCl_4]$(**6**) or dimer of mononuclear $[Zn(Dach)Cl_2]$complexes? Six different $[Zn(Dach)Cl_2]_2$ dimers has been found. The optimized structures of the most and the less stable $[Zn(Dach)Cl_2]_2$ complexes are illustrated in Figure 3.8.

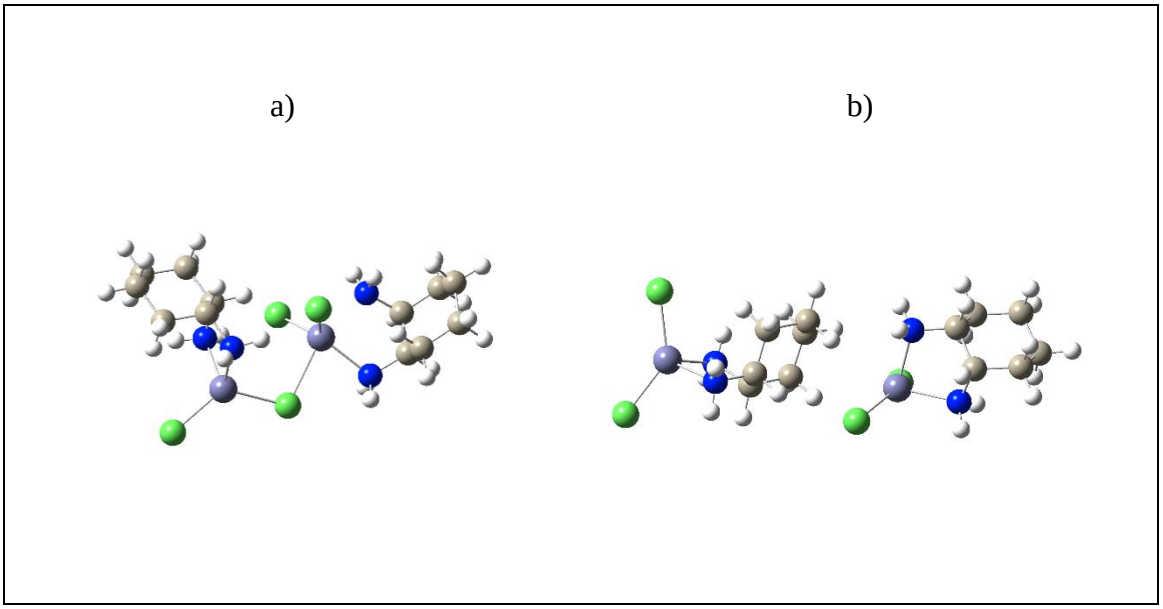

Figure 3.8 Optimized structures of the most (a) and the less (b) stable $[Zn(Dach)Cl_2]_2$ complex (6)

According to the DFT calculations, the most stable $[Zn(Dach)Cl_2]_2$ complex (structure a in Figure 3.8) is more stable than fully optimized $[Zn(Dach)_2][ZnCl_4]$ complex (**6**) by 22.48 kcal mol^{-1}, while the less stable dimer of homonuclear $[Zn(Dach)Cl_2]$ complexes (structure b in Figure 3.8) has been found to be less stable than (**6**) by 1.80 kcal mol^{-1}.

The NBO method allows to calculate the charges on the atoms in $[Zn(Dach)_2][ZnCl_4]$ $(\mathbf{6})_3$. The NBO charges on the selected atoms of $[Zn(Dach)_2][ZnCl_4]$ $(\mathbf{6})_3$ are collected in Table 3.7. The NBO charge on the Zn(1) cation surrounded by two neutral *cis*-1,2-diaminocyclohexane ligands is 1.398 e, and is larger by 0.547 e than that found on Zn(2) surrounded by four chlorine anions. The natural electron configuration on the Zn(1) cation is $[core]4s^{0.34}3d^{9.98}4p^{0.28}$ and slightly differ from that on the Zn(2) ion, where the electron configuration is $4s^{0.44}3d^{9.99}4p^{0.70}5p^{0.01}$. The charge on the nitrogen atoms in the isolated *cis*-1,2-diaminocyclohexane molecule is about -0.93 e, while in the $[Zn(Dach)_2][ZnCl_4]$ complex the values of these charges decrease and range from -1.046 to -1.026 e. With respect to the charges on the chlorine ions, they increase by about 0.33 e with respect to that in isolated ligands.

Table 3.6 Selected structural parameters of $\{[Zn(Dach)_2][ZnCl_4]\}_3$ (**6**)$_3$ complex.

Bond distance (Å)	Exp.[a]	Theory[b]	Bond angle(°)	Exp.[a]	Theory[b]
Zn(1)-N(1)	2.037(4)	2.094	N(1)-Zn(1)-N(2)	86.41(17)	85.74
Zn(1)-N(2)	2.020(4)	2.091	N(1)-Zn(1)-N(3)	126.94(18)	117.87
Zn(1)-N(3)	2.028(4)	2.103	N(1)-Zn(1)-N(4)	117.27(18)	113.54
Zn(1)-N(4)	2.058(4)	2.102	N(2)-Zn(1)-N(3)	130.91(17)	132.97
Zn(2)-Cl(1)	2.2542(13)	2.398	N(2)-Zn(1)-N(4)	112.43(18)	123.39
Zn(2)-Cl(2)	2.2624(14)	2.389	N(3)-Zn(1)-N(4)	85.36(17)	85.82
Zn(2)-Cl(3)	2.2870(14)	2.463	Cl(1)-Zn(2)-Cl(2)	113.45(6)	116.23
Zn(2)-Cl(4)	2.2737(12)	2.355	Cl(1)-Zn(2)-Cl(3)	111.30(6)	112.84
C(1)-N(1)	1.492(7)	1.491	Cl(1)-Zn(2)-Cl(4)	112.09(5)	104.88
C(12)-N(4)	1.485(6)	1.502	Cl(2)-Zn(2)-Cl(3)	106.03(5)	100.56
C(7)-N(3)	1.489(6)	1.501	Cl(2)-Zn(2)-Cl(4)	107.85(5)	112.36
C(6)-N(2)	1.491(6)	1.501	Cl(3)-Zn(2)-Cl(4)	105.63(5)	110.11

Table 3.7 NBO charges [e] on selected atoms of the central $[Zn(Dach)_2][ZnCl_4]$ complex in $(\mathbf{6})_3$

Atom	Charge (e)
Zn (1)	1.398
Zn (2)	0.851
N(1)	-1.026
N(2)	-1.041
N(3)	-1.037
N(4)	-1.046
Cl (1)	-0.676
Cl (2)	-0.667
Cl (3)	-0.676
Cl (4)	-0.671

$[Zn(Dach)(NCS)_2]$ (7), $[Zn(TMEDA)(NCS)_2]$ (9) and $[Zn(en)(NCS)_2]$ (13)

As shown in Figure 3.9, the fully optimized structure of the $[Zn(Dach)(NCS)_2]$ complex (**7**) surrounded by seven frozen complex molecules is similar to that obtained in the experiment (*vide infra*). The additional frozen complexes have the similar structure, observed in the solid-state (thus the crystal packing effects are covered). They are required to stabilize the position of the NCS^- ligands.

Full optimization of only one $[Zn(Dach)(NCS)_2]$ complex in the gas phase leads to the final structure significantly different from the experimental one as shown in Figure 3.10. In this case, the NCS^- ligands are twistedin such a waythat the sulfur atoms are situated next to the hydrogen atoms of Dach ligand. The S···H distances are only about 3 Å.

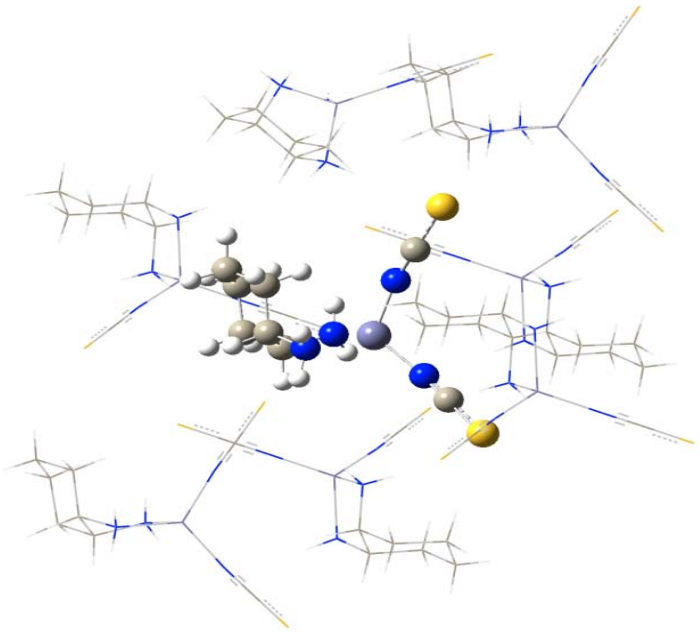

Figure 3.9 Fully optimized structure of the model [Zn(Dach)$(NCS)_2$] (**7**) complex surrounded by seven frozen complexes based on calculations performed at the B3LYP-D3 level

With respect to the [Zn(TMEDA)$(NCS)_2$] (**9**) and [Zn(en)$(NCS)_2$] (**13**) complexes, the same problem with final positions of the NCS^- ligands as a result of full geometry optimization of single complex has been found. To solve this problem, we decided to perform geometry optimization of all complexes studied with frozen position of sulfur atoms. Figure 3.11 illustrates the structures of these complexes, optimized at the BLYP-D3level.

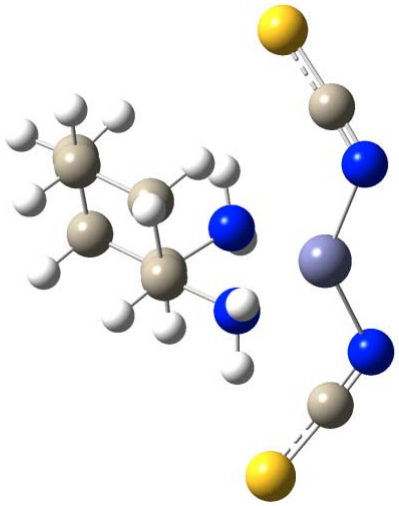

Figure 3.10 Fully optimized structure of the [Zn(Dach)$(NCS)_2$] (**7**) complex without additional frozen molecules

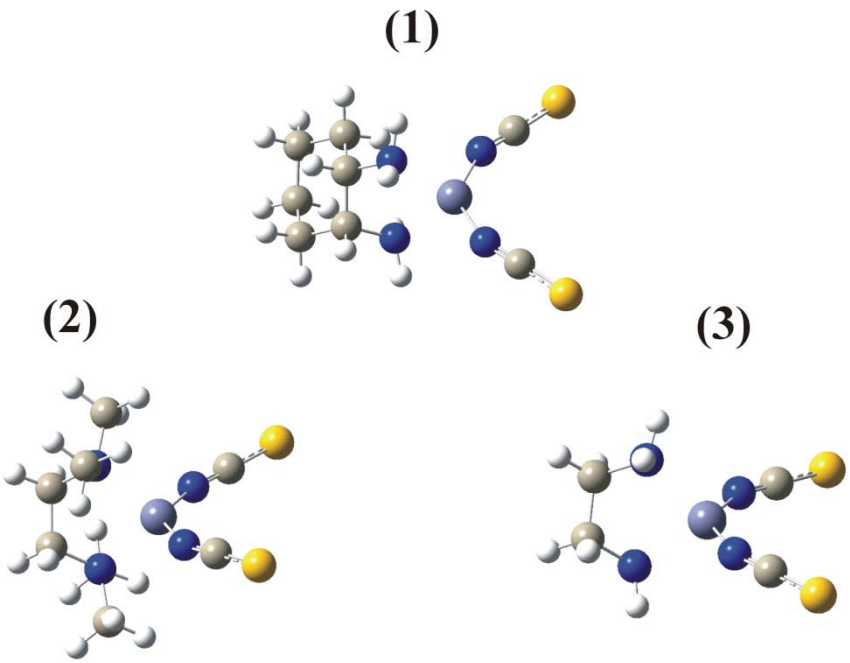

Figure 3.11 Optimized structure of the model [Zn(Dach)$(NCS)_2$] (**7**), [Zn(TMEDA)$(NCS)_2$] (**9**) and [Zn(en)$(NCS)_2$] (**13**) complexes with frozen positions of sulfur atoms.

The selected, experimentally determined and B3LYP-D3 calculated interatomic distances, and bond angles of the $[Zn(Dach)(NCS)_2]_8$ (**7_8**), $[Zn(Dach)(NCS)_2]$ (**7**), $[Zn(TMEDA)(NCS)_2]$ (**9**) and $[Zn(en)(NCS)_2]$ (**13**) complexes are collected in Table 3.8. In the optimized structure of $[Zn(Dach)(NCS)_2]_8$ complex (**7_8**), the tetrahedron around the zinc ion is slightly more distorted than that found from the X-ray diffraction. The N(1)-Zn(1)-N(2) and N(2)-Zn(1)-N(4) bond angles are 105.7° and 129.8°, respectively, whereas they are 117.1° and 110.8° in the crystal. With respect to the $[Zn(Dach)(NCS)_2]$ (**7**), $[Zn(TMEDA)(NCS)_2]$ (**9**) and $[Zn(en)(NCS)_2]$ (**13**) complexes, the bond angle for N(2)-Zn(1)-N(4) is significantly smaller than that in crystal and $[Zn(Dach)(NCS)_2]_8$ (**7_8**). In the complexes with frozen positions of S atoms the value of this angle is almost equal to the value of the bond angles for N(1)-Zn(1)-N(4) , N(2)-Zn(1)-N(3) and N(1)-Zn(1)-N(3) bonds. In contrast, the value of the bond angle for N(1)-Zn(1)-N(2) bond in the complexes (**7**), (**9**) and (**13**) is significantly larger than that found in the X-ray structure and calculated for (**7_8**) complex. It is worth to mention that this angle was found to be even larger in fully optimized complexes studied (without frozen positions of the sulfur atoms).

In (**7**) and (**7_8**) complexes, the calculated Zn(1)–N(1) bond distances are overestimated with respect to the corresponding experimental data by less than 0.13 Å. Similar discrepancies between the calculated and X-ray determined Zn–N distances have been found for the $\{[Zn(L\text{-}Arg)(Hox)_2]\cdot 4H_2O\}$ and $\{[Zn(L\text{-}tyr)_2(\mu\text{-}4,4'\text{-}bpy)]\cdot 4H_2O\}_n$ complexes [220,221].

The interaction energies (ΔE) corrected for the basis set super position error (BSSE) between selected ligands and the rest of the complex for studied systems (**7**, **9**, **13**) are collected in Table 3.9. Inspection of Table 3.9 reveals that the ΔE between NCS^- ligands and the rest of the complex are comparable. They are ranging from -139.9 to -143.8 kcal mol^{-1}. Thus, the differences between them are smaller than 3%. It is worth to mention that in the $\{[Zn(L\text{-}Arg)(Hox)_2]\cdot 4H_2O\}$ complex, the interaction energies for L-arginine zwitterion and two oxalate anions ligands were obtained as –144.03, –142.62, and –145.61 kcal mol^{-1}, respectively [220].

Table 3.8 Selected structural parameters (bond distances in Å, bond angles in degrees) of $[Zn(Dach)(NCS)_2]_8$ (**7_8**), $[Zn(Dach)(NCS)_2]$ (**7**), $[Zn(TMEDA)(NCS)_2]$ (**9**) and $[Zn(en)(NCS)_2]$ (**13**) complexes

Bond length (Å)	Experimental[a]	Theory[b]			
		(**7_8**)	(**7**)	(**9**)	(**13**)
Zn(1)-N(1)	1.927(5)	2.005	1.952	1.953	1.946
Zn(1)-N(2)	1.923(6)	1.998	1.949	1.953	1.946
Zn(1)-N(3)	2.036(4)	2.128	2.167	2.17	2.18
Zn(1)-N(4)	2.041(4)	2.1	2.166	2.165	2.18
N(1)-C(1)	1.138(6)	1.184	1.198	1.197	1.198
N(2)-C(2)	1.137(8)	1.184	1.198	1.197	1.198
N(3)-C(3)	1.492(6)	1.493	1.491	1.485	1.487
N(4)-C(4)	1.492(6)	1.507	1.495	1.487	1.487
S(1)-C(1)	1.612(7)	1.663	1.637	1.637	1.636
S(2)-C(2)	1.613(7)	1.661	1.637	1.637	1.636
Bond angle (°)		(**7_8**)	(**7**)	(**9**)	(**13**)
N(1)-Zn(1)-N(2)	110.8(2)	105.7	133.9	132.4	135.9
N(1)-Zn(1)-N(3)	111.5(2)	106.4	108.7	106.6	106.5
N(1)-Zn(1)-N(4)	115.38(19)	115.6	105.8	107.6	106.2
N(2)-Zn(1)-N(3)	113.1(2)	110.1	106.8	107.1	106.2
N(2)-Zn(1)-N(4)	117.10(19)	129.8	107.3	107.4	106.5
N(3)-Zn(1)-N(4)	86.80(18)	84.9	82.3	85.8	82.7
Zn(1)-N(1)-C(1)	175.1(6)	170.4	154.1	154.8	153
N(1)-C(1)-S(1)	179.2(7)	179.3	178.9	179	178.9

[a]Experimental values.

[b]Theoretical values calculated at the DFT (B3LYP-D3) level.

Table 3.9 DDFT calculated interaction energies (ΔE in kcal mol^{-1}) corrected for the BSSE between selected ligand and the rest of the complex in $[Zn(Dach)(NCS)_2]$ (**7**), $[Zn(TMEDA)(NCS)_2]$ (**9**) and $[Zn(en)(NCS)_2]$ (**13**)

Complex	ΔE (kcal mol^{-1})		
	N(1)S(1)C(1)	N(2)C(2)S(2)	Organic ligand
(**7**)	-140.1	-139.9	-77.2
(**9**)	-141	-141	-78.7
(**13**)	-143.8	-143.8	-72.8

With respect to the ΔE between the neutral organic ligand and the rest of the complex, for Dach and TMEDA ligands similar values of the ΔE were obtained -77.2 and -78.7 kcal mol^{-1}, while for the en ligand the absolute value of the ΔE was found to be smaller by about 5 kcal mol^{-1} (-72.8 kcal mol^{-1}).

The NBO charges on selected atoms of the complexes studied (**7**, **9** and **13)** are reported in Table 3.10. As follows from this table the charges on the zinc(II) ion in complexes (**7**, **9** and **13)** are, 1.688, 1.699 and 1.684 e respectively. Thus, the charge on the central ion in the $[Zn(TMEDA)(NCS)_2]$ complex is larger by 0.011 and 0.015 e than that in the $[Zn(Dach)(NCS)_2]$ and $[Zn(en)(NCS)_2]$ complexes, respectively. With respect to the charges on the nitrogen atoms of the NCS^- ligands in the investigated complex, they are equal to about -0.94 e.

The differences between the charges on the nitrogen atoms of the NCS^- ligands and the charges on the zinc(II) ions are comparable in all cases under discussion. They are 2.63 e (in **7** and **13**) and 2.64 e (in **9**). With respect to the charges on the nitrogen atoms of the organic ligands, they are equal about -1.03 e in the cases of the complexes (**7**) and (**13**), and much smaller -0.67 e in complex (**9**). As was mentioned before, the largest ΔE was calculated for the $[Zn(TMEDA)(NCS)_2]$ (**9**) complex. Therefore, the smallest differences between the charges on N atoms of TMEDA ligand and the charges on the central ion correspond to larger value of the interaction energy. This could be explained as a

consequence of the additional interactions between CH_3 groups of the TMEDA ligand and the rest of the complex.

According to the NBO results, in complexes studied, all of the interactions between the zinc(II) ion and all of nitrogen donor atoms were recognized as coordination bonds (N→Zn). These interactions correspond to a donation of the electron density from the lone pair orbital on the nitrogen atoms, LP(N) to the antibonding lone pair orbital on the zinc ion LP*(Zn).

Table 3.10 NBO charges [e] on selected atoms of the $[Zn(Dach)(NCS)_2]$ (**7**), $[Zn(TMEDA)(NCS)_2]$ (**9**) and $[Zn(en)(NCS)_2]$ (**13**) complexes

Atom	(**7**)	(**9**)	(**13**)
Zn	1.688	1.699	1.684
N(1)	-0.941	-0.941	-0.942
N(2)	-0.937	-0.941	-0.942
N(3)	-1.033	-0.669	-1.027
N(4)	-1.038	-0.671	-1.027
C(1)	0.198	0.199	0.197
C(2)	0.198	0.2	0.199
C(3)	-0.002	-0.207	-0.188
C(4)	-0.009	-0.207	-0.199
S(1)	-0.145	-0.146	-0.141
S(2)	-0.148	-0.146	-0.141

$[Zn(Dap)(NCS)_2][Zn(Dap)(NCS)_2]_3$ (8)

To answer the question whether the structure **8** is more stable than a simple polymeric structure (**8b**), we also performed calculations for the following two systems: $[Zn(Dap)(NCS)_2][Zn(Dap)(NCS)_2]_3$ and $[Zn(Dap)(NCS)_2]_4$ as models of the complex **8** and simple polymeric structure (**8b**) respectively (Figure 3.12).

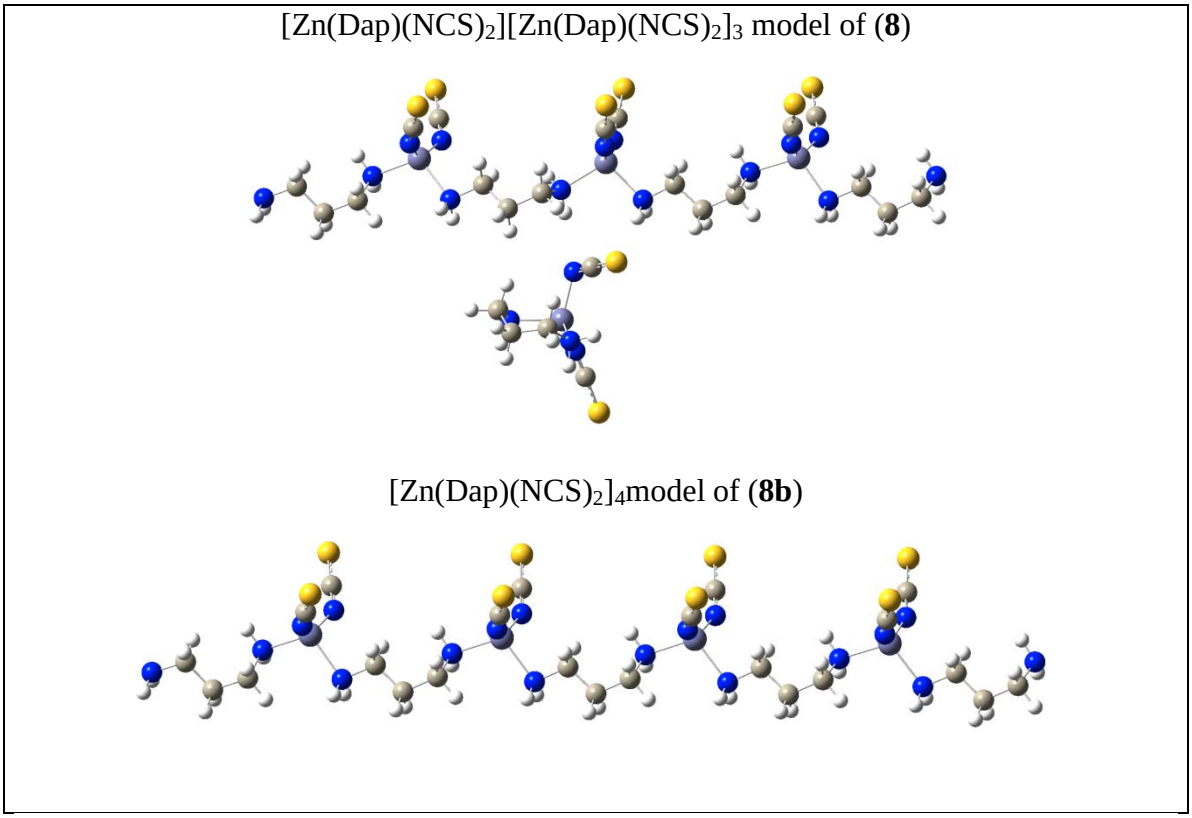

Figure 3.12 B3LYP-D3 optimized structures of the models of (**8**), $[Zn(Dap)(NCS)_2][Zn(Dap)(NCS)_2]_3$ and simple polymeric structure (**8b**), $[Zn(Dap)(NCS)_2]_4$

Each of the considered models consists of four $[Zn(Dap)(NCS)_2]$ units. As the starting geometries in the optimization procedures, the fragment of the crystallographic structure of (**8**) was used. During optimization, the positions of all sulfur atoms and external nitrogen atoms of the polymeric chains were frozen, while the positions of the rest of the atoms were relaxed. It should be mentioned that the full geometry optimization of the

models considered, leads to the final structures significantly different from the experimental one. According to the DFT results, the absolute value of the electronic energy of the $[Zn(Dap)(NCS)_2][Zn(Dap)(NCS)_2]_3$ complex is greater than that of $[Zn(Dap)(NCS)_2]_4$ by 11.05 kcal mol^{-1}. Therefore, the DFT results support the fact that the structure of complex (**8**) is more stable than a simple polymeric structure.

For the optimized structure of the $[Zn(Dap)(NCS)_2][Zn(Dap)(NCS)_2]_3$ complex, the interaction energy (ΔE) between the monomeric $[Zn(Dap)(NCS)_2]$ and the polymeric $[Zn(Dap)(NCS)_2]_3$ units was calculated to be -11.98 kcal mol^{-1}.The values of ΔE between each of the ligands and the rest of the complex were calculated for the optimized structure of polymeric $[Zn(Dap)(NCS)_2]_4$complex as well as for the isolated monomeric $[Zn(Dap)(NCS)_2]$ complex. With respect to the polymeric complex, the calculations were performed for one of the middle $[Zn(Dap)(NCS)_2]$ unit (Figure 3.12). With respect to the isolated monomeric $[Zn(Dap)(NCS)_2]$ complex, the optimization procedure was performed in the same way as described above (with frozen positions of the S atoms). In the case of NCS^- anions the B3LYP-D3 calculated values of ΔE are: -145.40, -146.81, -142.99 and -143.23 kcal mol^{-1} for the polymeric and isolated complexes, respectively. The ΔE values for the 1,3-diaminopropane ligands are: -65.28 and -78.26 kcal mol^{-1} for $[Zn(Dap)(NCS)_2]_4$and the monomeric $[Zn(Dap)(NCS)_2]$ complexes, respectively.

The X-ray structure of (**8**) shows that the complex is stabilized mainly by hydrogen bonds. We also found that some other weak interactions like a chalcogen bond can play an additional role in the stabilization of (**8**). We found that some of the intermolecular S···N distances were smaller than the sum of the van der Waals radii of the corresponding atoms (3.35 Å) which is a first indication of the interaction. Chalcogen bonded S···N and S···π interactions have been recently the subject of experimental and theoretical works [222-224]. Recently, Hobza et al. [224] demonstrated in the case of Ph-*closo*-1-$SB_{11}H_{10}$ that the pentavalent sulfur was involved in the S···π chalcogen bond. They found this interaction surprisingly strong, -8 kcal mol^{-1}. To the best of our knowledge, in our study, the evidence of the S···π chalcogen bond, where trivalent sulfur is involved, is described for the first time in the literature.

Let us mention that the interaction between the sulfur atom and electronegative region (like a lone pair of electrons or π-electrons) is possible since the region of positive potential called "σ-hole" located along the S-C bond. Figure 3.13 shows the electrostatic potential surface (ESP) of the model neutral HNCS molecule calculated at the B3LYP-D3/Def2TZVP level. The σ-hole on the sulfur atom is shown as the green circle. The electrostatic potential ($V_{s,max}$) on the sulfur atom of the isolated HNCS is 2.78 kcal mol^{-1}. As seen in Figure 3.13 the sulfur atom possess the positive σ-hole as well as the region of negative potential. Therefore, it can interact electrostatically with both electrophiles and nucleophiles.

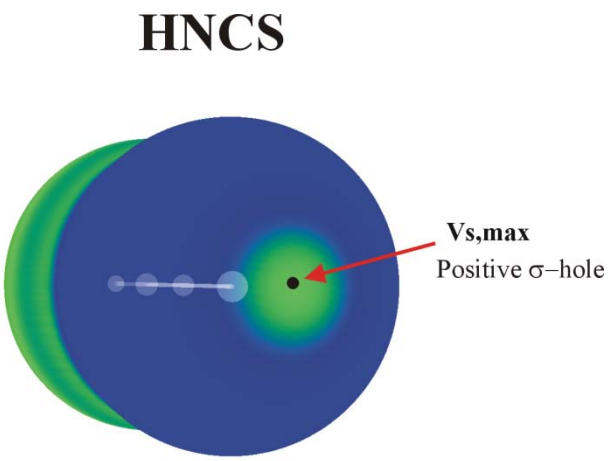

Figure 3.13 Molecular surface of electrostatic potential (ESP, kcal mol^{-1}) of neutral isolated HNCS molecule computed on the 0.001 a.u. contour of the electrostatic density at the B3LYP-D3/Def2TZVP level.Color ranges, in kcal mol^{-1}, are: red greater than 20, yellow between 20 and 10, green between 0 and 10, blue less than 0. Selected surface critical point, $V_{s,max}$ on the sulfur atom is indicated (its value is 2.78 kcal mol^{-1}). The σ-hole on the sulfur atom is demonstrated as a green circle.

In Figure 3.14, the fragment of the crystal structure of (**8**) with selected geometrical parameters is illustrated. The positions of hydrogen atoms were optimized at the DFT level. As it can be seen in Figure 3.14, the sulfur atom is simultaneously involved in the interactions with the H atom and π-electrons of the bond between the N and C atoms of NCS^-. Both the intermolecular S···N and S···H distances (3.331 and 2.956 Å) are shorter than the sum of the van der Waals radii of the corresponding atoms, 3.35 and 3.00 Å, respectively. The distance between the S and C atoms is 3.629 Å and is longer than the sum of the van der Waals radii of the S and C atoms by 0.129 Å. The difference in the S···N and S···C intermolecular distances testifies the fact that the maximum of the electron density of the NC bond is located closer to the nitrogen atom. The NBO charges on the N and C atoms of the NCS anion are -0.774 and 0.216e, respectively. The B3LYP-D3 calculated interaction energy between these two $[Zn(Dap)(NCS)_2]$ fragments is -5.17 kcal mol^{-1}. Therefore, one can assume that ΔE of the S···πchalcogen bond in the $[Zn(Dap)(NCS)_2]_2$ complex is about half of this value (-2.6 kcal mol^{-1}). The interaction energies calculated for the S···πchalcogen bonded complexes between the SF_2 or SF_4 and the C-C multiple bonds range between -3.60 and -6.63 kcal mol^{-1} [223].

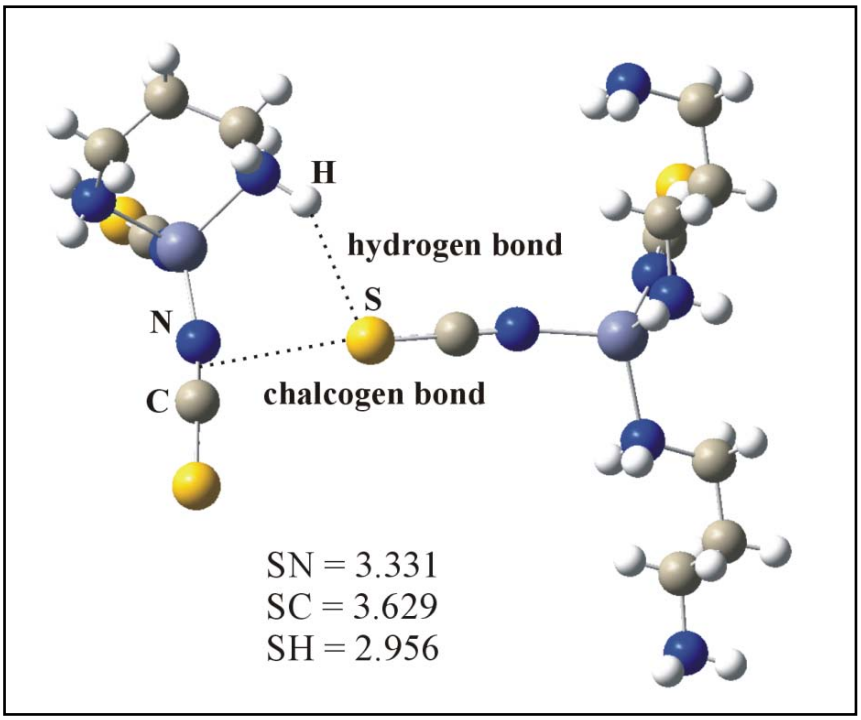

Figure 3.14 Fragment of the crystal structure of complex (**8**) with DFT optimized positions of hydrogen atoms. Selected distances are in Å. The dashed lines represent the S···π chalcogen and S···H hydrogen bonds.

It should be mentioned that in (**8**) the sulfur atom is also involved in two more hydrogen bonds with the H atoms of other two [Zn(Dap)$(NCS)_2$] units, not illustrated in Figure 3.14. The interactions indicated in Figure 3.14 should be considered as the S···π chalcogen bonds not as the S···N chalcogen bond. The main reason is that the lone pair of the N atom is involved in the interactions with the Zn(II) cation. According to the NBO results, the interaction between zinc(II) and the nitrogen atom is recognized as coordination bond (N→Zn). This interaction corresponds to a donation of electron density from the lone pair orbital on the nitrogen LP(N) to the antibonding LP*(Zn) orbitals. The strength of these donor-acceptor interactions was estimated by the second-order interaction energy, E^2. The value of E^2 of the LP(N) → LP^*(Zn) interaction is 123 kcal mol^{-1}. Further, according to the NBO results, there are weak donor- acceptor π*(N-C) →σ^*(S-C),π(N-C) →σ^*(S-C) and π(N-C) → Ry^*(S) interactions. The E^2 values of these

interactions are: 0.14, 0.11 and 0.06 kcal mol^{-1}, respectively. Also some back donation interactions were found.

To check the region of the non-covalent interactions between the fragments of the $[Zn(Dap)(NCS)_2]$ complex, the non-covalent interaction (NCI) method introduced by Yang et al. was used [225, 226]. In Figure 3.15, it is demonstrated that the stabilization interactions appears between the S atom and the NC multiple bond (the green area). Also the S···H hydrogen bond is seen in this Figure.

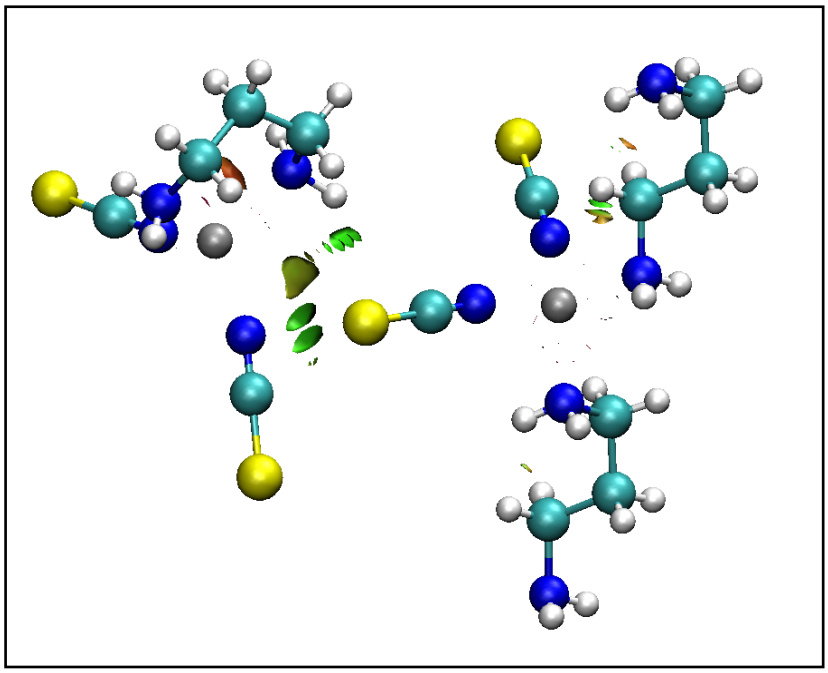

Figure 3.15 Plots of the non-covalent interactions (NCI) for $[Zn(Dap)(NCS)_2]\cdots[Zn(Dap)(NCS)_2]$(**8**) complex. The green parts of surfaces mean attractive interactions, while the red mean repulsive interactions.

3.3.4 Description of X-ray structures

$[Zn(Dach)_2][ZnCl_4]$ (6)

An ORTEP view of complex (**6**) is shown in Figure 3.16 and the geometrical features are listed in Table 3.11. The crystal structure of compound (**6**) is built up from discrete *bis*(*cis*-1,2-diaminocyclohexane)zinc(II) cations and tetrachloridozincate(II) anions. The Zn(II) ion in $[Zn(Dach)_2]^{2+}$ is coordinated by four nitrogen atoms of two chelating Dach ligands displaying a distorted tetrahedral geometry. The angles around zinc are in the range of 85.36(17) - 130.91(17)^o. The distortion from the regular tetrahedral geometry may be associated with the steric constraints of the cyclic Dach molecules. The two chelating N—Zn—N bite angles in (**6**) are almost identical (Table 3.11). The five-membered chelate rings in the dication of (**6**) approximate to an envelope. The Dach entities exhibit a regular spatial conformation (chair conformation for both cyclo-hexanediamine rings) with normal distances and angles. The $[ZnCl_4]^{2-}$ anion adopts a slightly distorted tetrahedral stereochemistry with the variation of bond angles from 105.63(5) to 113.45(6)^o. The average Zn–N and Zn—Cl bond distances are in agreement with the values reported for other Zn(II)-Dach [37, 38, 49, 50] and $[ZnCl_4]^{2-}$ complexes [227-229]. Among the reported Zn-Dach complexes, only one i.e.$[Zn(Dach)_2](ClO_4)_2$ involves a *bis* chelated environment as observed in (**6**) [37].

The crystal packing is stabilized by extensive hydrogen-bonding interactions between the N-H groups (or C-H) of the Dach ligands and $[ZnCl_4]^{2-}$ anions. All N-H hydrogen atoms are involved in hydrogen bonding. The details of hydrogen bonding are given in Table 3.12. The linking of cations and anions through N-H···Cl hydrogen bonds, leads to the formation of a two-dimensional network. The hydrogen bonding pattern is believed to stabilize the encountered distorted tetrahedral geometry.

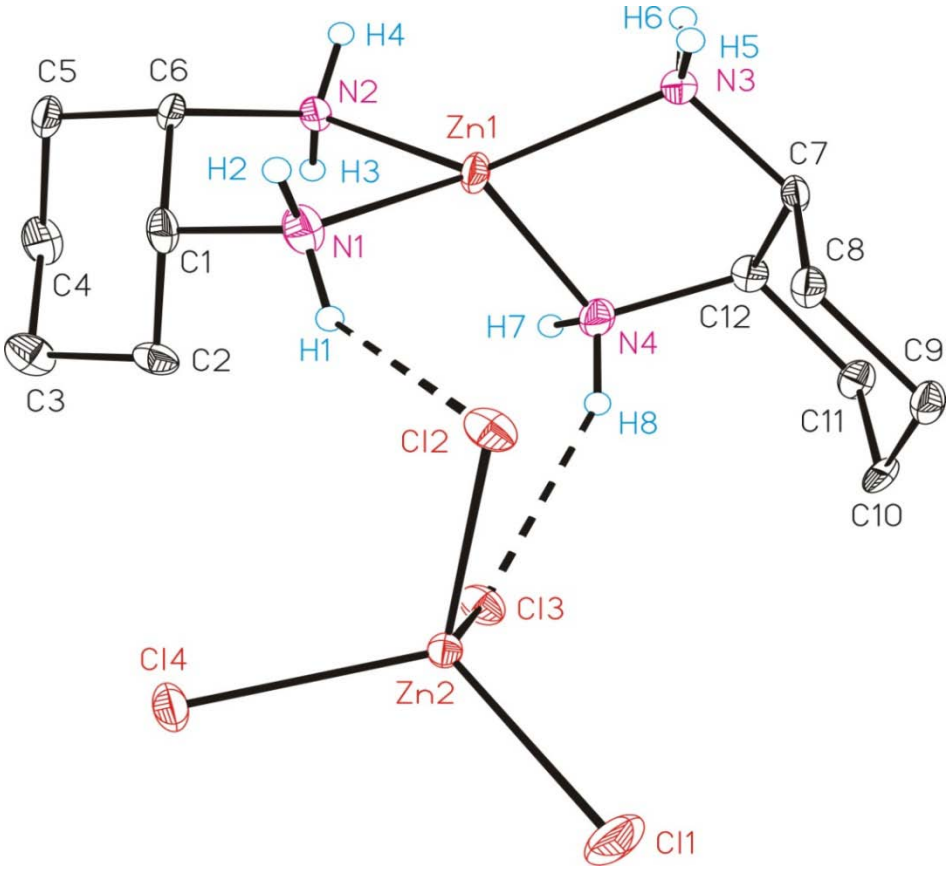

Figure 3.16 ORTEP diagram (50 % ellipsoid probability) of the molecular structure of (**6**) according to the orientation of the $[Zn(dach)_2]^{2+}$ cation towards the $[ZnCl_4]^{2-}$ anion in the asymmetric unit. All carbon bonded hydrogen atoms are omitted for clarity. Dotted lines refer to interionic hydrogen bonds.

Table 3.11 Selected bond distances (Å) and bond angles (˚) of $[Zn(Dach)_2][ZnCl_4]$ (**6**)

Bond distance		Bond angle	
Zn(1)-N(1)	2.037(4)	N(1)-Zn(1)-N(2)	86.41(17)
Zn(1)-N(2)	2.020(4)	N(1)-Zn(1)-N(3)	126.94(18)
Zn(1)-N(3)	2.028(4)	N(1)-Zn(1)-N(4)	117.27(18)
Zn(1)-N(4)	2.058(4)	N(2)-Zn(1)-N(3)	130.91(17)
Zn(2)-Cl(1)	2.2542(13)	N(2)-Zn(1)-N(4)	112.43(18)
Zn(2)-Cl(2)	2.2624(14)	N(3)-Zn(1)-N(4)	85.36(17)
Zn(2)-Cl(3)	2.2870(14)	Cl(1)-Zn(2)-Cl(2)	113.45(6)
Zn(2)-Cl(4)	2.2737(12)	Cl(1)-Zn(2)-Cl(3)	111.30(6)
C(1)-N(1)	1.492(7)	Cl(1)-Zn(2)-Cl(4)	112.09(5)
C(12)-N(4)	1.485(6)	Cl(2)-Zn(2)-Cl(3)	106.03(5)
C(1)-C(2)	1.523(8)	Cl(2)-Zn(2)-Cl(4)	107.85(5)
		Cl(3)-Zn(2)-Cl(5)	105.63(5)

Table 3.12 Hydrogen bonds in complex $[Zn(Dach)_2][ZnCl_4]$ (**6**) (Å, º)

Donor-H···Acceptor	Code	D-H	H···A	D···A	∠Δ–H&A
N1-H1…Cl2	1555.02	0.92(4)	2.62(4)	3.325(4)	134(5)
N1-H2…Cl1	3655.02	0.93(3)	2.61(3)	3.531(5)	171(5)
N2-H3…Cl2	3654.02	0.91(3)	2.49(3)	3.335(4)	155(5)
N2-H4…Cl4	1565.02	0.92(4)	2.65(4)	3.360(4)	135(5)
N3-H5…Cl4	3655.02	0.93(3)	2.56(4)	3.482(4)	173(6)
N3-H6…Cl1	1565.02	0.94(2)	2.81(4)	3.550(4)	137(5)
N4-H7…Cl2	3654.02	0.93(5)	2.35(5)	3.259(5)	167(5)
N4-H8…Cl3	1555.02	0.95(3)	2.46(4)	3.346(4)	155(5)
C8-H8A…Cl2	1555.02	0.97	2.78	3.601(5)	142

Translation of ARU-Code to CIF and Equivalent Position Code

[1565.] = [1_565] = x,1+y,z

[3654.] = [3_654] = 3/2-x,1/2+y,-1/2+z

[3655.] = [3_655] = 3/2-x,1/2+y,1/2+z

[Zn(Dach)$(NCS)_2$] (7)

The molecular structure of (**7**) is shown in Figure 3.17. The particular bond lengths (Å) and bond angles (^{o}) are listed in Table 3.13. The structure of complex (**7**) contains discrete nonionic molecules, [Zn(Dach)$(NCS)_2$]. The coordination environment around zinc is distorted tetrahedral attained by two, two N-atoms of each Dach and thiocyanate ions. Except the N-Zn-N angle of 86.79(17)^o corresponding to Dach ligand, the angles around zinc {110.8(2)^o– 117.10(19)^o} are in agreement with the tetrahedral geometry. The smaller value of Dach bite angle with respect to 109.5° could be related to its chelating mode. The Zn-N distances are in accordance with those found in other [ZnL$(NCS)_2$] type zinc(II) complexes [39-41, 80, 206, 207] such as, [Zn(en)$(NCS)_2$] [41]. The somewhat shorter Zn-N (NCS) distances [1.968(2) Å] as compared to Zn-N(Dach) [(2.009(2) Å] indicate the stronger binding of thiocyanate. The Zn-N=CS units are slightly bent with the bond angles of 170.9(5) and 175.1(6)^o. The angles around N atoms of Dach {C3-N3-Zn1 = 106.3(3)^o} represent a tetrahedral environment. The SCN moieties are almost linear with a bond angle of 179.2(7)^o. The compound (**7**) is somewhat similar to a known zinc(II) complex, [Zn(en)$(NCS)_2$] [41].

There exists strong H-bonding between N-H hydrogen atoms of Dach and sulfur atoms of thiocyanate. The hydrogen bonding parameters are listed in Table 3.14. Due to intermolecular N-H---S interactions, the molecules are stabilized in the 1D polymeric grid along the ***a*** axis as shown in Figure 3.18. The H-bonds in (**7**) are not branched as they were found for other en-based [Zn(diamine)$(SCN)_2$] complexes [41]. The N-H hydrogen atoms in these complexes were fully involved in N–H(N) ---S bonds and the most of such bonds were branched either bifurcated or trifurcated.

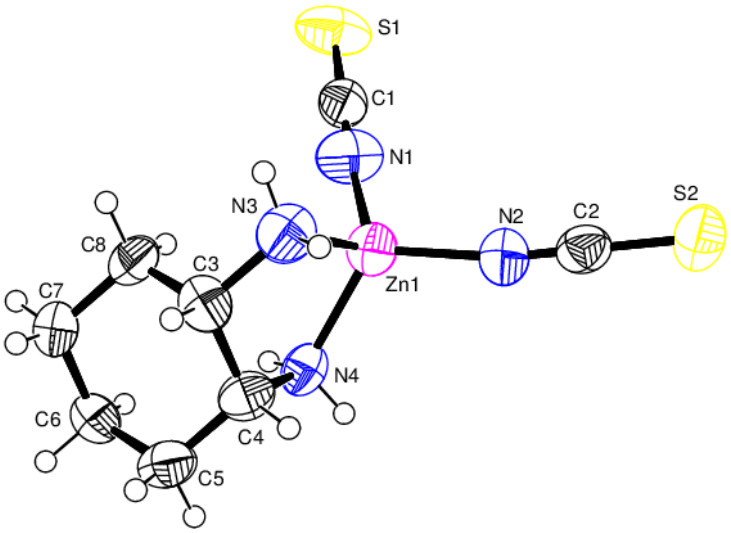

Figure 3.17 Molecular structure of (**7**) along with crystallographic numbering scheme of the molecular unit.

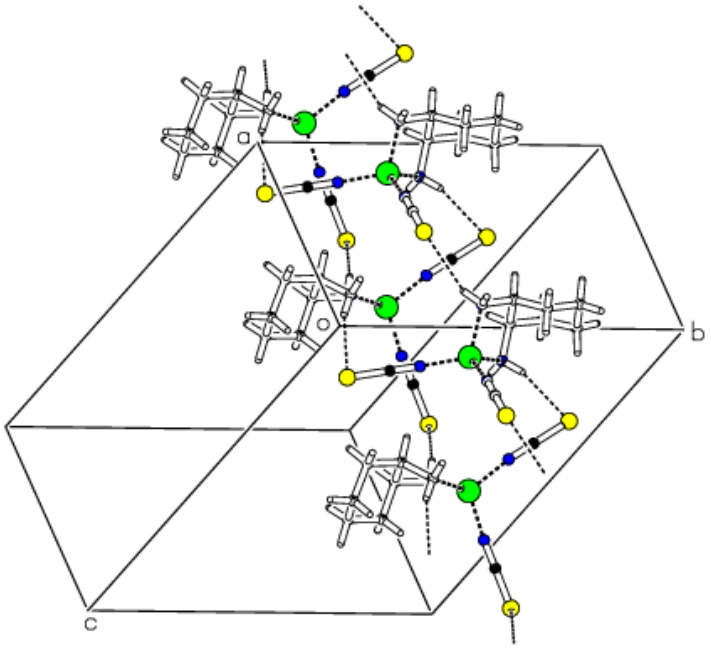

Figure 3.18 Crystalpacking diagram of (**7**) showing H-bonds

Table 3.13 Selected bond distances (Å) and bond angles (˚) for (**7**)

Bond distance		Bond angle	
Zn(1)-N(1)	1.927(5)	N(1)-Zn(1)-N(2)	110.8(2)
Zn(1)-N(2)	1.923(6)	N(1)-Zn(1)-N(3)	111.5(2)
Zn(1)-N(3)	2.036(4)	N(1)-Zn(1)-N(4)	115.38(19)
Zn(1)-N(4)	2.041(4)	N(2)-Zn(1)-N(3)	113.1(2)
N(1)-C(1)	1.138(6)	N(2)-Zn(1)-N(4)	117.10(19)
N(3)-C(3)	1.492(6)	N(3)-Zn(1)-N(4)	86.80(18)
S(1)-C(1)	1.612(7)	Zn(1)-N(1)-C(1)	175.1(6)
S(2)-C(2)	1.613(7)	N(1)-C(1)-S(1)	179.2(7)

Table 3.14 Hydrogen bonds in the complex (**7**) (Å, º)

Donor-H···Acceptor	D-H	H···A	D···A	∠Δ–H$^{\&}$A
N3-H3A…S1	0.89	2.7	3.476	145.8
N3-H3B…S1	0.89	2.92	3.808	173.8
N4-H4A…S2	0.89	2.73	3.586	161.7

$[Zn(Dap)(NCS)_2][Zn(Dap)(NCS)_2]_n$ (8)

The molecular structure of (**8**) is shown in Figure 3.19. The designated bond lengths (Å) and bond angles (°) are given in Table 3.15. The crystal structure of (**8**) comprises two kinds of molecules, a discrete monomer and a polymeric one. The Zn(II) ions in both adopt a somewhat distorted octahedral geometry, with two N donor atoms from diamine ligand and two SCN^- nitrogen atoms completing the coordination sphere. In the monomeric species, Dap binds as a chelating ligand leading to a hexacyclic ring, whereas in the polymeric unit, it coordinates in a bridging mode forming a linear chain. In the linear polymeric chain, the distance between adjacent Zn-atoms *i.e.*, Zn1-$Zn1^{i,ii}$ (i = -1+x, y, z and ii = 1+x, y, z) is 7.6966(4) Å, which is much greater than the distance 5.3001(6) Å between polymeric and discrete molecules, Zn1...$Zn2^{iii}$ (iii = -x+1/2, y+1/2, z). The thiocyanate ions in both species act as terminal ligands. The angles around zinc {100.58(8)° - 114.94(6)°} are in agreement with the tetrahedral geometry. The N-Zn-N angle of chelating Dap ligand 100.58(8)° is significantly smaller than the same angle attained by the open chain ligand (114.94(6)°). The Zn-N distances are in accordance with those found in other $[ZnL(NCS)_2]$ type zinc(II) complexes [17-21,49]. The SCN moieties are almost linear with the bond angle in the range of 178.35(19)-179.7(2)°. The structure of compound (**8**) is very much different from the known structures, which exist in the form of $[Zn(en)(NCS)_2]$ [41].

There exists strong H-bonding between N-H or C-H hydrogen atoms of Dap and sulfur atoms of thiocyanate. However, any C-H···π or π···π interactions were not observed. The hydrogen bonding parameters are listed in Table 3.16. The molecules are stabilized in the shape of asymmetrical polymeric grid along the *a* axis due to intermolecular N-H---S (except N1-H1B…S3, which is intramolecular) interactions as shown in Figure 3.20. The monomeric and polymeric molecules are arranged alternatively and stabilized due to H-bonding interactions. The H-bonds in (**8**) are not branched as they were found for other en-based $[Zn(diamine)(SCN)_2]$ complexes [41].

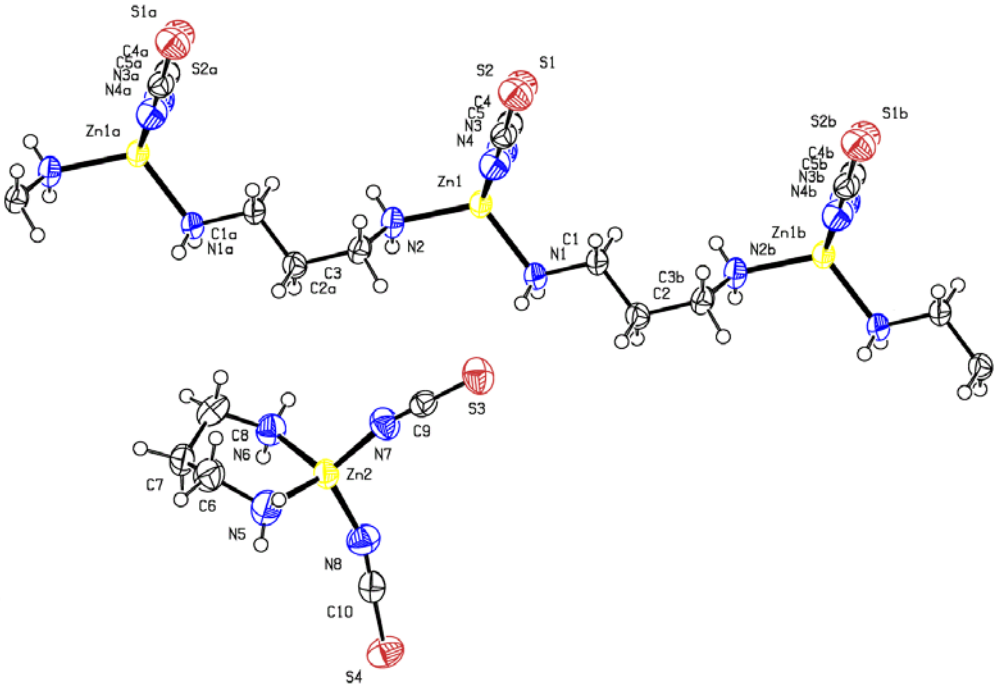

Figure 3.19 Molecular structure of (**8**) along with crystallographic numbering scheme.

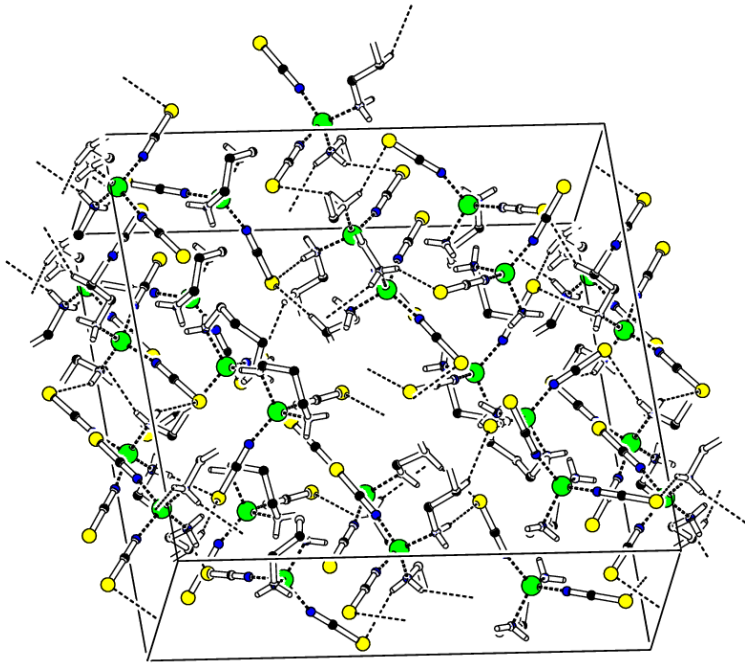

Figure 3.20 Crystalpacking diagram of compound (**8**) showing H-bonds

Table 3.15 Selected bond distances (Å) and bond angles (˚) for (**8**)

Bond distance		Bond angle	
Zn(1)-N(1)	2.0170(15)	N(1)-Zn(1)-N(2)	114.94(6)
Zn(1)-N(2)	2.0153(15)	N(1)-Zn(1)-N(3)	108.60(7)
Zn(1)-N(3)	1.9655(17)	N(1)-Zn(1)-N(4)	106.52(7)
Zn(1)-N(4)	1.9471(17)	N(2)-Zn(1)-N(3)	105.54(7)
Zn(2)-N(5)	2.0030(19)	N(2)-Zn(1)-N(4)	110.62(7)
Zn(2)-N(6)	2.0174(17)	N(3)-Zn(1)-N(4)	110.65(8)
Zn(2)-N(7)	1.9263(18)	N(5)-Zn(2)-N(6)	100.58(8)
Zn(2)-N(8)	1.9466(18)	N(5)-Zn(2)-N(7)	111.59(9)
C(1)-N(1)	1.473(2)	N(5)-Zn(2)-N(8)	109.08(9)
C(4)-N(3)	1.145(2)	N(6)-Zn(2)-N(7)	114.62(8)
C(5)-N(4)	1.152(2)	N(6)-Zn(2)-N(8)	107.81(8)
C(9)-N(7)	1.144(2)	N(7)-Zn(2)-N(8)	112.43(8)
C(10)-N(8)	1.149(3)	Zn(1)-N(1)-C(1)	112.20(15)
C(4)-S(1)	1.627(2)	Zn(1)-N(3)-C(4)	170.33(18)
C(5)-S(2)	1.613(2)	Zn(1)-N(4)-C(5)	172.21(17)
C(9)-S(3)	1.611(2)	Zn(2)-N(7)-C(9)	167.45(18)
C(10)-S(3)	1.613(2)	Zn(2)-N(8)-C(10)	160.91(18)
		N(3)-C(4)-S(1)	178.92(19)
		N(4)-C(5)-S(2)	179.33(19)
		N(7)-C(9)-S(3)	179.7(2)
		N(8)-C(8)-S(4)	178.35(19)

Table 3.16 Hydrogen bonds in complex (**8**) (Å, º)

Donor-H···Acceptor	D-H	H···A	D···A	∠Δ–H&A
N1-H1A···S4^{i}	0.85(1)	2.89(1)	3.6431(17)	148(2)
N1-H1B···S3	0.86(1)	2.64(1)	3.4951(17)	173(2)
N2-H2A···S1^{ii}	0.85(1)	2.78(1)	3.5416(18)	150(2)
N2-H2B···S4^{iii}	0.84(1)	2.78(2)	3.5319(17)	149(2)
N5-H5B···N4^{iv}	0.84(1)	2.66(2)	3.381(3)	145(3)
N6-H6A···S1^{iv}	0.84(1)	2.89(1)	3.712(3)	165(2)
C2-H2C···S4^{i}	0.97	2.94	3.730(2)	139
C2-H2D···S3^{v}	0.97	2.85	3.6796(19)	143

Symmetry codes: (i) *x*+1/2, −*y*+1/2, −*z*; (ii) −*x*+1, −*y*+1, −*z*; (iii) −*x*+1/2, *y*+1/2, *z*;
(iv) −*x*+1/2, *y*−1/2, *z*; (v) *x*+1/2, *y*, −*z*+1/2

$(TMEDA\text{-}H_2)^{2+}[ZnCl_4]^{2-}$ (10)

The crystal structure of (**10**) is shown in Figure 3.21. The certain bond lengths (º) and bond angles (Å) are given in Table 3.17. The structure is ionic in nature. The asymmetric unit contains one tetrachloridozincate anion and two halves of tetramethylethylenediammonium cations, situated on inversion (*i*) centers. Each of the two diammonium cations is positioned about an inversion (*i*) center and one of them is muddled over two sets of sites in a 0.780 (17):0.220 (17) ratio. The Zn atom, coordinated by four chloride anions, shows a distorted tetrahedronal geometry (Fig. 3.21). The bond angles around zinc fluctuate from 105.92(7)^{o} to 115.82(7)^{o}. The complex (**10**) is iso-structural with its cobalt equivalent [230]. In the crystal, the cations and anions are connected by N---H...Cl hydrogen bonds into chains spreading along the [011] direction (Fig. 3.22). The H-bonding details are given in Table 3.18. The displacement ellipsoids are drawn at the 30% probability level. For clarity, only H atoms of N-H group are exposed.

[Symmetry codes: (i) 1-x, 2- y, 1-z; (ii) 1-x, 1-y, 1-z; (iii) x, y, 1 +z].

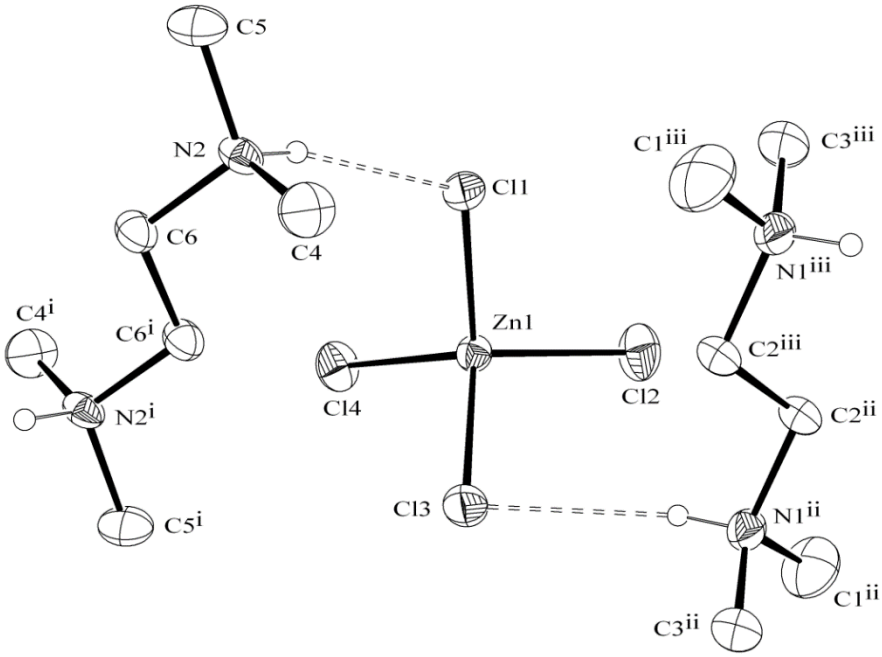

Figure 3.21 Molecular structure of compound (**10**) showing the atomic numbering scheme.

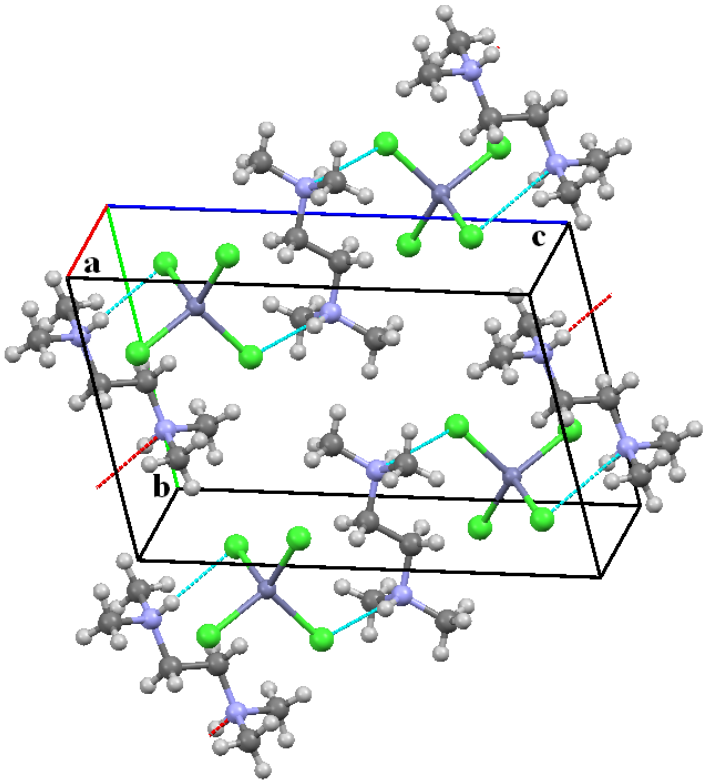

Figure 3.22 Crystal packing diagram of compound (**10**) showing the H-bonding interactions.

Table 3.17 Selected bond distances (Å) and bond angles (˚) for (**10**)

Bond distance		Bond angle	
Zn(1)-Cl(1)	2.2404(15)	Cl(1)-Zn(1)-Cl(2)	105.93(6)
Zn(1)-Cl(2)	2.2516(13)	Cl(1)-Zn(1)-Cl(3)	106.21(6)
Zn(1)-Cl(3)	2.2596(17)	Cl(1)-Zn(1)-Cl(4)	112.86(7)
Zn(1)-Cl(4)	2.2949(16)	Cl(2)-Zn(1)-Cl(3)	107.45(6)
		Cl(2)-Zn(1)-Cl(4)	115.80(6)
		Cl(3)-Zn(1)-Cl(4)	108.07(6)

Table 3.18 Hydrogen bonds in complex (**10**) (Å, º)

Donor-H···Acceptor	D-H	H···A	D···A	∠Δ–H&A
N2-H2…Cl1	0.91	2.3	3.157(3)	158
N1-H1…Cl3	0.85	2.44	3.227(4)	155

[Zn(Mnt-Mnt)(en)]·H_2O (11)

The asymmetric unit of complex (**11**) is illustrated in Figure 3.23 and consists of a zinc(II) as central metal ion bound to two Mnt ligands (in the form of a disulfide), an ethylenediamine molecule and a water of crystallization. The asymmetric units are connected in the shape of 1D polymer chains extending along the *b*-axis. The structure of the polymeric compound is shown in Figure 3.24. The important bond distances and bond angles are given in Table 3.19. As can be seen from Figure 3.24, each zinc atom is five coordinated with three carboxylic oxygen atoms of Mnt ligand and two N atoms of en ligand resulting in a greatly distorted trigonal bipyramidal (TBP) geometry. The S atoms of Mnt did not participate in coordination. In the presence of diamines, the two Mnt molecules coupled to each other to form disulfide with S-S bond distance of 2.0247(7) Å. The R-S-S-R unit is not linear as the angles around sulfur are in the range of tetrahedral geometry. The angles around zinc {86.70(7) - 124.7(5)^o} show significant distortions from the normal values of trigonal bipyramidal geometry. The equatorial plane of the bipyramid is defined by two oxygen atoms of bidentate carboxylic group of Mnt and an amine nitrogen atom. The axial plane is involved by an O donor atom of the monodentate carboxylate and a nitrogen atom of diamine. The coordinated oxygen atoms exhibit different geometry. The oxygen atom of monodentate carboxylate shows a tetrahedral environment, while those of chelating carboxylic group display a trigonal planar environment. The Zn-N/O bond distances are similar to those observed in other Zn-diamines and Zn-carboxylate complexes.

In the crystal packing of the complex, polymeric chains are interlinked due toD-H--S and D-H--O (here D is either N or O) H-bonds. The H-bonding interactions are illustrated in Figure 3.25 and Table 3.20. A 2D grid structure is formed because of the H-bonding interactions, as shown in Figure 3.25.

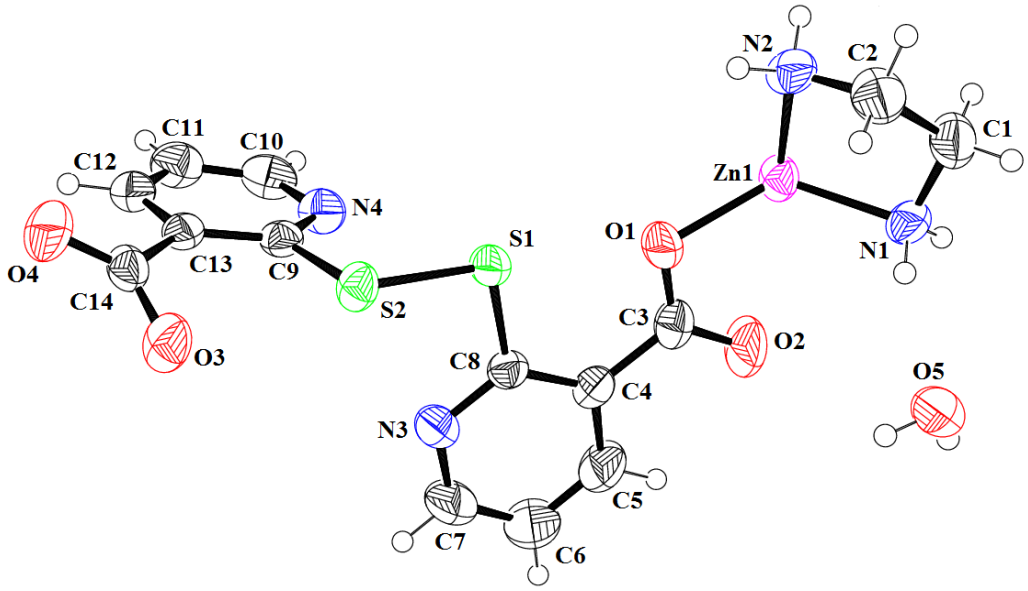

Figure 3.23 The asymmetric unit of (**11**) with thermal ellipsoids drawn at 50 % probability level

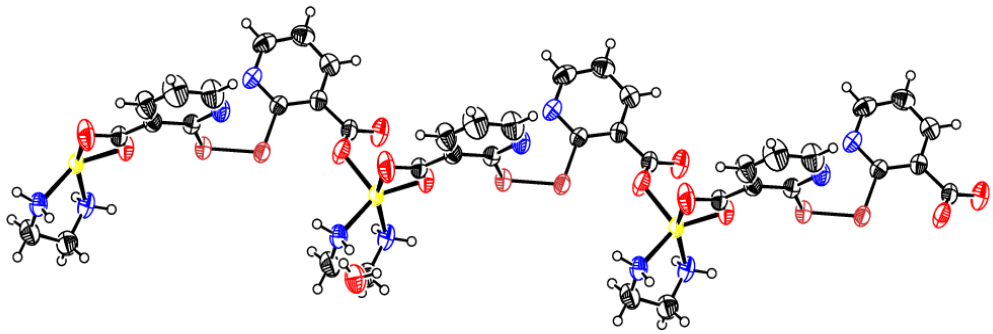

Figure 3.24 Formation of one-dimensional polymeric chains along the ***b***axis in (**11**)

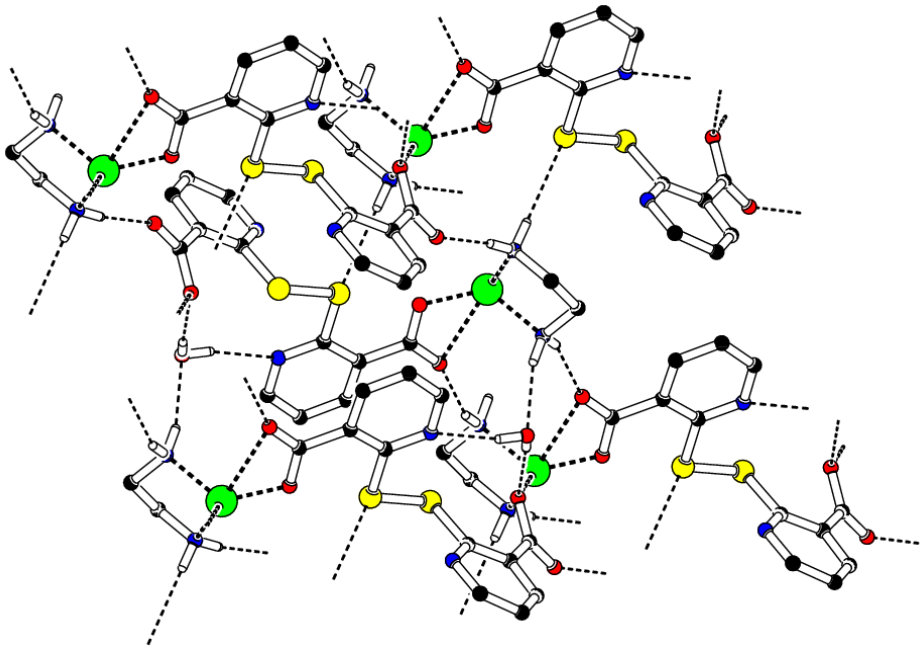

Figure 3.25 Crystal packing diagram of (**11**) showing H-bonding interactions

Table 3.19 Selected bond distances (Å) and bond angles (˚) for (**11**)

Bond distance		Bond angle	
Zn(1)-N(1)	2.0287(16)	N(1)-Zn(1)-N(2)	86.70(7)
Zn(1)-N(2)	2.0524(18)	N(1)-Zn(1)-O(1)	124.75(7)
Zn(1)-O(1)	1.9511(14)	N(1)-Zn(1)-O(3)	101.45(7)
Zn(1)-O(3)	1.9423(14)	N(2)-Zn(1)-O(1)	108.94(7)
S(1)-S(2)	2.0247(7)	N(2)-Zn(1)-O(3)	113.56(7)
O(1)-C(3)	1.812(5)	O(1)-Zn(1)-O(3)	117.65(7)
O(2)-C(3)	2.0304(19)	Zn(1)-O(1)-C(3)	107.37(12)
O(3)-C(14)	1.278(3)	Zn(1)-O(3)-C(14)	119.21(13)
O(4)-C(14)	1.212(3)	S(2)-S(1)-C(8)	102.74(7)

Table 3.20 Hydrogen bonds in complex (**11**) (Å, º)

Donor-H···Acceptor	D-H	H···A	D···A	∠Δ–H$^{\&}$A
N1-H1C···O5	0.89	2.12	2.975(3)	160.1
N1-H1D···O2	0.89	2.11	2.993(2)	153.8
N2-H2C···S1	0.89	2.73	3.6218(19)	179.3
N2-H2D···O4	0.89	2	2.891(2)	173.6
O5-H5A···S2	0.8	2.89	3.4289(19)	127(3)
O5-H5A···N3	0.8	2.14	2.910(3)	162(3)
O5-H5B···O3	0.8	2.22	3.000(3)	166(4)

Conclusions

This study presents thespectroscopic data, crystal structure and theoretical investigation of a eightzinc(II)-diaminecomplexes, which include: $[Zn(Dach)_2][ZnCl_4]$ (**6**), $[Zn(Dach)(NCS)_2]$ (**7**), $Zn(Dap)(NCS)_2][Zn(Dap)(NCS)_2]_n$ (**8**), $[Zn(TMEDA)(NCS)_2]$ (**9**), $(TMEDA\text{-}H_2)^{2+}[ZnCl_4]^{2-}$ (**10**) and $[Zn(en)(Mnt\text{-}Mnt)]\cdot H_2O$ (**11**) [Zn(Dap)(Mnt)]Cl (**12**) and $[Zn(en)(NCS)_2]$ (**13**).The X-ray structure of (**6**) shows that the complex exists in the ionic form and zinc atom in both components adopts a distorted tetrahedral geometry. According to the density functional theory (DFT) calculations, the fully optimized structure of the $[Zn(Dach)_2][ZnCl_4]$ complex (**6**) is more stable in comparison to the less stable nonionic dimer of homonuclear $[Zn(Dach)Cl_2]$ complex by 1.80 kcal mol^{-1}. The X-ray structures of zinc thiocyanate complexes, $[Zn(Dach)(NCS)_2]$ (**7**) and $Zn(Dap)(NCS)_2][Zn(Dap)(NCS)_2]_n$(**8**) show that $[Zn(Dach)(NCS)_2]$ (**7**) exists as a discrete monomer, while the Dap compound is a unique combination of monomeric and polymeric components, $[Zn(Dap)(NCS)_2]$and $[Zn(Dap)(NCS)_2]_n$.The DFT calculations of Zn-diamine-NCS complexes confirmthat calculated geometrical parameters are in agreement with the experimental data. We have also found that in addition to hydrogen bonding and weak S···πchalcogen bonds play a role in stabilization of (**8**).

In the reaction of $ZnCl_2$ with tetramethylethylenediamine (TMEDA) and 2-mercaptosuccinic acid (Msa), an ionic complex $(TMEDA\text{-}H_2)^{2+}[ZnCl_4]^{2-}$ was obtained.The mixed ligand complex, $[Zn(Mnt\text{-}Mnt)(en)].H_2O$ (**11**) is polymeric consisting of $[Zn(Mnt\text{-}Mnt)(en)].H_2O$ monomeric units. Each zinc atom in (**11**)assumes trigonal bypyramidal geometry that is attained by three oxygen atoms of two bridging Mnt-Mnt ligands and two nitrogen atoms of an en molecule.

Chapter – 4
Zinc(II) Complexes of Phenanthroline

4.1 Introduction

Due to the ambidentate nature of CN^-,transition metal cyanides such as $[Fe(CN)_6]^{3-}$ [231–236], $[Ni(CN)_4]^{2-}$ [237–241], $[Au(CN)_2]^-$ [242–251] and $[Ag(CN)_2]^-$ [251–264] have been widely used as bridging/linker/spacer ligands for the formation of coordination polymers with one-, two- or three-dimensional networks. The structural stability is an important factor in the study of the microporous functions of coordination polymers [235]. Therefore, due to their high stability, cyanidometallates may find extensive applications as microporous materials [231,242,247,262].The coordination polymers of coinage metal cyanides are of great interest in this respect because the unusually low 2-coordination of the metal centers allows them to reversibly adsorb nucleophiles offering applications in separations and sensing technologies [266].Another unique feature of these structures is that the central silver or gold atoms are capable of forming d^{10}-d^{10} M–M bonds, which are useful tools in crystal engineering of polymeric structures [242,250,264,267-270].For example, the linear chains in $[\{Cd(en)_2Ag(CN)_2\}\{Ag(CN)_2\}]_n$ (en = 1,2-diaminoethane) [256] are assembled through Ag-Ag interactions to form a chain structure or a 2D network. In $[Ni(en)_2Ag_3(CN)_5]_n$, the 2D hexagonal grids are constructed using cyanides as bridges, and the Ag---Ag interactions between layers lead to a three dimensional network [261]. The threshold limit of distance for feasible argentophilic d^{10}-d^{10} interactions is the Ag–Ag distance below the twice of van der Walls radius of silver atom (<1.72 x 2=3.44 Å)[262-264,270].

The metal-cyanide units, *e. g.*, $[Au(CN)_2]^-$ and $[Ni(CN)_4]^{-2}$ usually remain preserved in supramolecular assemblies. The $[Ag(CN)_2]^-$ unit in many cases also remains preserved [252-261], but sometimes it may undergo secondary interactions forming a variety of products consisting of $[Ag_2(CN)_3]^-$ [262], $[Ag_3(CN)_5]^{2-}$[261] and $[Ag(CN)_2^-]_5$ [262] anions. They may be explained by the following equilibria:

$$K[Ag(CN)_2] \rightleftharpoons KCN + AgCN$$

$$AgCN + K[Ag(CN)_2] \rightleftharpoons K[Ag_2(CN)_3]$$

$$AgCN + 2K[Ag(CN)_2] \rightleftharpoons K_2[Ag_3(CN)_5]$$

The existence of these equilibria provide a thermodynamic driving force for the oligomerization of $[Ag(CN)_2]^-$ ions.We present here thestructural characterization of a new one dimensional heterobimetallic coordination polymer with formula $\{[Zn(phen)_2(H_2O)\{Ag(CN)_2\}][Ag(CN)_2]\cdot MeOH\}_n$ (phen = 1,10-phenanthroline), assembled by significant argentophilic interactions.H-bonds and π-π interactions extend the chains,leading to the formation of 3D assembly.

4.2 Experimental

4.2.1 Materials

$ZnCl_2$ and1,10-phenanthroline (phen) weresupplied byMerck., Germany.Thiolates wereprocured from Arcos Organics, Belgium. $AgNO_3$ was a product of Panreac, Spain. $AgNO_3$ mixed with KCN in a 1:2 mol ratio in water to form $K[Ag(CN)_2]$.

4.2.2 Synthesis of complexes

[Zn(phen)(Thiolate)Cl] (14)

A solution of 0.14 g (1mmol) $ZnCl_2$ in 10 mL of water was added slowly to a 10 mL methanolic solution of 0.20 g (1mmol) of phenanthroline (phen). The solution was magnetically stirred for 15 minutes to obtain a clear solution. At this point, 1 mmol of thiolate in 15 mL methanol was added. The solution was stirred for 30 minutes and then filtered. The filtrate was kept at room temperature to result off-white crystals.

For the preparation of complex (**14**), 0.16 g (1 mmol) 2-mercaptonicotinc acid was dissolved in 20 mL water containing 0.06 g (1 mmol) ethylendiamine and then added to Zn-phen solution. White precipitates were formed, which were washed with methanol. Analysis of (**14**): Found (Calculated): 47.06 (47.69); 2.39 (2.64); 9.17 (9.27); 6.91 (7.06).

{[Zn(phen)$_2$(H$_2$O){Ag(CN)$_2$}][Ag(CN)$_2$]·MeOH}$_n$ (15)

The amorphous complex was prepared by the procedure as described earlier [271]. Crystals of (**15**)were obtained by dissolving some of the precipitated product in a 1:1 water-methanol mixtureon heating and keeping the filtrate in air for overnight. The crystals were washed with methanol and finally dried in air.M.P. = 283-284^{o}C. IR: ν = 1618, 1589 cm^{-1} (C=N), ν = 1505, 1423 cm^{-1} (C=C), ν = 2163, 2138 cm^{-1} (C≡N).

4.2.3 X-ray structure determination

X-ray diffraction data of (15) were measuredwith an Oxford Gemini S diffractometer [Mo$K\alpha$ (λ= 0.71073 Å) at 110 K]. The structure wasexplained by Direct Methods with SHELXS-97 [186] and refined by full-matrix least-squares methods on F^2employing the software SHELXL-97 [186]. Crystal data including the data collection are briefed in Table 4.1.

Table 4.1 Crystal data and refinementdetailsforcomplex(**15**)

Formula	$C_{29}H_{22}Ag_2N_8O_2Zn$
Formula weight	795.66
Crystal system	Triclinic
Space Group	P_1
a, Å	10.3619(5)
b, Å	12.0360(5)
c, Å	12.3670(6)
α,°	109.019(4)
β, °	91.090(4)
γ,°	99.812(4)
V,Å^3	1432.22(11)
Z	2
ρ_{calc}, g cm^{-3}	1.85
μ(Mo$K\alpha$), μμ^{-1}	2.2
F(000)	784
Crystal size (mm)	0.2 x 0.2 x 0.1
Temperature (K)	110(2)
λMo$K\alpha$ (Å)	0.71073
2θrange,deg	2.95 - 25.00
h, k, l limits	-12:12, -14:14, -11:14
Max. and min. transmission	1.0, 0.82
Reflections; collected/Uniq.	8839/4987 [*R(int)*= 0.0223]
Reflections: observed [$I > 2\sigma(I)$]	4061
Data / restraints / parameters	4987 / 2 / 390
R_1,wR_2, S [$I > 2\sigma(I)$]	0.0308, 0.0737, 0.960
Largest diff. peak, hole (e Å^{-3})	1.84, -0.71

4.3 Results and discussion

The reaction of $ZnCl_2$, phenanthroline (phen) and thiolates yielded only the [(phen)$ZnCl_2$] complex instead of mixed ligand complexes as given below.

$$ZnCl_2 + phen + RSH \rightarrow [(phen)ZnCl_2]$$

The thiolate ligands include; cysteine, cysteamine, mecrcaptosuccinic acid and mecrcaptonicotinic acid.

A comparison of ^{13}C NMR spectrum of [Zn(phen)Cl_2] and the expected complex [Zn(Phen)(Cys)]Cl show similar appearance suggesting that cysteine has not coordinated and the compound formed is only [Zn(phen)Cl_2] as shown in Figure 4.1. The X-ray measurementsalso furnished the same information. The crystal structure of [Zn(phen)Cl_2] was measured but it was found to be the same as already reported one [65]. This observation reflects the greater stability of [Zn(phen)Cl_2] in comparison to the mixed ligand complexes.In these cases, the Zn-Cl bond is strong to be replaced by a Zn-SR bond.

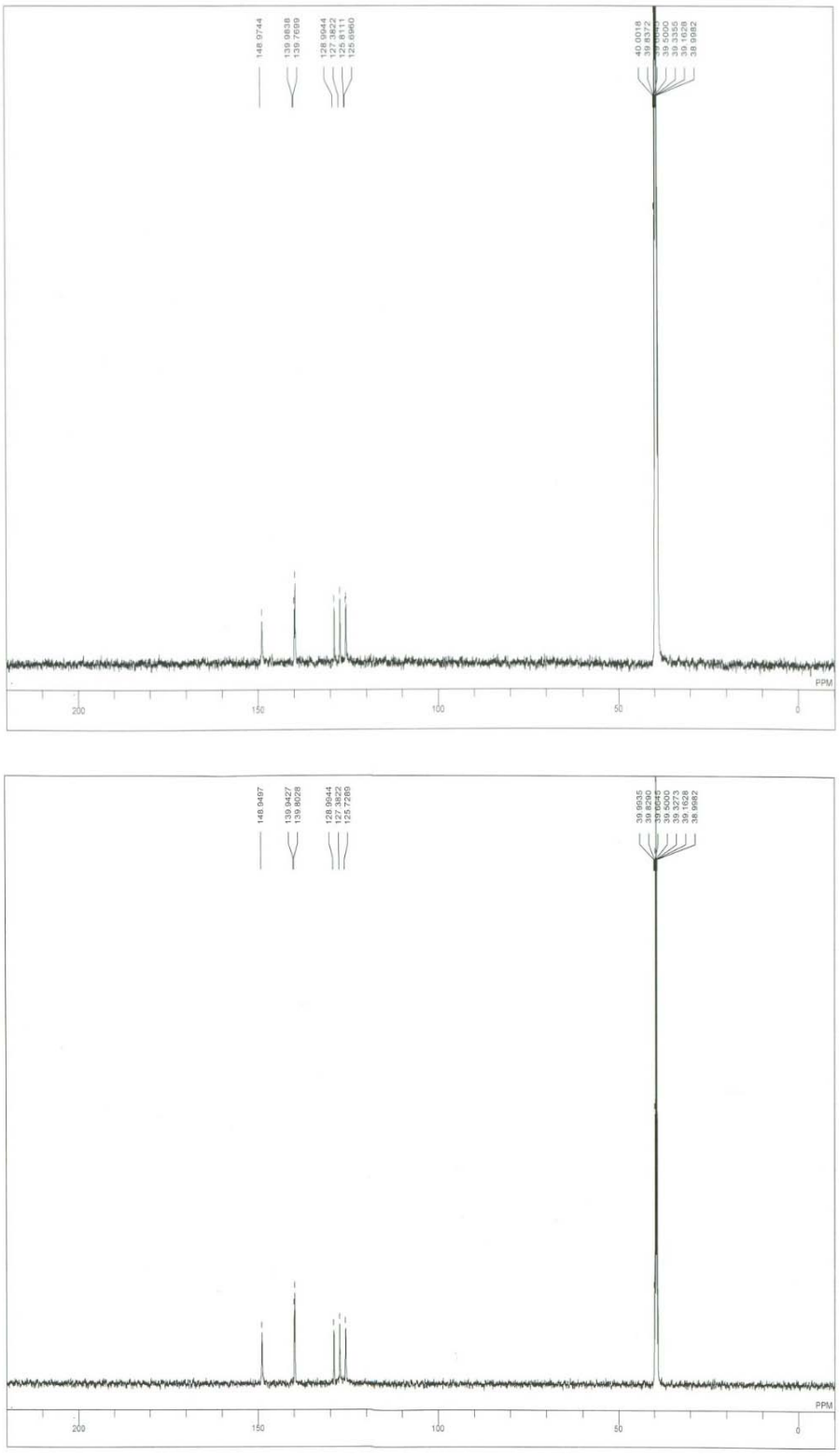

Figure 4.1 A comparison of ^{13}C NMR of [Zn(Phen)Cl_2] (lower) and expected [Zn(Phen)(Cys)Cl] product(upper)

In the reaction of 2-mercaptonicotinic acid, however, a mixed ligand complex could be successfully obtained, as indicated by the ^{13}C NMR spectrum as shown in Figure 4.2.

The phen-Zn-$Ag(CN)_2$ complex was prepared by the reaction of $ZnCl_2$, 1,10-phenanthroline (phen) and $K[Ag(CN)_2]$ in a 1:2:2 molar ratio. In the IR spectrum of the residual product (not of the crystals) of complex(**15**), two ν(CN) bands are seen, at 2163 cm^{-1} and 2138 cm^{-1}, while for $K[Ag(CN)_2]$ only one ν(C≡N)appears at 2140 cm^{-1}. The presence of two bands indicates that the complex contains both bridging and terminal cyanide groups. Generally, the stretching frequency of the terminal cyanide is lower relative to that of bridging one [244,255,272].In the IR spectrum of 1,10-phenanthroline (phen), the characteristic bands observed are; ν(C=N) at 1618 and 1589 cm^{-1}, and ν(C=C) at 1505 and 1423 cm^{-1}. For complex (**15**), the ν(C=N) vibrations of phen were observed at1626 and1579 cm^{-1}, while the ν(C=C) bands appeared at 1505 and 1424 cm^{-1}.The presence of these bands indicates the coordination of phen ligand to the metal.

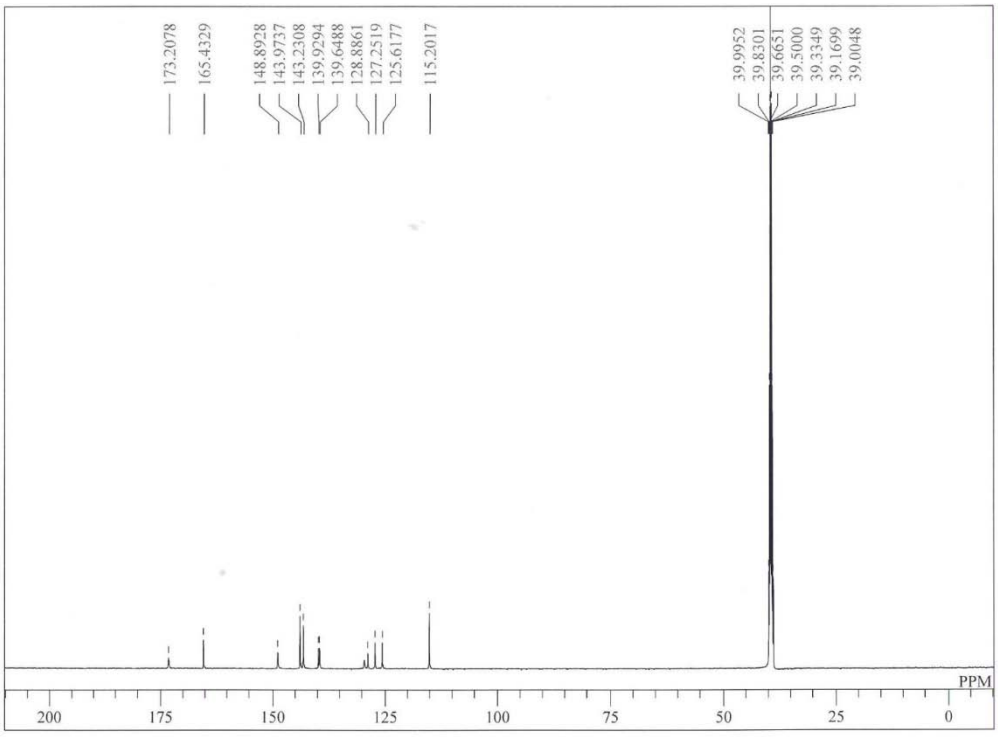

Figure 4.2 $^{13}C\{^{1}H\}$ NMR of [Zn(Phen)(Mnt)Cl] (**14**) showing the resonances of both ligands

4.3.1 Crystal structure description of(15)

The molecular structure of the asymmetric unit of (**15**)is shown in Figure 4.3. Certain bond lengths (Å) and bond angles (°) are recorded in Table 4.2. The crystal structure of (**15**) comprises $[Zn(phen)_2(H_2O)\{Ag(CN)_2\}]^+$cations, $[Ag(CN)_2]^-$ anions and one molecule of methanol.The Zn(II) ions are coordinated to 4 N donor atoms of phen ligands, one water molecule and one $[Ag(CN)_2]^-$ ion assuming a slightly distorted octahedral geometry. The *cis* N-Zn-N bond angles differ from 89.31(14) - 90.59(14)°, whereas the *trans* N-Zn-N bond angle is 179.31(14)°. The *cis* N-Zn-N(CN) angles are greater than the *cis* N-Zn-N(phen) angles. The Zn-N≡C unit is closely linear with a bond angle of 166.0(3)°. The coordination environments of the coordinated and non-coordinated$[Ag(CN)_2]^-$ ionsarenear to linear (Ag-C-N = 176.7(3) - 179.0(5)°).The cyanido groups are bent away from each other so that the silver(I)ions reach the closest contacts between the $[Ag(CN)_2]^-$ anions. The Zn-N bond lengths, 2.096(3) - 2.247(3)Å, are comparable to those in known structures, *e.g.,* in $[Zn(Phen)_3]Cr_2O_7{\cdot}4H_2O$[68]. The comparable Zn-N(CN) and Zn-N(phen) bond lengths indicate the absence of Jahn-Teller distortion in the complex.

The coordinated and noncoordinated$[Ag(CN)_2]^-$ ions are linked to each other through argentophilic interactions. The Ag-Ag interactions are extending in one dimension forming a zigzag chain as shown in Figure 4.3. The Ag–Ag distances ranging from 3.0463(3)-3.0697(3)Å are below the twice of the van der Walls radius of silver atom(1.72 Å) showingthe presence ofsignificant argentophilicinteractions [262-264,270]. The Ag1–Ag2–Ag1A and Ag2–Ag1–Ag2A angles involved in this bonding are 153.411(14)and 179.998(1)° respectively.Such Ag…Ag distances are observed that confirm the presence of argnetophilic interactions in the given examples: $[Cd(en)_2Ag(CN)_2]\{Ag(CN)_2\}]$ with 3.1750 Å [256], $[Ni(en)_2Ag(CN)_2]\{Ag(CN)_2\}$with 3.289 Å [257], $[Cu(en)_2Ag(CN)_2]\{Ag(CN)_2\}$ with 3.1580 Å [258], $[Zn(en)_2Ag(CN)_2]\{Ag(CN)_2\}$with 3.221 Å [259].

In the crystal structure, the chains do interact with each other by both hydrogen bond and π-π contacts (Figure 4.4a). The particular data of the H-bonds are recorded in Table 4.3, while Figure 4.4b demonstrates the π-π interactions in more detail.The results of present study have shownthat $[Ag(CN)_2]^-$ can be used as a bridging ligand as well as counter-ion in the formation of polymetallic complexes. The dimensionality of such complexes can be increased by argentophilic (Ag---Ag) interactions [249-255]. We have isolated and crystallographically characterized a rare example of a 1D coordination polymer (**15**), assembled bysuchinteractions.

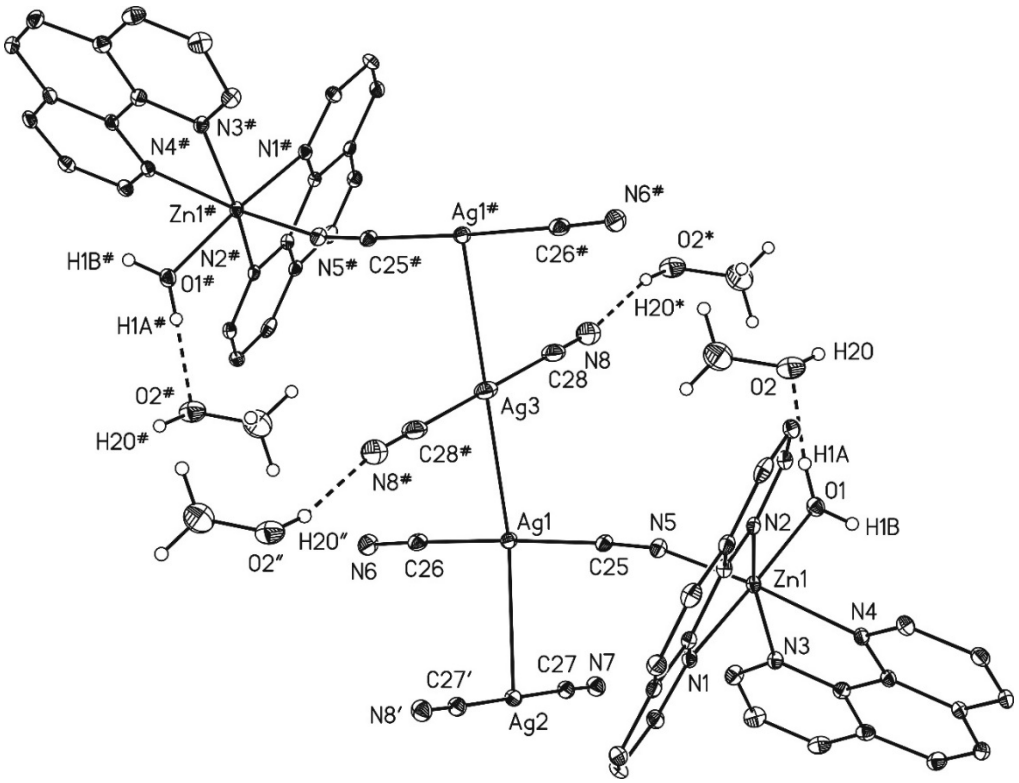

Figure 4.3 Graphical representation of a selected part of the chains formed by (**15**) in the solid state due to argentophilic interactions and interactions with theMeOH molecules in chains. All *C*-bonded hydrogen atoms of the phen ligands are omitted for clarity.

Symmetrycodes: (‘) *-x+1, y, -z+1/2*; (#) *x, -y+1/2, -z+3/2*; (*) *3-x, -y, -z*; (“) *x-1, y, z*.

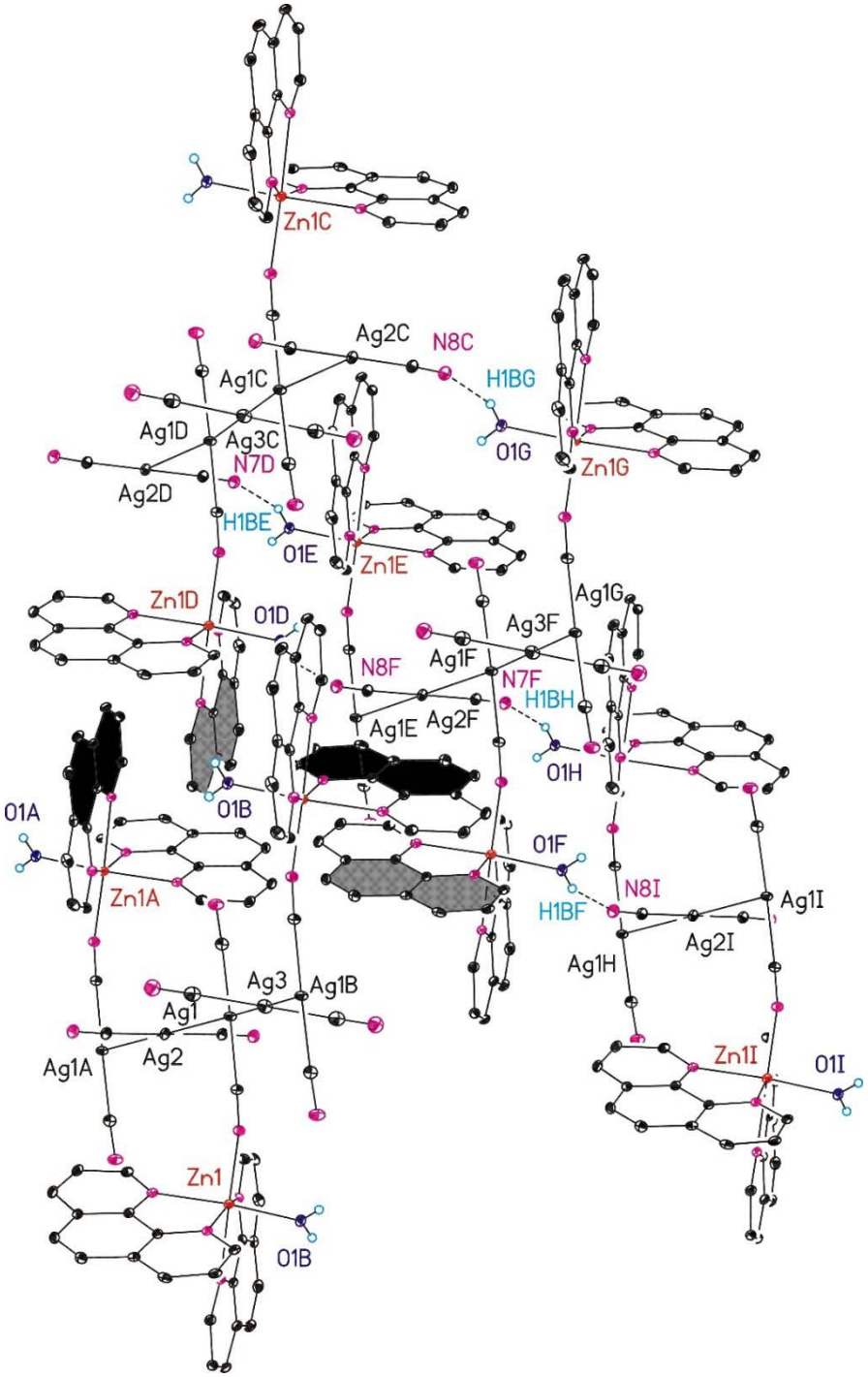

Figure 4.4 (a) Selected part of the 3D network of(**15**) in the solid state. Hydrogen bonds are indicated by dotted lines.π-π-interacting aromatic rings are filled with black and grey colours. MeOH molecules and *C*-bonded hydrogen atoms are omitted. Labels 'A' to 'I' refer to a first to the ninth symmetry-generated asymmetric unit of (**15**).

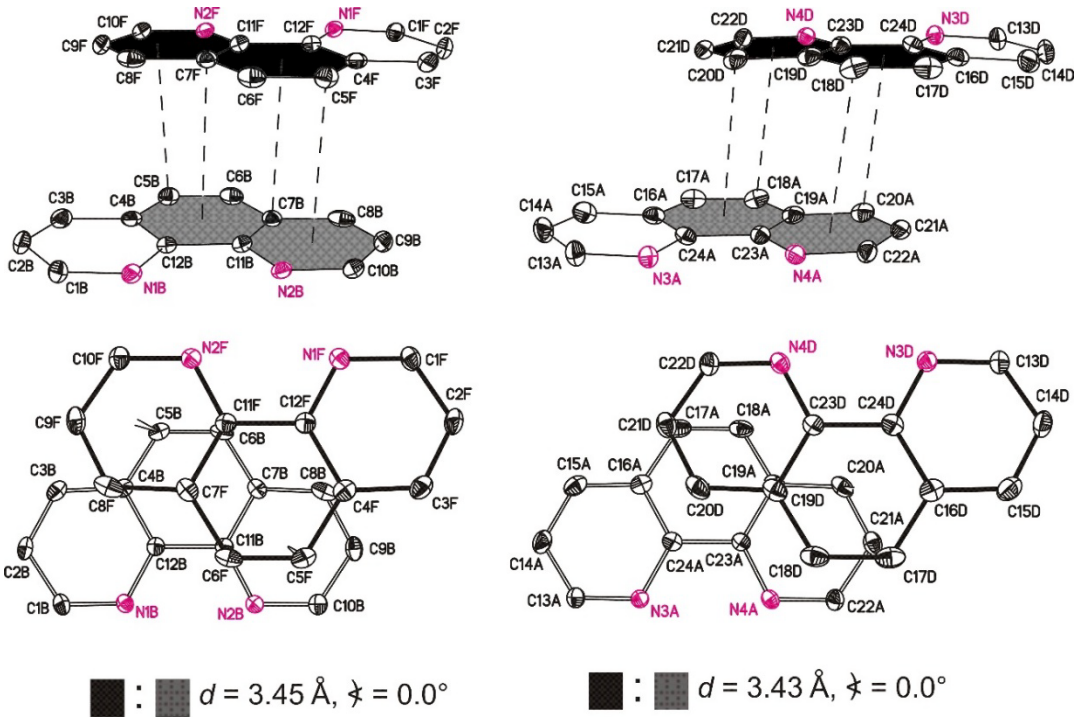

Figure 4.4(b) Graphical illustration of the parallel-displaced sandwich type π-π interactions of phen ligands in (**15**) in the solid state, where*d* gives the distances of interacting phen ligands and ∢ the interplanar angles, respectively. The labelling refers to the code given in Figure 4.3.

Table 4.2 Selected bond lengths (Å) and bond angles (º) for compound (**15**)

Bond distance		Bond angle	
Ag(1)-C(26)	2.063(4)	C(26)-Ag(1)-C(25)	177.63(14)
Ag(1)-C(25)	2.064(4)	C(27)-Ag(2)-C(27)‘	180
Ag(1)-Ag(2)	3.0463(3)	C(28)-Ag(3)-C(28)#	180
Ag(1)-Ag(3)	3.0697(3)	C(25)-Ag(1)-Ag(2)	87.14(10)
Ag(2)-C(27)	2.059(4)	C(26)-Ag(1)-Ag(2)	90.52(11)
Ag(2)-C(27)‘	2.059(4)	N(2)-Zn(1)-N(1)	77.77(11)
Ag(2)-Ag(1)‘	3.0463(3)	N(3)-Zn(1)-N(1)	95.88(11)
Ag(3)-C(28)	2.061(6)	N(1)-Zn(1)-N(4)	92.14(11)
Ag(3)-C(28)	2.061(6)	N(5)-Zn(1)-N(1)	89.28(12)
Ag(3)-Ag(1)	3.0697(3)	N(3)-Zn(1)-N(2)	162.07(11)
Zn(1)-O(1)	2.077(3)	N(5)-Zn(1)-N(2)	102.25(11)
Zn(1)-N(1)	2.165(3)	N(5)-Zn(1)-N(3)	94.34(12)
Zn(1)-N(2)	2.161(3)	N(5)-Zn(1)-N(4)	170.52(11)
Zn(1)-N(3)	2.147(3)	O(1)-Zn(1)-N(2)	92.96(11)
Zn(1)-N(4)	2.247(3)	O(1)-Zn(1)-N(3)	92.65(11)
Zn(1)-N(5)	2.096(3)	O(1)-Zn(1)-N(4)	86.18(11)
N(1)-C(1)	1.316(5)	O(1)-Zn(1)-N(5)	93.89(12)
N(1)-C(12)	1.350(5)	C(25)-N(5)-Zn(1)	166.0(3)
N(5)-C(25)	1.145(5)	N(5)-C(25)-Ag(1)	176.7(3)
N(6)-C(26)	1.142(5)	N(6)-C(26)-Ag(1)	177.9(4)
N(7)-C(27)	1.151(5)	N(7)-C(27)-Ag(2)	177.4(4)
N(8)-C(28)	1.126(6)	N(8)-C(28)-Ag(3)	179.0(5)

Symmetrycodes: *(‘) -x+1, y, -z+1/2; (#) x, -y+1/2, -z+3/2*.

Table 4.3 Selected bond lengths (Å) and bond angles (º) of hydrogen bonds of (**15**)

Donor-H···Acceptor	D···A	∠Δ–H&A
O1–H1A···O2	2.649(5)	161(7)
O1–H1B···N7	2.813(4)	157(6)
O2–H20···N8	2.752(5)	164(6)

Conclusions

In this study, we have isolated and crystallographically characterized a rare example of a 1D coordination polymer assembled through argentophilic and π-π interactions, $\{[Zn(phen)_2(H_2O)\{Ag(CN)_2\}]\ [Ag(CN)_2]\cdot MeOH\}_n$ (**15**). The structure of (**15**)consists of dinuclear $[Zn(phen)_2(H_2O)\{Ag(CN)_2\}]^+$ cations and $[Ag(CN)_2]^-$ anions linked through argentophilic interactions. Argentophilic interactions play a significant role in increasing the dimensionality of such complexes. The study also shows that $[Ag(CN)_2]^-$ can be used as a bridging ligand as well as a counter-ion in the formation of polymetallic complexes.Attempts to prepare the mixed ligand zinc(II) complexes of phenanthroline and thiolates led to the formation of $[Zn(phen)Cl_2]$ except in case of 2-mercaptonicotinic acid, where, the complex [Zn(phen)(Mnt)Cl] (**14**) was obtained.

The overall, spectroscopic, theoretical and structural data presented in this thesis would provide useful information about the nature of bonding and properties of the zinc(II) complexes with diamines and thiolates or thiocyanates.

References

1 W. Kaim, B. Schwederski, *Bioinorganic Chemistry: Inorganic Elements in the Chemistry of Life*, J. Wiley, New York (1994) p.367.

2 G. Parkin, *Chem. Commun.*, (2000) 1971-1985.

3 W. N. Lipscomb, N. Strater, *Chem. Rev.*, 96 (1996) 2375-2433.

4 S. F. Sousa, A. B. Lopes, P. A. Fernandes, M. J. Ramos, *Dalton Trans*., (2009) 7946–7956.

5 W. Maret, *J. Inorg. Biochem.*, 111 (2012) 110–116.

6 D. S. Auld, *Biometals*, 14 (2001) 271–313.

7 I. L. Alberts, K. Nadassy, S. J. Wodak, *Protein Science*, 7 (1998) 1700-1716.

8 M. L. Zastrow, V. L. Pecoraro, *Biochemistry*, 53 (2014) 957–978.

9 B. L. Vallee, D. S. Auld, *Acc. Chem. Res.*, 26 (1993) 543-551.

10 R. J. P. Williams, *Polyhedron*, 6 (1987) 61-69.

11 F. Namuswe, J. M. Berg, *J. Inorg. Biochem.*, 111 (2012) 146-149.

12 G. Henkel, B. Krebs, *Chem. Rev.*, 104 (2004) 801-824.

13 H. Fleischer, *Coord. Chem. Rev.*, 249 (2005) 799-827.

14 H. Fleischer, Y. Dienes, B. Mathiasch, V. Schmitt, D. Schollmeyer, *Inorg. Chem.*, 44 (2005) 8087-8096.

15 H. Fleischer, S. Hardt, D. Schollmeyer, *Inorg. Chem.*, 45 (2006) 8318-8325.

16 I. Casals, P. González-Duarte, C. López, X. Solans, *Polyhedron*, 9 (1990) 763-768.

17 M. Ji, H. Vahrenkamp, *Eur. J. Inorg. Chem*., 200 (2005) 1398-1405.

18 M. Ji, B. Benkmil, H. Vahrenkamp, *Inorg. Chem*., 44 (2005) 3519-3538.

19 U. Lehmann, B. Kersting, *Z. Anorg. Chem. Allg*., 639 (2013) 1543-1551.

20 R. Vogler, M. Gelinsky, L. F. Guo, H. Vahrenkamp, *Inorg.Chim. Acta*, 339 (2002) 1-8.

21 J. G. Melnick, G. Zhu, D. Buccella, G. Parkin, *J. Inorg. Biochem.*, 100 (2006) 1147–1154.

22 M. M. Ibrahim, *J. Sulfur Chem*., 31 (2010) 395-403.

23 J. Penner-Hahn, *Curr. Opin. Chem. Biol.*, 11 (2007) 166.

24 M. C. Bagley,Z. Lin, S. J. A. Pope, *Dalton Trans.*, 39 (2010) 3163-3166.

25 S. Enthaler, X.-F. Wu, Zinc *Catalysis, Applications in Organic Synthesis*, Wiley-VCH Verlog GmbH & Co., Weinheim, Germany (2015) 149.

26 M. Dochnahl, J.-W. Pissarek, S. Blechert, K. Lohnwitz, P. W. Roesky, *Chem. Commun*., (2006) 3405-3407.

27 Q. Dong, X. Ma, J. Guo, X. Wei, M. Zhou, D. Liu, *Inorg. Chem. Commun.*, 11 (2008) 608-611.

28 S. Nayab, J. H. Jeong, *Polyhedron*, 59 (2013) 138–143.

29 I. E. Sajo, L. Kotai, G. Keresztury, I. Gacs, G. Pokol, J. Kristof, B. Soptrayanov, V. M. Petrusevski, D. Timpu, P. K. Sharm, *Helv. Chim. Acta*, 91 (2008) 1646-1658.

30 A. Mohamadou, C. Gerhard, *J. Chem. Soc., Dalton Trans.*, (2001) 3320-3328.

31 J. L. Huang, Y. L. Feng, *Acta Cryst.*, E63 (2007) m1395.

32 Y.-I. Kim, S.-Y. Yun, T. Lee, S. K. Kang, *Acta Cryst.*,E66 (2010) m940.

33 P. L. Zick, D. K. Geige, *Acta Cryst*., E72 (2016) 1037–1042.

34 A. Johansson, M. Håkansson, *Acta Cryst.,* E60 (2004) m955-m957.

35 D. M. Chen, X. J. Ma, B. Tu, W. J. Feng, Z. M. Jin, *Acta Cryst.*,E62 (2006) m3174-m3175.

36 H. Citeau, O. Conrad, D. M. Giolando, *Acta Cryst*., E57 (2001) m5-m6.

37 P. Sureshbabu, A. A. J. S. Tjakraatmadja, C. Hanmandlu, K. Elavarasan, N. Kulak, S. Sabiah, *RSC Adv.*, 5 (2015) 22405-22418.

38 J.-Y. Miao, *Synth. React. Inorg. Met.-Org. Nano-Met. Chem.,* 45 (2015) 1683–1686.

39 C-Y. Wang, A-F. Ke, X. Wu, *Acta Cryst.,* E66 (2010) m350.

40 Z. Hong, *Acta Cryst.,* E63 (2007) m132-m134.

41 E. M. Cameron, W. E. Louch, T. S. Cameron, O. Knop, *Z. Anorg. Allge. Chemie*, 624 (1998) 1629–1641.

42 M-H. Ding, S. W. Ng, *Acta Cryst.,* E66 (2010) m1356.

43 A. Fowkes, W. T. A. Harrison, *Acta Cryst.,* E63 (2007) m1249-m1251.

44 D. Neill, M. J. Riley,C. H. L. Kennard, *Acta Cryst.,*C53 (1997) 701-703.

45 L. Cheng, Y.-Y. Sun, Y.-W. Zhang, G. Xu, *Acta Crystallogr*., E64 (2008) m1246.

46 Y. Guo, R. Weiss, R. Boese, M. Epple, *Thermochim. Acta,* 446 (2006) 101–105.

47 A. J. Finney, M. A. Hitchman, C. L. Raston, G. L. Rowbottom, A. H. White, *Austr. J. Chem.,* 34 (1981) 2061 – 2067.

48 K. Karimnejad, H. Khaledi, H. M. Ali, *Acta Cryst*.,E67 (2011) m421.

49 Z. S. Sahin, F. Sevindi, H. Icbudak, S. Isik, *Acta Cryst*., C66 (2010) m314-m318.

50 N. Y. Lee, J. U. Yoon, J. H. Jeong, *Acta Cryst.*, E63 (2007) m2471.

51 J. D. Lee, *Concise Inorganic Chemistry*, 5th Ed. Wiley-Blackwell, (2007).

52 A. G. Massey, *Main Group Chemistry*, 2nd Ed., John Willey & Sons Ltd. Chichester, New York, Weicheim, Brisbane, Toronto, Singapore (2000).

53 F. A. Cotton, J. Wilkinson, C. A. Murillo, M. Bochmann, *Advanced Inorganic Chemistry*, 6th Ed. (2007) 598.

54 N. N. Greenwood, A. Earnshaw, *Chemistry of the Elements*, Oxford, Eng. Pergamon Press, (1986) 1420.

55 M. Baumann,I. R. Baxendale, *Beilstein J. Org. Chem.,* 9 (2013) 2265–2319.

56 A. Naqvi, R. Malasoni, A. Srivastava, R. R. Pandey, A. K. Dwivedi, *Bioorg. & Med. Chem. Letters,* 24 (2014) 5181–5184.

57 N. W. Alcock, A. C. Benniston, P. Moore, G. A. Pike, S. C. Rawle, *J. Chem. Soc., Chem. Commun.,* (1991) 706-708.

58 J. L. Sesslor, T. Murai, V. Lynch, *Inorg. Chem.,* 28 (1989) 1333-341.

59 A. Hergold-Brundić, B. Kaitner, B. Kamenar, V. M. Leovac, E. Z. Ivegeš, N. Juranić, *Inorg. Chim. Acta,* 188 (1991) 151-158.

60 L. Y. Zhu, D. Xu, X. Q. Wang, G. Yu, *J. Chem. Crystallogr*., 38 (2008) 609–612.

61 C. J. Adams,M. A. Kurawa, M. Lusi, A. G. Orpen, *Cryst. Eng. Comm.***,**10(2008) 1790-1795.

62 X.-M. Chen, X.-C. Huang, Z.-T. Xu and X.-Y. Huang, *Acta Cryst.*, C52 (1996) 2482-2484.

63 U. Brand, H. Vahrenkamp, *Inorg. Chim. Acta*, 198-200 (1992) 663-669.

64 H. Zhong, X.-M. Yang, Q.-Y. Luo, Y.-P. Xu, *Acta Cryst.*, E63 (2007) m2208.

65 C. W. Reimann, S. Block, A. Perloff, *Inorg. Chem*., 5 (1966) 1185-1189.

66 M. A. Khan, D. G. Tuck, *Acta Crystallogr*.,C40 (1984) 60–62.

67 C. H. Yu, R. C. Zhang, *Acta Crystallogr.*, E62 (2006) m1758–m1759.

68 K. Ejsmont, M. Wasielewski, J. Zaleski, *Acta Cryst*., E58 (2002) m200-m202.

69 K. Manna, T. Zhang, F. X. Greene, W. Lin, *J. Am. Chem. Soc.*, 137 (2015) 2665–2673.

70 A. F. Holleman, E. Wiberg, *Inorg. Chem.*, Academic Press, A Harcourt Science and Technology Company (2001) 1301.

71 J. McMurry, *Organic Chemistry*, 5thEd. National Book Foundation, Islamabad, Pakistan (2000) 1976.

72 J. Cusacka, M.G.B. Drewb, T. R. Spalding, *Polyhedron*, 23 (2004) 2315–2321.

73 N. Srinivasan S. Thirumaran, S. Kohli, Rajnikant, *J. Chem. Crystallogr*., 40 (2010) 505-509.

74 B. Luo, B. E. Kucera, W. L. Gladfelter, *Polyhedron*, 25 (2006) 279–285.

75 A. Hazari, L. K. Das, A. Bauzá, A. Frontera, A. Ghosh, *Dalton Trans*., 43 (2014) 8007.

76 B. G. Chand, U.S. Ray, G. Mostafa, J. Cheng, T.-H. Lu, C. Sinha, *Inorg. Chim. Acta*, 358 (2005) 1927–1933.

77 B. Notash, N. Safari, V. Amani, *Acta Cryst.,* E67 (2011) m418.

78 S. R. Petrusenko, V. N. Kokozay, I. O. Fritsky, *Polyhedron,* 16 (1997) 267–274.

79 M. Daković, Z. Popović, G. Giester, M. Rajić-Linarić, *Polyhedron*, 27 (2008) 210–222.

80 M. H. Sadhu, A. Solanki, S. B. Kumar, *Polyhedron*, 100 (2015) 206–214.

81 M. Akhtar, M. A. Alotaibi, A. I. Alharthi, W. Zierkiewicz, M. N. Tahir, M. Mazhar, A. A. Isab, M. Monim-ul-Mehboob, S. Ahmad, *J. Mol. Struc.*, 1128 (2017)455-461.

82 M. A. Alotaibi, A. I. Alharthi, W. Zierkiewicz, M. Akhtar, M. N. Tahir, M. Mazhar, A. A. Isab, S. Ahmad, *J. Mol. Struc.*,1133 (2017) 271-277.

83 R. Canhan, T. Overton, *Descriptive Inorganic Chemistry*, 3rd Ed., W. H. Freeman and Company, New York (2002) 527.

84 J. C. Bailar Jr., H. J. Emeleus, S. R. Nyholm, A. F. Trotman -Dickenson, *Comprehensive Inorganic Chemistry*, Pergamon Press Ltd., Oxford, (1973).

85 J. R. Parga, J. L. Valenzuela, H. Moreno, J. E. Perez, *Advances in Chemical Engineering and Science*, 1 (2011) 191-197.

86 A. Monge, M. Martinex-Ripoll, S. Garcia-Blanco, *Acta. Cryst.*, B33 (1977) 2329-2331.

87 G. S. Kurkcuoglu, O. Z. Yesilel, O. Sahin, E. Sayın, O. Buyukgungor, *Z. Kristallogr.– Cryst. Mat*., 230 (2015) 407–412.

88 R.-F. Zhang, B. Zhao, H.-S. Wang, P. Cheng, *Inorg. Chem. Commun*., 10 (2007) 1226–1228.

89 J. Li, Z. P. Liang, C.-Y. Wang, X.-S. Tai, *J. Chem. Crystallgr*., 39 (2009) 638-641.

90 P. A. Vigato, S. Tamburini, *Coord. Chem. Rev*., 248 (2004) 1717-2128.

91 K. C. Gupta, A. K. Sutar, *Coord. Chem. Rev.*, 252 (2008) 1420–1450.

92 P. Espinet, M. A. Esteruelas, L. A. Oro, J. L. Serrano, E. Sola, *Coord. Chem. Rev*., 117 (1992) 215-274.

93 S. Chang. L. Jones. C. M. Wang. L. M. Henling, R. H. Gruubbs, *Organometallics*, 17 (1998) 3460.

94 A. D. Garnovskii, A. L. Nivorozhkin, V. I. Minkin, *Coord. Chem. Rev.*, 126 (1993) 1.

95 G. E. Batley, D. P. Graddon, *Aust. J. Chem.*, 20 (1967) 885-891.

96 C. Evans, D. Luneau, *J. Chem. Soc., Dalton Trans.*, (2002) 83-86.

97 M. Enamullah, G. Makhloufi, R. Ahmed, B. A. Joy, M. A. Islam, D. Padula, H. Hunter, G. Pescitelli, C. Janiak, *Inorg. Chem.*, 55 (2016) 6449–6464.

98 C. Maxim, T. D. Pasatoiu, V. Kravtsov, S Shova, C. A. Muryn, R. E.P. Winpenny, F. Tuna, M. Andruh, *Inorg. Chim. Acta*, 361 (2008) 3903–3911.

99 S. Uhlenborck, R. Wegner, B. Krebs, *J. Chem. Soc., Dalton Trans*., (1996) 3731.

100 M. X. Li, L. Z. Zhang, C. L. Chen, J. Y. Niu, B. S. Ji, *J. Inorg. Biochem*., 106 (2012) 117-25.

101 X. J. Yao, Y. W. Xuan, W. Wu, *Acta Cryst.*, E64 (2008) m1132.

102 J. S. Lum, P. E. Chen, A. L. Rheingold, L. H. Doerrer, *Polyhedron*, 58 (2013) 218-228.

103 I. Abrahams, M. A. Malik, M. Motevalli, P. O'Brien, *J. Chem. Soc., Dalton Trans.*, vol. (1995) 1043-1046.

104 H. E. A. El Abdallaoui, P. Rubini, P. Tekely, D. Bayeul, C. Lecomte, *Polyhedron*, 11 (1992) 1795-1800.

105 B.-H. Ye, X.-Y. Li, I. D. Williams, X.-M. Chen, *Inorg. Chem.*, 41 (2002) 6426-6431.

106 U. Kumar, M. Singh, N. Thirupathi, *Polyhedron*, 55 (2013) 233-240.

107 R. L. Rardin, W. B. Tolman, S. J. Lippard, *New. J. Chem*., 15 (1991) 417-430.

108 H. Chun, D. N. Dybtsev, H. Kim, K. M. Kim, *Chem. Eur. J.*, 11 (2005) 3521-3529.

109 R. S. Crees, M. L. Cole, L. R. Hanton, C. J. Sumby, *Inorg. Chem*., 49 (2010) 1712-1719.

110 Y.-L. Liu, K.-F. Yue, B.-H. Shan, L.-L. Xu, C.-J. Wang, Y.-Y. Wang, *Inorg. Chem. Commun.*, 17 (2012) 30-33.

111 E. Katsoulakou, D. Dermitzaki, K. F. Konidaris, E. E. Moushi, C. P. Raptopoulou, V. Psycharis, A. J. Tasiopoulos, V. Bekiari, E. Manessi-Zoupa, S. P. Perlepes, T. C. Stamatatos, *Polyhedron*, 52 (2013) 467-475.

112 B. V. D. Marco, A. Tapparo, A. Dolmella, G. G. Bombi, *Inorg. Chim. Acta*, 357 (2004) 135–142.

113 M. Darawsheh, H. A. Alia, A. L. Abuhijleh, E. Rappocciolo, M. Akkawi, S. Jaber, S. Maloul, Y. Hussein, *Eur. J. Med. Chem*., 82 (2014) 152-163.

114 L. Radovanovic, J. Rogan, D. Poleti, M. Milutinovic, M. V. Rodic, *Polyhedron*, 112 (2016) 18-26.

115 K. M. Doxsee, J. R. Hagadorn, T. J. R. Weakley, *Inorg. Chem*., 33 (1994) 2600-2606.

116 P. Harbach, H.-W. Lerner, M. Bolte, *Acta Cryst.*, E59 (2003) m724.

117 H. Montgomery, E. C. Lingafelter, *Acta Cryst.*,16 (1963) 748–752.

118 M. J. Bennett, F. A. Cotton, R. Eiss, R. C. Elder, *Nature*, 213 (1967) 174.

119 A. Hubner, D. Stroybusch, H.-W. Lerner, M. Bolte, *J. Chem. Crystallogr.*, 38 (2008) 953–957.

120 W. A. Herrmann, N. W. Hubar, O. Runte. *Angew. Chem. Int. Ed. Engl.*, 34 (1995) 2187.

121 K. G. Caulton, L. G. Huberts-Pfalzgrof, *Chem. Rev.*, 90 (1990) 969.

122 J. A. McCleverty, *Prog. Inorg. Chem*., 10 (1968) 49.

123 C. A. Downes, S. C. Marinescu, *Dalton Trans*., 45 (2016) 19311-19321.

124 S. C. Ratvasky, B. Mogesa, M. J. van Stipdonk, P. Basu, *Polyhedron*, 114 (2016) 370-377.

125 V. Madhu, S. K. Das, *Dalton Trans*., 40 (2011) 12901-12908.

126 S. C. Debnath, D. K. Basu, *J. Appl. Poly. Sci*., 52 **(**2003) 597 – 603.

127 C. Ouyang, S. Wang, Y. Zhang, Y. Zhang, *Poly. Degrad. Stability*, 91 (2006) 795-804.

128 J. K. Kurian, N. R. Peethambaran, K. C. Mary, B. Kuriakose, *J. Appl. Poly. Sci*., 78 (2000) 304-10.

129 S. Agarwal, S. G. Aggarwal, P. Singh, *Talanta*, 65 (2005) 104–110.

130 L. A. Vermeulen, A. J. Reinecke, S. A. Reinecke, *Ecotox. Envir. Safety (B)*, 48 (2001) 183-189.

131 H. P. Klug, *Acta Cryst*.,21 (1966) 536.

132 M. Bonamico, G. Mazzone, A. Vaciago, L. Zambonelli, *Acta Cryst*., 19 (1965) 898.

133 M. Shahid, T. Rüffer, H. Lang, S. A. Awan, S. Ahmad, *J. Coord. Chem*., 62 (2009) 440-445.

134 F. A. Almeida Paz, M. C. Neves, T. Trindade, J. Klinowski, *Acta Cryst*., E59 (2003) m1067-m1069.

135 K. A. Fraser, M. M. Harding, *Acta Cryst*., 22 (1967) 75.

136 N. R. Kunchur, M. R. Truter, *J. Chem. Soc*., (1958) 3478-3784.

137 L. Cavalca, G. F. Gasparri, D. Andreetti, P. Domiano, *Acta Cryst*., 22 (1967) 90-98.

138 T. S. Lobana, R. Sharma, R. Sharma, R. Sultana, R. J. Butcher, *Z. Anorg. Allg. Chem*., 634 (2008) 718-723.

139 A. D. Burrows, R. W. Harrington, M. F. Mahon, *Acta Cryst.*, E60 (2004) m1317.

140 M. Bonamico, G. Dessy, V. Fares and L. Scaramuzza, *J. Chem. Soc. A*, (1971) 3195- 3198.

141 M. R. Malik, V. Vasylyeva, K. Merz, N. Metzler-Nolte, M. Saleem, S. Ali, A. A. Isab, K. S. Munawar, S. Ahmad, *Inorg. Chim. Acta*, 376 (2011) 207-211.

142 S. Baggio, R. F. Baggio, P. K. de Perazzo, *Acta Cryst.*, B30 (1974) 2166.

143 Z. Atherton, D. M. L. Goodgame, S. Menzer, D. J. Williams, *Inorg. Chem*., 1998, 37, 849-858.

144 G. Faraglia, R. Graziani, Z. Guo, U. Casellato, S. Sitran, *Inorg. Chim. Acta*, 192 (1992) 17-23.

145 A. Castineiras, D. X. West, *J. Mol. Struc*., 604 (2002) 113-116.

146 V. Z. Vassileva, P. P. Petrova, *Croatica Chim. Acta,* 78 (2005) 295.

147 Y. Matsunaga, K. Fujisawa, N. Amir, Y. Miyashita, K.-I. Okamoto, *J. Coord. Chem.,* 58 (2005) 1047-1061.

148 M. Fettouhi, M. I. M. Wazeer and A. A. Isab, *Z. Kristallogr. NCS*, 221 (2006) 221-222.

149 M. Fettouhi, M. I. M. Wazeer, A. A. Isab, *J. Coord. Chem.,* 60 (2007) 369-377.

150 D. J. Williams, J. J. Concepcion, M. C. Koether, K. A. Arrowood, A. L. Carmack, T. G. Hamilton, S. M. Luck, M. Ndomo, C. R. Teel, D. V. der veer, *J. Chem. Crystallgr*., 36 (2006) 453-357.

151 J. Packer, J. Vaughan, *A Modern Approach in Organic Chemistry,* Oxford, Clarendon Press, (1958) 200.

152 S. Patai (Ed.), *The chemistry of the thiol group*, Wiley, London (1974).

153 R. J. Cremlyn, *An Introduction to Organosulfur Chemistry*, John Wiley and Sons, Chichester (1996).

154 G. Rabbani, A. A. Isab, A. R. Al-Arfaj, S. Ahmad, M. Saleem, A. Hameed, E. Akbar, *Spectroscopy*, 23 (2009) 45-50.

155 L. G. Wade Jr., *Organic Chemistry.* 5th Ed., Amazon prime, (2005) 437-439.

156 J. Reece, L. A. Urry, M. L. Cain, S. A. Wasserman, *Campbell Biology*, 9th Ed., Pearson Benjamin Cummings, New York (2011) 65, 83.

157 J. A. Vilensky, K. Redman, *Ann. Emerg. Med*., 41 (2003) 378-383.

158 B. Muller, A. Schneider, M. Tesmer, H. Vahrenkamp, *Inorg. Chem*., 38 (1999) 1900-1907.

159 U. Brand, M. Rombach, J. Seebacher, H. Vahrenkamp, *Inorg. Chem*., 40 (2001) 6151-6157.

160 S-J. Chiou, C. G. Riordan, A. L. Rheingold, *Proc. Natl. Acad. Sci., U.S.A.*, 100 (2003) 3695–3700.

161 M. M. Ibrahim, J. Seebacher, G. Steinfeld, H. Vahrenkamp, *Inorg. Chem.*, 44 (2005) 8531-8538.

162 T-W. Ngan, C-Ch. Ko, N. Zhu, V. W-W Yam, *Inorg. Chem.*, 46 (2007) 1144-1152.

163 G. Ohanessian, D. Picot, G. Frison, *Int. J. Quant. Chem.*, 111 (2011) 1239-1247.

164 S. Y. Shaban, *Inorg. Chim. Acta*, 367 (2011) 212–216.

165 D. A. Suhy, K. D. Simon, D. I. H. Linzer, T. V. O'Halloran, *J. Biol. Chem.*, 274 (1999) 9183-9192.

166 N. Lihi, A. Grenacs, S. Timari, I. Turi, I. Banyai, I. Sovago, K. Varnagy, *New J. Chem.*, 39 (2015) 8364-8372.

167 C. A. Blindauer, *J. Inorg. Biochem.*, 102 (2008) 507-521.

168 C. A. Blindauer, M. D. Harrison, J. A. Parkinson, A. K. Robinson, J. S. Cavet, N. J. Robinson, P. J.Sadler, *Proc. Natl. Acad. Sci., U.S.A.*, 98 (2001) 9593-9598.

169 N. J. Pace, E. Weerapana, *Biomolecules*, 4 (2014) 419-434.

170 R. Kassim, C. Ramseyer, M. Enescu, *Inorg. Chem*., 50 (2011) 5407.

171 D. Picot, G. Ohanessian, G. Frison, *Inorg. Chem*., 2008, 47, 8167–8178.

172 L. Koziol, C. A. Valdez, S. E. Baker, E.Y. Lau, W. C. Floyd, S. E.Wong, J. H. Satcher, F. C. Lightstone, R. D. Aines, *Inorg. Chem*., 51 (2012) 6803.

173 N. Strater, W. N. Lipscomb, T. Klabunde, B. Krebs, *Angew. Chem., Int. Ed. Engl*., 35 (1996) 2024-2055.

174 N. Strater, W. N. Lipscomb, *Biochemistry*, 34 (1995) 14792.

175 H. Vahrenkamp, *Dalton Trans.*, (2007) 4751-4759.

176 H. Vahrenkamp; *Acc. Chem. Res*., 32 (1999) 589-596.

177 R. Burth, H. Vahrenkamp, *Inorg. Chim. Acta*, 282 (1998) 193-199.

178 J. Notni, H. Görls, E. Anders, *Eur. J. Inorg. Chem.*, (2006) 1444–1455.

179 J. Notni, W. Günther, and E. Anders, *Eur. J. Inorg. Chem.*,(2007) 985–993.

180 J.Seebacher, M. Ji, H. Vahrenkamp, *Eur. J. Inorg. Chem., (*2004) 409-417.

181 J. P. Glusker, A. K. Katz and C.W. Bock, *The Rigaku Journal*, 16 (2) (1999) 8-16.

182 C. S. Lai, Y. X. Lim, T. C. Yap, E. R. T. Tiekink, *Cryst. Eng. Comm.***,** 4 (2002) 596-600.

183 R. Baggio, M. T. Gerland, M. Perec, , *J. Chem. Soc*., *Dalton Trans*, (1993) 3367.

184 D. T. Crown, S. A. Koch, *Inorg. Chem.*, 27 (1988) 493-496.

185 D. T. Crown, E. C. Gruff, S. A. Koch, *J. Chem. Soc., Chem. Commun.*, (1987) 966-967.

186 G. M. Sheldrick, *Acta Cryst.*,A64 (2008) 112–122.

187 G. M. Sheldrick, *Acta Cryst.*, C71 (2015) 3-8.

188 A. L. Spek, Acta Cryst., D65 (2009)148-155.

189 G. Kresse, J. Hafner, Phys. Rev., B47 (1993) 558-561.

190 G. Kresse, J. Hafner, Phys. Rev., B49 (1994) 14251-14269.

191 G. Kresse, J. Furthmuller, Phys. Rev., B54 (1996) 11169-11186.

192 J. P. Perdew, K. Burke, M. Ernzerhof, Phys.l Rev. Lett., 77 (1996) 3865-3868.

193 G. Kresse, D. Joubert, Phys. Rev., B59 (1999) 1758-1775.

194 S. L. Dudarev, G. A. Botton, S. Y. Savrasov, C. J. Humphreys, A. P. Sutton, Phys. Rev., B57 (1998) 1505-1509.

195 M. Ernzerhof, G. E. Scuseria, J. Chem. Phys.,110 (1999) 5029-5036; C. Adamo, V. Barone, J. Chem. Phys., 110 (1999) 6158-6170

196 M. J. Frisch, G. W. Trucks, H. B. Schlegel, G. E. Scuseria, M. A. Robb, J. R. Cheeseman, G. Scalmani, V. Barone, B. Mennucci, G. A. Petersson, H. Nakatsuji, M. Caricato, X. Li, H. P. Hratchian, A. F. Izmaylov, J. Bloino, G. Zheng, J. L. Sonnenberg, M. Hada, M. Ehara, K. Toyota, R. Fukuda, J. Hasegawa, M. Ishida, T. Nakajima, Y. Honda, O. Kitao, H. Nakai, T. Vreven, J. A. Montgomery, Jr., J. E. Peralta, F. Ogliaro, M. Bearpark, J. J. Heyd, E. Brothers, K. N. Kudin, V. N. Staroverov, R. Kobayashi, J. Normand, K. Raghavachari, A. Rendell, J. C. Burant, S. S. Iyengar, J. Tomasi, M. Cossi, N. Rega, J. M. Millam, M. Klene, J. E. Knox, J. B. Cross, V. Bakken, C. Adamo, J. Jaramillo, R. Gomperts, R. E. Stratmann, O. Yazyev, A. J. Austin, R. Cammi, C. Pomelli, J. W. Ochterski, R. L. Martin, K. Morokuma, V. G. Zakrzewski, G. A. Voth, P. Salvador, J. J. Dannenberg, S. Dapprich, A. D. Daniels, Ö. Farkas, J. B. Foresman, J. V. Ortiz, J.

Cioslowski, and D. J. Fox, *The Gaussian 09, Gaussian, Inc.,* Wallingford CT, Revision D.01 (2009).

197 http://www.chemcraftprog.com.

198 V. Barone, M. Cossi, *J. Phys. Chem*., A102 (1998) 1995-2001; M. Cossi, N. Rega, G. Scalmani, V. Barone, *J. Comput. Chem*., 24 (2003) 669-681

199 J. P. Snyder, N. Nevins, S. L. Tardif, D. N. Harpp, *J. Am. Chem. Soc*., 119 (1997) 12685-12686.

200 M. Hanif, A. Saddiqa, S. Hasnain, S. Ahmad, G. Rabbani, A. A. Isab, *Spectroscopy*, 22 (2008) 51-56.

201 Y. Matsunaga, K. Fujisawa, N. Amir, Y. Miyashita, K. Okamoto, *Appl. Organomet. Chem.*, 19 (2005) 208.

202 B. M. Vedavathi, K. Vijayan, *Curr. Sci. India*, 48 (1979) 1028.

203 L. Riauba, G. Niaura, O. Eicher-Lorka, E. Butkus, *J. Phys. Chem.*, A110 (2006) 13394-13404.

204 H. E. Vanwart, H.A. Scheraga, *Proc. Natl. Acad. Sci. U.S.A*., 83 (1986) 3064.

205 S. Ahmad, A. A. Isab, S. Ali, A. R. Al-Arfaj, Polyhedron, 25 (2006) 1633.

206 A. Ferrari, A. Braibranti, G. Bigliardi, A. M. Lanfredi, *Acta Cryst.*,18 (1965) 367.

207 J. Pickardt, G. Gong, S. Wischnack, C. Steinkopff, *Z. Naturforsch.,* B 49 (1994) 325-329.

208 M. Kabesova, R. Boca, M. Melnik, D. Valigura, M. Dunaj-Jurco, *Coord. Chem. Rev.*, 140 (1995) 115-135.

209 A. Espinosa, M. Sohail, M. Habib, K. Naveed, M. Saleem, Habib-ur Rehman, I. Hussain, A. Munawar, S. Ahmad, *Polyhedron*, 90 (2015) 252-257.

210 F. Naureen, T. Ruffer, H. Lang, A. A. Isab, S. Ahmad, *J. Chem. Cryst*., 38 (2008) 765-768.

211 L. Tchertanov, C. Pascard, *Acta Cryst*., B53 (1997) 904-915.

212 L. A. Aslanov, V. M. Ionov, K. Kynev, *Kristallografiya*, 21 (1976) 1198-1199.

213 S. Grimme, J. Antony, S. Ehrlich, H. Krieg, *J. Chem. Phys.,* 132 (2010) 154104.

214 P. J. Hay, W. R. Wadt, *J. Chem. Phys.,* 82 (1985) 299.

215 T. H. Dunning Jr., P. J. Hay, *in Modern Theoretical Chemistry, Ed. H. F. Schaefer III*, *Plenum*, New York, Vol. 3 (1976) 1.

216 S. F. Boys, F. Bernardi, *Mol*. *Phys*., 19 (1970) 553.

217 A. E. Reed, L. A. Curtiss, F. Weinhold, *Chem. Rev.*, 88 (1988) 899.

218 E. D. Glendening, J. K. Badenhoop, A.E. Reed, J. E. Carpenter, J. A. Bohmann, C. M. Morales, F. Weinhold, *NBO 5.0.*, (Theoretical Chemistry Institute, University of Wisconsin, Madison, WI, (2001).

219 N. Ozturk, S. Bahceli, *Z. Naturforsch*., 61A (2006) 399-401.

220 A. Wojciechowska, A. Kochel, W. Zierkiewicz, *J. Coord. Chem.*, 69 (2016) 5.

221 A. Wojciechowska, J. Janczak, W. Zierkiewicz, A. Dylong, E. Matczak-Jon, *Polyhedron*, 85 (2015) 665.

222 U. Adhikari,S. Scheiner, *J. Phys. Chem. A*, 118 (2014) 3183–3192.

223 V. P. N. Nziko, S. Scheiner, *J. Phys. Chem. A*, 119 (2015) 5889–5897.

224 J. Fanfrlík, A. Prada, Z. Padelkova, A. Pecina, J. Machacek, M. Lepsik, J. Holub, A. Ruzicka, D. Hnyk, P. Hobza, *Angew. Chem. Int. Ed. Engl*., 53 (2014) 10139-10142.

225 J. Contreras-Garcia, E. R. Johnson, S. Keinan, R. Chaudret, J.-P. Piquemal, D. N. Beratan, W. Yang, *J. Chem. Theory Comput*., 7 (2011) 625.

226 E. R. Johnson, S. Keinan, P. Mori-Sanchez, J. Contreras-Garcia, A. J. Cohen, W. Yang, *J. Am. Chem. Soc*., 132 (2010) 6498-6506.

227 P. A. Sutherland, W. T. A. Harrison, *Acta Cryst.*, E65 (2009) m565.

228 Z. Dong, B. Liu, *Acta Cryst.*, E68 (2012) m131.

229 E. Govindan, S. Thirumurugan, A. S. Ganeshraja, K. Anbalagan, A. Subbiah Pandi, *Acta Cryst.*, E70 (2014) m53.

230 R. G. Baughman, R. S. Shane, J. M. McCormick, *Acta Cryst*., E67 (2011) m1.

231 R. Lescouezec, L. M. Toma, J. Vaissermann, M. Verdaguer, F. S. Delgado, C. Ruiz-Perez, F. Lloret, M. Julve, *Coord. Chem. Rev*., 249 (2005) 2691.

232 H. Miyasaka, H. Takahashi, T. Madanbashi, K. Sugiura, R. Clerac, H. Nojiri, *Inorg. Chem*., 44 (2005) 5969.

233 E. Colacio, M. Ghazi, H. Stoeckli-Evans, F. Lloret, J. M. Moreno, C. Perez, *Inorg. Chem.*, 40 (2001) 4876-4883.

234 M. Nayak, P. Kundu, P. Lemoine, R. Koner, H. H. Wei, S. Mohanta, *Polyhedron*, 25 (2006)2007.

235 A. Rodriguez-Dieguez, R. Kivekaes, R. Sillanpaeae, J. Cano, F. Lloret, V. McKee, H. Stoeckli-Evans, E. Colacio, *Inorg. Chem.*, 45 (2006) 10537.

236 H.-X. Zhang, Y.-X. Tong, Z.-N. Chen, K.-B. Yu, B.-S. Kang, *J. Organomet. Chem.*, 598 (2000) 63–70.

237 E. Colacio, F. Lloret, M. Navarrete, A. Romerosa, H. Stoeckli-Evans, J. Suarez-Varela, *New J. Chem.*, 29(2005) 1189-1194.

238 D. Ghoshal, A. K. Ghosh, T. K. Maji, J. Ribas, G. Mostafa, E. Zangrando, N. R. Chaudhuri, *Inorg. Chim. Acta*, 359 (2006) 593-602.

239 T. Akitsu, Y. Einaga, *Inorg. Chim. Acta*, 361 (2008) 36–42.

240 J. Paharova, J. Cernak, R. Boca, Z. Zak, *Inorg. Chim. Acta*, 346 (2003) 25-31.

241 A. Karadag, H. Pasaoglu, G. Kastas, O. Buyukgungor, *Acta Cryst.*, C60 *(*2004) m581-m583.

242 A. Deak, T. Tunyogi, C. Jobbágy, Z. Károly, P. Baranyai, G. Palinkas, *Gold Bull.*, 45 (2012) 35–41.

243 D. B. Leznoff, B. Y. Xue, R. J. Batchelor, F. W. B. Einstein, B. O. Patrick, *Inorg. Chem.*, 40 (2001) 6026.

244 D. B. Leznoff, B. Y. Xue, C.L. Stevens, A. Storr, R. C. Thompson, B. O. Patrick, *Polyhedron*, 20 *(*2001) 1247.

245 D. B. Leznoff, B. Y. Xue, B. O, Patrick, V. Sanchez, R. C. Thompson, *Chem. Commun.*,(2001) 259.

246 E. Colacio, F. Lloret, R. Kivekas, J. S. Varela, M. R. Sundberg, R. Uggla, *Inorg. Chem*., 42 (2003) 560.

247 E. Colacio, F. Lloret, R. Kivokas, J. Ruiz, J. Suarez-Varela, M. R. Sundberg, *Chem. Commun.*, (2002) 592.

248 M. J. Katz,V. K. Michaelis, P. M. Aguiar, R. Yson, H. Lu, H. Kaluarachchi, R. J. Batchelor, G. Schreckenbach, S. Kroeker, H. H. Patterson, D. B. Leznoff, *Inorg. Chem.*,47 (2008) 6353-6363.

249 M. J. Katz, D. B. Leznoff, *J. Am. Chem. Soc*., 131 (2009) 18435.

250 F. Baril-Robert, X. Li, M. J. Katz, A. R. Geisheimer, D. B. Leznoff, H. Patterson, *Inorg. Chem*., 50 (2011) 231.

251 Y. Guo, Y. Ma, N. Zhou, Z.-Q. Liu, Q.-L. Wang, S.-P. Yan, D.-Z. Liao, *Z. Anorg. Allg. Chem*., (2010) 865–871.

252 S. Nawaz, T. Rüffer, H. Lang, M. A. Shaheen, S. Ahmad, J. H. Shah, *Z. Naturforsch. B*, 70 (2015) 455-459.

253 S. Nawaz, A. Ghaffar, M. Monim-ul-Mehboob, M. N. Tahir, M. A. Alotaibi, A. A. Isab, S. Ahmad, *Z. Naturforsch. B*, 72 (2017)43-47.

254 S. Ahmad, M. N. Tahir, H. M. Javaid, M. Monim-ul-Mehboob, M. A. Shaheen, R. Mahmood, *J. Chem. Crystallogr.*, 42 *(*2012) 401-404.

255 S. Ahmad, M. Monim-ul-Mehboob, M. Altaf, H. Stoeckli-Evans, R. Mehmood, *J. Chem. Crystallogr.*,37 *(*2007) 685-689.

256 H. X. Zhang, B. S. Kang, L. R. Deng, C. Ren, C. Y. Su, Z. N. Chen,*Inorg. Chem. Commun*., 4(2001) 41.

257 Y-P. Ren, L-S. Long, R-B. Huang, L-S. Zheng, *Appl. Organomet. Chem*., 19 (2005) 1071.

258 J. Cernak, J. Chomic, P. Gravereau, A. Orendacova, M. Orendac, J. Kovac, A. Feher, C. Kappenstein, *Inorg. Chim. Acta,* 281 *(*1998) 134.

259 C. Kappenstein, A. Ouali, M. Guerin, J. Cernak, J. Chomic, *Inorg. Chim. Acta*, 147 (1988) 189.

260 J. Cernak, K. A. Abboud, J. Chomic, M. W. Meisel, M. Orendac, A. Orendacova, A. Feher, *Inorg. Chim. Acta*, 311 (2000) 126.

261 H. X. Zhang, Z. N. Chen, C. Y. Sue, C. Ren, B. S. Kang, *J. Chem. Crystallogr*., 29 (1999) 1239.

262 C. J. Shorrock, B. Y. Xue, P. B. Kim, R. J. Batchelor, B. O. Patrick, D. B. Leznoff, *Inorg. Chem*., 41 (2002) 6743.

263 H. Zhang, Y. Zhang, C. Wang, L. Cai, Y. Xie, G. Xue, *Inorg. Chem. Commun*., 41 (9)(2006) 555–558.

264 H. Schmidbaur, A. Schier, *Angew. Chem. Int. Ed.*, 54 *(*2015) 746–784.

265 S. Kitagawa, R.Kitaura, S.-I. Noro, *Angew. Chem. Int. Ed*., 43 (2004) 2334.

266 C. A. Bayse, J. L. Ming, K. M. Miller, S. M. McCollough, R. D. Pike, *Inorg. Chim. Acta,* 375 *(*2011) 47-52.

267 J. Cernak, M. Orendac, I. Potocnak, J. Chomic, A. Orendacova, J. Skorsepa, A. Feher, *Coord. Chem. Rev.*, 224 *(*2002) 51–66.

268 H. Schmidbaur, A. Schier, *Chem. Soc. Rev.*, 37 (2008) 1931.

269 H. Schmidbaur, A. Schier, *Chem. Soc. Rev.*, 41 (2012) 370.

270 P. Pyykko, *Chem. Rev.*, 97 (1997) 597-636.

271 M. Ramzan, *M.Phil Thesis*, University of Engineering and Technology, Lahore, Pakistan (2009).

272 L. Trisciıkova, I. Potocnak, J. Chomic, T. Müller, *Thermochimica Acta*, 419 *(*2004) 231.

List of Publications

1) M. Monim-ul-Mehboob, M. Ramzan, T. Rüffer, H. Lang, S. Nadeem, **M. Akhtar**, S. Ahmad,*A Zinc(II)-Silver(I) Bimetallic Coordination Polymer Assembled Through Argentophilic and π-π Interactions, {[Zn(phen)$_2$(H$_2$O){Ag(CN)$_2$}][Ag(CN)$_2$].MeOH}$_n$ (phen = 1,10-Phenanthroline),* **Z. Naturforsch.B**,68 (**2013**).161-167.

2) **M. Akhtar**, M. Fettouhi, M. Ahmed, I. U. Khan, S. Ahmad, *N,N,N'N'-Tetramethylethylenediaminium tetrachloridozincate(II),* **Acta Cryst.E**, 69 (**2013**) m642.

3) **M. Akhtar**, M. N. Tahir, M. Saleem, M. Mazhar, A. Rauf, A. A. Isab, S. Ahmad, S. Nadeem, *Crystal structure and biological properties of a tetranuclear Zinc(II) complex of cysteamine, [Zn$_4$Cym$_4$Cl$_4$] prepared in the presence of diamines*, **Russ. J. Inorg. Chem.,**60(**2015**).1568-1572.

4) **M. Akhtar**, A. I. Alharthi, M. A. Alotaibi, N. Trendafilova, I. Georgieva, M. N. Tahir, M. Mazhar, A. A. Isab, M. Hanif, Saeed Ahmad, *Synthesis, X-ray structure, spectroscopic (IR, NMR) analysis and DFT modeling of a new polymeric Zinc(II) complex of cystamine, [Zn(Cym-Cym)Cl$_2$]$_n$,* **Polyhedron**, 122 (**2017**) 105-115

5) **M. Akhtar**, M. R.Malik, M. N.Tahir, S. Nadeem, M. Altaf, M. Sohail, S. Ali, S. Ahmad, **J. Struct. Chem.**, 8 (1) (**2017**) 178–182.

6) **M. Akhtar**, M. A. Alotaibi, A. I. Alharthi, W. Zierkiewicz, M. N. Tahir, M. Mazhar, A. A. Isab, M. Monim-ul-Mehboob, S. Ahmad, *Spectroscopic and DFT studies of zinc(II) complexes of diamines and thiocyanate; crystal structure of (cis-1,2-diaminocyclohexane) bis(thiocyanato-κN)zinc(II),* **J. Mol. Structure**, 1128 (**2017**). 455-461.

7) M. A. Alotaibi, A. I. Alharthi, W. Zierkiewicz, **M. Akhtar**, M. N. Tahir, M. Mazhar, A. A. Isab, S. Ahmad,*Synthesis, crystal structure and DFT studies of a Zinc(II) complex of 1,3-diaminopropane (Dap), [Zn(Dap)(NCS)$_2$][Zn(Dap)(NCS)$_2$]$_n$. The additional stabilizing role of S-π chalcogen bond*, **J. Mol. Structure**, 1133 (**2017**) 271-277.

8) **M. Akhtar**, W. Zierkiewicz, M. Michalczyk, T. Rüffer, H. Lang, A. A. Isab, M. Mazhar, S. Ahmad, *Crystal Structure and Theoretical Investigation of Bis(cis-1,2-diaminocyclohexane)zinc(II) tetrachloridozincate(II),***Z. Naturforsch.B**,72(8)b (**2017**) 627-630.

9) **M.Akhtar**,I.Georgieva,N. Trendafilova, T. Ahmad, A. Noor, M.N.Tahir, M.Mazhar, A.A. Isab, S.Ahmad, *Synthesis, X-ray Structure and DFT Modelling of a New Polymeric Zinc(II) Complex of 2-Mercaptonicotinic acid (Mnt-H), {[Zn(Mnt-Mnt)(en)].H$_2$O}$_n$*, submitted to **J. Mol. Structure** (**2017**).